MICROENVIRONMENTAL STIMULATION OF CARDIAC PROGENITOR CELLS

A Dissertation

Presented to

The Academic Faculty

by

Kristin Marie French

In Partial Fulfillment

of the Requirements for the Degree

Doctor of Philosophy in the

Wallace H. Coulter Department of Biomedical Engineering

Georgia Institute of Technology

August 2015

MICROENVIRONMENTAL STIMULATION OF CARDIAC PROGENITOR CELLS

Approved by:

Dr. Michael E. Davis, Advisor
School of Biomedical Engineering
Emory University

Dr. W. Robert Taylor
School of Medicine, Cardiology
Emory University

Dr. Thomas H. Barker
School of Biomedical Engineering
Georgia Institute of Technology

Dr. Manu O. Platt
School of Biomedical Engineering
Georgia Institute of Technology

Dr. Alejandra San Martin
School of Medicine, Cardiology
Emory University

Date Approved: April 30th 2015

This work is dedicated to my grandparents, who through hard work, love and sacrifice built our family and made our education possible.

ACKNOWLEDGEMENTS

Many people have contributed directly to this work or provided support along the way. I would like to thank those people here and hope that I do not leave anyone out. First and foremost, I would like to thank my advisor, Mike Davis for his unwavering support and enthusiasm. He has afforded me the freedom to explore my own scientific ideas and challenged me to take ownership of my data. It has been exciting to watch the lab grow and expand under his leadership.

I would also like to thank the members of my thesis committee. Dr. Barker provided meaningful insight early on by introducing me to silanization. He also asks very direct questions challenging me to truly evaluate the experimental set-up and is never short of novel ideas. Dr. San Martin has offered a strong biological perspective and challenged me to consider what is occurring on a sub-cellular level. She is also quick to provide a warm smile when passing in the hallway. I have truly enjoyed being a member of the cardiology division. It is a collaborative and supportive environment that propels everyone forward. Dr. Platt brings such cheer to science. It is sometimes overwhelming to talk to him, as he has an abundance of energy and ideas. He can go from big picture to small detail in two-seconds flat and has helped me to both streamline and expand my project. Dr. Taylor has been a grounding force. He has a skill for identifying the defining experiment in a project and asking the critical questions. His lab has graciously allowed me to borrow their space and time on numerous occasions. I am glad to engage in a little friendly rivalry, settled by sport, between our labs.

I would like to thank all of the members, past and present, of the Davis Lab. It has been a fun experiment. You all bring such unique perspectives to our group. Jay and Gokul were there from the beginning and were the first examples that I had to follow. I was naïve and four years behind, but they made it look easy. Archana continued to set

the bar high with her sweet demeanor and hard work. Inthu and Warren made the lab feel like a home with their sibling-like rivalry. They never failed to push the boundaries academically. Pauline and Bernadette joined the lab with me and made it a fun and warm environment. Milton has been a constant support that allows us all to flourish. Mario always offers humor. Srishti has been a constant source of support, optimism and cheer. To the newest Davis lab members, Josh, Udit and Aline, it has been a pleasure to work with each of you and I trust that you will keep up the spirt of our lab.

I would also like to thank my family for their endless support. From the very beginning, my parents gave me every opportunity possible to grow and excel and for that I can never repay them. From spell checking elementary homework to gardening in the yard and from replacing the garbage disposal to baking a pie, they have taught me so many things and set me on this path to learn even more. My brother Kyle is a big reason that I ended up in Atlanta for a Ph.D. and has always paved the path for my siblings and me. My sister has been a constant companion and was always willing to talk or listen. While not included in this thesis, she has also contributed artwork to manuscripts in our lab. My younger brother Brian has been my sidekick from early on and nowadays dorks out even harder than I do. To my fiancé Orlando, thank you for making me wake up at the crack of dawn in order to beat traffic into lab, for always making me run faster than I care to, for making what I do look easy because you always manage to work harder than I do and for relieving the stress of a long week. I have enjoyed sharing this part of the journey with you and know that you will continue to challenge me in the future.

It turns out that I did not know what I was getting myself into when I started graduate school. It has definitely been challenging, but thanks to an awesome cohort of colleagues and friends it has been more enjoyable than I ever could have imagined. I am so thankful to get to work (and play) alongside these fine people. I have met some spectacular scientists and leaders and I am excited to see where their futures taken them. They have also, perhaps unknowingly, pushed me to be better every day.

TABLE OF CONTENTS

LIST OF TABLES

LIST OF FIGURES

LIST OF SYMBOLS AND ABBREVIATIONS

a-MHC	alpha myosin heavy chain
ANOVA	analysis of variance
bFGF	beta fibroblast growth factor
CADUCEUS	Cardiosphere-derived autologous stem cells to Reverse Ventricular Dysfunction
cECM	naturally-derived, cardiac extracellular matrix
Cnx43	connexin 43
COL	collagen I
CPCs	cardiac progenitro cells
ECM	extracellular matrix
ELISA	enzyme-linked immuno assay
ERK	extracellular signal-regulated kinase
FAK	focal adhesion kinase
FBS	fetal bovine serum
FDA	Food and Drug Administration
FN	fibronectin
FSP	fibroblast-specific protein 1
GAPDH	Glyceraldehyde 3-phosphate dehydrogenase
HBSS	Hank's Balanced Salt Solution
HGF	hepatocyte growth factor
HRP	horseradish peroxidase
ITS	insulin transferrin selenium
LINC	linker of nucleoskeleton and cytoskeleton
LN	laminin
MAGIC	Myoblast Autologous Grafting in Ischemic Cardiomyopathy

MCP	monocyte chemoattractant
MDR	multi-drug resistance protein
MI	myocardial infarction
MSC	mesenchymal stem cell
NRVM	neonatal rat ventricular myocytes
P/S/G	penicillin-streptomycin-glutamine
PBS	phosphate buffered saline
PDGF	platelet-derived growth factor
PDMS	Polydimethylsiloxane
qPCR	quantitative polymerase chain reaction
SCF	stem cell factor
SCIPIO	Stem Cell Infusion in Patients with Ischemic Cardiomyopathy
SDS	sodium dodecyl sulfate
SERCA	sarcoendoplasmic reticulum calcium transport ATPase
SIS	small intestine submucosa
SPARC	Secreted protein acidic and rich in cysteine
TBS-T	tris buffered saline with tween
VEGF	vascular endothelial growth factor
vWF	von Willibrand Factor

SUMMARY

Heart failure, predominately caused by myocardial infarction (MI), is the leading cause of death in the United States [1]. During MI, the occlusion of a coronary artery results in a loss of contractile cells and formation of scar tissue in the myocardium. Changes in tissue structure induce altered mechanical loads that lead to chronic remodeling and progression to heart failure. Currently, the only treatment for heart failure is cardiac transplantation, but studies show that progenitor cell, biomaterial, or combined therapies have improved cardiac function post-MI. While cell therapy studies show promise at a clinical level, the mechanism through which benefits are achieved is unclear [2]. A thorough understanding of cardiac progenitor cell interactions with their microenvironments is necessary to understand how cellular and biomaterial treatments could synergistically improve cardiovascular therapy. This dissertation aims to fill this mechanistic gap created by ongoing clinical studies through evaluating the interaction of cardiac progenitor cells (CPCs) with their microenvironment, specifically through the application of extracellular matrix proteins or mechanical strain.

The endogenous environment of CPCs is drastically different than commonly used culture conditions. Further the endogenous environment changes with disease state. We evaluated the behavior of CPCs cultured on a naturally-derived, cardiac extracellular matrix (cECM) as compared to the standard culture coating collagen I, which also mimics fibrotic tissue. In this study, CPCs cultured on cECM had improved cell numbers and cardiomyogenic maturation.

The microenvironmental cues responsible for stimulating CPC activation are largely unknown. During development, aging and disease the myocardium changes in matrix composition and stiffness exposing endogenous cells to a wide variety of stimuli. In a combinatorial study, we evaluate the effect of cyclic strain and extracellular matrix composition on CPC behavior. The response of CPCs to signals from the microenvironment is complex, with more matrix-dependency observed at lower strains. Alignment, cell division and paracrine signaling are extracellular matrix and strain dependent. Extracellular matrix conditions affect CPC maturation and calcium signaling. Mechanotransduction pathways, including focal adhesion kinase are activated through adhesion and maintained under cyclic strain.

This dissertation addresses the interaction between CPCs and extracellular matrix proteins, including cECM, as well as the interaction between CPCs and cyclic strain. The impact of this work is significant because it will build a basic scientific understanding of CPC interactions with the microenvironment. These insights will advance pragmatic cell therapy attempts to regenerate healthy myocardium post-MI.

CHAPTER 1 INTRODUCTION

Coronary artery disease accounts for half of all cardiovascular disease, greatly contributing to the number one cause of death in the United States [1]. Advances in surgical techniques, pharmacological agents and an understanding of risk factors have reduced the mortality of cardiovascular disease over the last several decades [3]. However, the majority of current therapies are palliative and while slowing the progression of heart failure, are unable to regenerate tissue after an injury such as myocardial infarction (MI). To fill this need, the fields of cell therapy and tissue engineering have grown exponentially of late.

1.1 Motivation

Annually there are over 1 million estimated cases of MI, with the estimated direct and indirect costs of the disease totaling $315 billion dollars [1]. A myocardial infarction begins with the occlusion of a coronary artery, preventing blood flow to the serviced region of myocardium. The hypoxic environment leads to a loss of myocytes, further triggering an immune response. Fibroblasts are recruited to the injury site and deposit extracellular matrix leading to the formation of a non-contractile scar. As the heart adjusts to changes in its altered mechanical load it undergoes maladaptive chronic remodeling leading to decreased function and heart failure. In a clinical setting, coronary angioplasty restores blood flow to the myocardium, acutely resulting in the production of reactive oxygen species and additional damage.

Cell therapy shows great promise in regenerating injured tissues. Several clinical trials are underway to evaluate the safety and efficacy of these therapies after MI. SCIPIO and CADUCEUS have both demonstrated safety with functional improvements seen in patients with more severe heart failure [4]. One of the greatest challenges of cell therapy is adequate retention and survival of implanted cells [2]. Combination therapies of cells

delivered in a biomaterial vehicle are being used to improve cell retention. Biomaterials may also serve to provide implanted cells with a controlled microenvironment, shielding them from the harsh condition of the diseased myocardium. Currently, a number of cell types have been evaluated in combination with several biomaterials for cell therapy. In many cases though, these studies lack a thorough understanding of how the cell behavior is tied to their microenvironment. Evaluating and understanding how specific microenvironmental cues affect cell behavior will allow for pragmatic design of cell therapy studies.

CHAPTER 2 SPECIFIC AIMS AND HYPOTHESES

The central hypothesis of this dissertation is that cardiac progenitor cells (CPCs) sense their microenvironment and that providing CPCs with the appropriate microenvironmental cues will improve their potential to regenerate healthy myocardium through proliferation, cardiogenic differentiation, paracrine signaling and connectivity. The microenvironment consists of many complex signals including biochemical (i.e. extracellular matrix composition) and biomechanical (i.e. tensile strain) cues. Moreover, endogenous microenvironments are spatially and temporally distinct. This dissertation focuses on understanding the relationship between microenvironmental cues and CPC behavior.

Aim 1: Evaluate the effect of cECM on CPC behavior.[1]

We hypothesize that a complex, naturally-derived exctracellular microenvironment (cECM) would improve CPC culture over standard collagen I. CPCs were isolated from adult, male Sprague-Dawley rats and cultured on cECM or collagen I (COL) at 1 mg/mL for 2 – 7 days. Following culture, CPCs were harvested for qPCR, Western, Annexin V and Coulter Counting to assess maturation, survival and proliferation. Additionally, a microfluidic experiment was performed to determine CPC adhesion to each substrate. We found that CPC behavior was improved by culture on cECM as compared to collagen I.

Aim 2: Assess the matrix composition dependency of mechanical loading on CPCs.

We hypothesize that CPCs would respond to cyclic strain and that the response would be specific to matrix culture conditions. Bioflex plates were functionalized with poly-L-

---

[1] French KM et al. A naturally derived cardiac extracellular matrix enhances cardiac progenitor cell behavior in vitro. Acta Biomaterialia. 2012; 8(12): 4357-64.

lysine, laminin, fibronectin, collagen I or cECM at 10 ug/cm^2 before seeding with CPCs. The plates were then exposed to 0%, 5%, 10% or 15% strain for 24 hours on a Flexcell 5000. The effects of strain and matrix coating on CPC behavior were evaluated by immunofluorescence, qPCR, Western, calcium oscillations and ELISA to assess alignment, differentiation, proliferation and paracrine signaling. Further, effective strain transfer and biochemical pathways were evaluated for mechanistic insight. CPCs respond to biochemical and biomechanical cues in a complex manner.

CHAPTER 3 LITERATURE REVIEW

3.1 Myocardial Infarction

3.1.1 Prevalence of Myocardial Infarction

Cardiovascular disease is responsible for more deaths in the United States than any other cause, accounting for almost one-third of all deaths [1]. Every 40 seconds there is a death contributed to cardiovascular disease. Coronary heart disease, including myocardial infarction (MI), contributes to 50% of all cardiovascular disease. MI has a current prevalence of 7.6 million people, with 620,000 new, 295,000 recurrent and a predicted 150,000 silent MIs annually. Thanks to an improved understanding of risk factors and therapeutic intervention, the death rate of all cardiovascular disease has decreased 31% since 2000. This had led to a 28% increase in the number of inpatient procedures performed and an increase in the prevalence of heart failure, currently at 5.1 million. Heart transplantation is ultimately the only cure for heart failure, with the number of available donor hearts far insufficient for the number of patients. Currently, fewer than 3,000 heart transplantations are performed annually. This equates to less than 1% of all heart failure patients. In 2010, the total direct and indirect cost of all cardiovascular disease was $315 billion, one-and-a-half times greater than the total estimated costs of all cancer combined. This places a burden on the health care system, with the predicted costs to reach one trillion dollars in the next 15 years [1].

3.1.2 Myocardial Infarction Progression

This section will describe the disease progression following a myocardial infarction (MI), with a specific focus on remodeling of the extracellular matrix and altered mechanics of the myocardium. An MI is initiated by the occlusion of a coronary artery. Within minutes of this event, myocytes loss begins through necrosis, programmed apoptosis and autophagy, with myocytes loss spanning the thickness of the myocardium within hours

[5, 6]. It is estimated that 1.7 x10^9 myocytes are lost in a severe infarct of the human left ventricle [7-9]. While there is some evidence of mitotic cardiomyocytes after MI, the degree of myocyte turnover is debated and ultimately, division of existing myocytes is insufficient to restore the myocardium [7]. Within 12 hours, the biochemical changes to surviving cells in the myocardium are irreversible [5]. Biochemical signaling events initiated by release of intracellular proteins from dying myocytes trigger an immune response in the myocardium [6]. In large mammals, this is identified as cytokine signaling induction and leukocyte infiltration beginning within an hour of infarct and lasting several days [10].

Loss of myocardium function is evident within minutes of the occlusion [9]. This loss of function leads to a reduced stroke volume and increased end diastolic pressure of the left ventricle. Cardiomyocycte slippage contributes to acute wall thinning [9]. To compensate for this remodeling, the end diastolic volume of the myocardium increases, but this adaptation is only successful for small infarcts [11]. In more severe infarcts, eccentric hypertrophy is induced in the infarct region resulting in further dilation of the ventricle. Infarct tissue is softest 4-7 days post-MI, leading to the greatest likelihood of ventricular rupture [5]. This is followed by fibrotic tissue deposition [10]. If chamber dilation is uncompensated by an increase in wall thickness, there is a decrease in wall motion indicating further loss of function. As the surviving myocardium must bear the mechanical load, this remodeling also results in an increase in wall tension, leading to concentric hypertrophy of remote regions of the myocardium [9, 11]. Increased wall tension can lead to a 70% increase in cardiomyocyte size through hypertrophy [8, 12]. However, myocyte hypertrophy, while increasing the mass of viable myocardium, is insufficient to functionally compensate for myocyte loss [13]. Additionally, scar tissue continues to develop through further matrix deposition and crosslinking over 2-3 months [5, 10]. This fibrosis contributes to contractile dysfunction and arrhythmia [6]. Acute

left ventricular remodeling including infarct expansion, i.e. the thinning and lengthening of scar tissue, and ventricle dilation are observed within several weeks of the initial coronary event. Chronic remodeling which is largely observed as chamber dilation occurs over several months to a year [8, 11]. The degree of functional loss and myocardial remodeling is proportional to the degree of injury after MI [9]. Further the degree of fibrosis correlates with morbidity and mortality due to arrhythmias and sudden cardiac death [6].

Additional changes are observed in the myocardium post-MI. In the remote and border zones, capillaries increase in diameter in order to maintain capillary volume after a decrease in capillary number [13]. Neurohumoral factors, i.e atrial natriuretic peptide, angiotensin II, and transforming growth factor beta, are released and further contribute to remodeling [11, 12]. Additionally pathophysiological loading of cardiomyocytes leads to increased production of reactive oxygen species [14]. Biochemical changes in cardiomyocytes may also contribute to loss of contractility. Decrease in the calcium handling proteins sarcoendoplasmic reticulum calcium transport ATPase, ryanodine receptor and L-type calcium channels, with an increase in inositol trisphosphate receptor and sodium calcium exchanger, result in a shift to a less mature phenotype [8]. Myocyte coupling may also be reduced by shifts in connexin 43 expression to the predominantly atrial connexin 40 [8]. The remainder of this work will focus on changes in extracellular matrix composition and biomechanical signaling in the myocardium.

3.1.2.1 Extracellular Matrix Remodeling

Ventricular remodeling was originally defined as global changes in the size and shape of the ventricle [11]. While this remains true from an organ-level perspective, remodeling also occurs at a sub-tissue level with changes in the extracellular matrix (ECM), cells and

local mechanical properties. As the myocardium is heterogeneous, the changes discussed here are likely to be region specific.

Initially after MI in the rat, increased expression and activity of cathepsins, matrix metalloproteinases and tissue inhbitors of matrix metalloproteinases induces early changes in matrix remodeling [15]. There is an initial decrease in collagen content and organization [8]. The controlled degradation of ECM leads to cardiomyocyte slippage and reduced stiffness of the myocardium. This process also generates ECM fragments that act as signaling moieties, contributing to the immune response and directing differentiation of fibroblast into myofibroblasts [8, 10]. Fibroblasts and myofibroblasts are largely responsible for matrix deposition in the myocardium [6, 16]. The ECM is responsible for surrounding cells to organize and orient them, provide mechanical support, allow for transfer of mechanical forces and to protect cells from over-stretching [8, 15]. In the healthy myocardium, cECM is composed of collagen I, collagen III, fibronectin, laminin, collagen IV, elastin and proteoglycans [8]. Under physiological conditions collagen turnover in the myocardium is 5-9%, greater than in other tissues [17, 18]. In adults, 85% of collagen in the heart is collagen I, thick fibers providing strength, and 11% is collagen III, thin resilient fibers [19]. Post-MI, fibronectin is the first matrix protein to be deposited [12, 20]. This is followed by pathophysiologic collagen turnover in the myocardium, which can be as high as 50% [18]. Full scar formation includes the accumulation of fibronectin and collagens I and III, with an increase in the ratio of collagen I to collagen III content [8, 19, 21]. In remote regions of the myocardium, reactive fibrosis occurs in response to increased wall stress. An increase in thin collagen fibers decreases the compliances of the remote myocardium and limits oxygen diffusion [6].

In addition to changes in ECM content post-MI the organization of ECM components is also altered [16]. Collagen fibers post-MI, due to changes in mechanical loading, tend to be larger in diameter and are more crosslinked [6, 8, 12, 22]. Assembly and organization of collagen fibrils is likely influenced by matricellular proteins such as secreted protein acidic and rich in cysteine. Secreted protein acidic and rich in cysteine (SPARC) levels are highest in development and after injury, tracking with collagen expression and SPARC null mice have fewer collagen fibrils [23]. Additionally, an increase in proteoglycans and glycoproteins, such as tenascin-C, osteopontin and hyaluronan, is observed post-MI [21, 24, 25]. Proteoglycans are less studied in the myocardium and regulated by their own processes. However, they may play a role in regulating folding, organization, degradation and activity of structural ECM components and have been shown to influence the outcome in cardiac disease studies [25]. Cells are reactive to changes ECM remodeling as demonstrated by a global increase in integrin alpha1, alpha3 and alpha5 subunits post-MI [20].

3.1.2.2 Altered Biomechanics

It is difficult to measure local forces in the myocardial wall in vivo. Therefore, biomechanics of the myocardium are typically discusses as tissue stress or strain measurements. These parameters are also dependent on location within the myocardium and active stress changes through the cardiac cycle. Rodent models are used for more invasive studies and will differ from human tissue. In rats, the elastic modulus of a healthy left ventricle is 18 kPa. This increases to 55 kPa post-MI [26]. Similar results were obtained in mice, but with further stiffening over time to 90 kPa in the infarct region [27]. Maximal in vivo active stresses for the healthy myocardium are 70-110 kPa in a canine model and 180 in humans during the cardiac cycle [28, 29]. In patients with pressure overload, the active wall stress doubles [29]. One study in decellularized murine myocardium evaluated local mechanical properties by atomic force microscopy. Andreu

et al. demonstrated that healthy myocardium is mechanically heterogeneous. Infarcted myocardium, while three-fold stiffer still displayed heterogeneity [30]. Interestingly, this study also demonstrated that ECM experiences stresses about 4-fold higher than stresses on cells, suggesting that ECM bears the load in the heart. Cells would experience higher stresses at the cell-ECM interface than internally [30]. Global strain in healthy myocardium of humans is 18% as demonstrated by echocardiography [31, 32]. This decreases to 7% post-MI [31]. Strain of the myocardium is also inversely proportional to wall motion score and decreases with cardiac dysfunction [32].

3.1.3 Current Therapies for Myocardial Infarction

Aside from heart transplantation a number of palliative therapies are available for MI treatment. These therapies come in the form of surgical intervention, pharmacological agents and mechanical support from a left ventricular assist device. Surgical intervention, such as coronary angioplasty and the placement of a stent, restore blood flow to the damaged myocardium [12]. Thrombolytics are also used to remove arterial occlusions. Early reperfusion is considered one of the most important interventions to prevent infarct expansion and negative myocardial remodeling [11]. Pharmacological agents include angiotensin-converting-enzyme inhibitors, angiotensin receptor blockers and beta-adrenergic blockers. Each of these has been shown to reduce mortality in clinical trials [3]. Angiotensin-converting-enzyme inhibitors and angiotensin receptor blockers target angiotensin II signaling, while the mechanisms of action for beta-adrenergic blockers are not fully understood. When given early, angiotensin-converting-enzyme inhibitors, in addition to improved survival, have been shown to improve contractility of the heart, as well as stroke volume and ejection fraction. They may work through a combination of mechanisms including peripheral vasodilation, myocyte unloading and reduced myocyte hypertrophy [12]. Left ventricular assist devises are typically reserved for patients with late-stage heart failure and are considered a bridge to

transplantation. The device aids the heart in its pump function, while also alleviating mechanical loads. Implantation is invasive and success of the device is limited by risks of bleeding, infection, thrombosis and mechanical failure. However they lead to increases in patient survival and improve quality of life [3]. In addition to the currently available therapies, at least one clinical trial is underway assessing gene therapy for MI treatment. The Calcium Up-regulation by Percutaneous Administration of Gene Therapy in Cardiac Disease (CUPID) trial uses an adeno-associated virus to deliver sarcoendoplasmic reticulum calcium transport ATPase to the myocardium of heart failure patients [6]. As discussed in later sections, the recent growth in the field of regenerative medicine has raised hopes for cell therapy post-MI.

3.1.4 Endogenous Myocardial Regeneration

As cell therapy attempts are being considered for regeneration of the myocardium, the endogenous regenerative capacity of the myocardium is often questioned. For several decades, adult myocytes, and they myocardium as a whole, were considered to be post-mitotic. However, since the turn of the century, this notion has been questioned. Estimated rates of cardiomyocyte turnover in the normal adult mammalian heart range from <0.1% to 40%, with the consensus falling around 1% [33-35]. A large part of this discrepancy is due to the methods used to calculate turnover. Carbon-14 dating shows that about half of all human cardiomyocytes are replaced in a lifetime [35]. The field generally accepts that this level of regeneration is insufficient to repair a heart after infarct and merely supports maintenance due to aging and normal "wear and tear" of the myocardium. There is also unanimity that the regenerative capacity of the myocardium declines with age [6, 33-35]. Myocyte regeneration is increased after cardiac injury [7]. However the source of newly generated myocytes remains somewhat controversial and the pool of new cardiomyocytes is likely due to the contributions of circulating progenitors, division of existing myocytes and resident stem/progenitor cells [34]. A

study transplanted infarcted ventricular tissue into an immunodeficient mouse, eliminating the bone marrow as a potential cell source for regeneration, and showed induction of c-kit and cardiogenic differentiation within the transplant [36]. In this study, c-kit cells from young mice adopted myogenic and vascular fates, whereas only vascular fates were induced in older mice. Unfortunately, endogenous contributions are still insufficient to repair the myocardium after significant injury [6, 37]. Evolutionarily, resident stem/progenitor cells may not have evolved for rapid tissue regeneration after injury [37]. Efforts are being made to better understand stem cell niches and the roles they play in homeostasis and repair [38]. For example, microenvironmental stresses such as hypoxia, led to activation of endogenous stem/progenitor cells [34]. Further work is necessary to determine how to best activate, improve and harness the endogenous regenerative capacity of these cells.

3.1.5 Development of the Myocardium

Regenerative medicine can take many cues from the studies of developmental biology [39]. Toward this end, evaluating the ECM and biomechanics of the young myocardium may provide insight into the ideal microenvironments for myocardial regeneration post-MI. In animal models, myocardial collagen accumulation begins in the embryo and continues after birth. A study comparing the ECM composition of rat myocardium at different developmental ages showed that fibronectin was the most abundant protein in fetal and neonatal cardiac ECM, accounting for a fifth of all protein. Fetal and neonatal hearts also contained significant amounts of fibrillin-1, perlecan and collagen I, with periostin detected only in fetal ECM [40]. A separate study showed increasing collagen I, collagen III and laminin with increasing age of rat myocardium; while fibronectin and periostin decreased and collagen IV levels remained unchanged [41]. Fibronectin and collagen expression are often observed in parallel, with fibronectin being deposited temporally just before collagen, and are more present in development and after injury

than in the adult myocardium [42, 43]. Fibronectin plays many roles in development, including regulating cell growth, integration, adhesion, cytoskeletal organization and morphogenesis [20, 44]. While in a less relevant animal model, drosphilia, laminin has also been shown to be essential for heart development [45].

In addition to a unique ECM composition, biomechanical forces are important during development. Cell tension may contribute to sorting progenitor cells and organizing germ layers in the zebrafish embryo and altering fluid forces in the developing myocardium has been linked to congenital heart disease [46, 47]. Stiffness of the fetal and neonatal rat myocardium is 5-10 kPa, where in the same studies the adult rat myocardium was observed to be about double, at 20-25 kPa [41, 48]. By both ultrasound and velocity vector imaging, global left ventricular strains in healthy human fetuses are 17%, with regional variability [49, 50]. This strain matches that observed in the adult myocardium as discussed above.

3.1.6 Cell Therapy for Myocardial Infarction

Cell therapy for regeneration is the transplantation of an expanded pool of cells into the injured host tissue. Current clinical trials that aim to regenerate the myocardium post-MI through cell therapy aim to replace the lost myocytes [34]. A number of cell types have been examined for their potential to regenerate the myocardium as reviewed by Mohsin et al. and discussed below [37]. Irrespective of cell type, cell therapy remains limited by the survival, proliferation and engraftment of transplanted cells. In addition to cell source, the ideal delivery time, method and dosage have yet to be identified. The delivery of cells alone may prove insufficient and many ongoing studies pair a biomaterial with cells to improve their successful transplantation and regeneration of host tissue.

Skeletal myoblasts were one of the first cell types evaluated for myocardial regeneration. The Myoblast Autologous Grafting in Ischemic Cardiomyopathy (MAGIC) trial while unsuccessful was an important step and lesson for cell therapy [51]. The trial was unable to show a significant improvement in heart function and increased the risk of arrhythmia in patients. Adult bone marrow-derived stem cells, or mesenchymal stem cells, are the most clinically evaluated cell type for myocardial regeneration. Meta-analysis of these trials shows that the therapy is safe and beneficial over standard treatments, with decreases in infarct size and end systolic volume and increases in ejection fraction [3]. Mesenchymal stem cell injection into the infarcted myocardium in animal models and clinical trials (i.e. POSEIDON, comparing autologous and allogenic cells) results in decreased fibrosis and improvement in certain heart function parameters [26, 52]. Other authors point out that these effects are sometimes small and short-lived [37]. The mechanism of action surrounding these cells, and all of cell therapy, is debated and improvements are attributed to paracrine signaling and increased angiogenesis and not reconstitution of the myocardium [2, 53, 54]. Additionally, in a mouse model the injection of and unpurified population of mesenchymal stem cells led to calcification in the myocardium, underscoring the importance of choosing an optimal cell type [55].

In addition to mesenchymal stem cells, several other stem/progenitor cell types have entered the arena of cell therapy for myocardial regeneration. Embryonic stem cells are able to improve cardiac function post-MI in animal models, but have not yet entered clinical trials due to ethical concerns and risks of immune rejection or teratoma formation [37, 56, 57]. Induced pluripotent stem cells are also considered to be an unsafe cell type at this time due to their potential to form teratomas and risks of somatic coding mutations or incomplete reprogramming [37]. Several stem or progenitor cells types endogenous to the adult myocardium have been identified, although the distinctions between these populations are blurry at this time and many of these populations are likely related or

overlapping based on their biological markers [34, 58]. As these populations are restricted to the cardiac lineages, they may prove safer than cells of a more pluripotent state and are being considered for regeneration of the myocardium. Cardiac stem/progenitor cells that express the receptor c-kit have been identified in mice, rats, dogs and humans [59-63] and will be discussed in more detail in Aim I. Intramyocardial injections of these cells have shown improvements in cardiac function after injury [60, 61, 64]. Cardiospheres have been formed from cells isolated from mice and human myocardium [65]. Cells within the cardiospheres express c-kit, hematopoietic progenitor cell antigen CD34 and sca-1. These cells originate from a single clone and are a mixture of stem, progenitor and differentiated cells. Mouse, but not human, cardiospheres beat spontaneously [65]. Cardiosphere-derived cells are acquired by plating cardiospheres on fibronectin coated dishes [66]. The phase I clinical trial Cardiosphere-derived autologous stem cells to Reverse Ventricular Dysfunction (CADUCEUS) reported few adverse events, observed a reduction in scar mass and increase in viable myocardium. However, improvements in functional cardiac parameters were not seen [67]. A separate phase I clinical trial, Stem Cell Infusion in Patients with Ischemic Cardiomyopathy (SCIPIO), evaluated the safety of cell therapy with c-kit positive cardiac progenitor cells. Left ventricular ejection fraction in treated patients increased from 30% before infusion to 42.5% at one year. A decrease in infarct size was also observed and no adverse events were reported [68]. CADUCEUS and SCIPIO included patients with similar ejection fractions, but differed in the average age of infarct, time until delivery of cells and dose of cells delivered. These studies are further reviewed by Xie et al. [3].

Cell therapy requires removing cells from their native environment, propagating them in a laboratory setting and introducing them into a new environment [69]. Injectable biomaterials have the potential to be attractive cell delivery vehicles as they can provide a suitable microenvironment and can potentially be delivered via minimally invasive

catheters [70]. Cellular therapies have been combined with various matrices and hydrogels to treat MI and are too numerous to review here [71-77]. Another advantage to the combined use of cells and biomaterial is the structural support and unloading provided to the myocardium by hydrogels [78]. The major disadvantage of the currently used biomaterials for myocardial regeneration is that they lack the complexity and specificity of the native myocardial extracellular matrix [79].

3.2 Microenvironmental Stimulation

3.2.1 Biochemical Signals

An early indication that cell-matrix interaction was cell type specific was the variable binding of myocytes of different developmental states to ECM components. Neonatal cardiomycoytes adhere rapidly to fibronectin, laminin and collagen IV. To a lesser degree, neonatal cells also adhere to fibrilar collagens. This was in contrast to adult cardiomyocytes which adhere strongly to laminin and collagen IV, but only weakly to fibronectin and not at all to fibrilar collagens [80]. Collagen IV supports culture of neonatal rat ventricular myocytes better than laminin over two weeks [81]. These results suggest that cells are influenced by their surrounding ECM and that the ideal microenvironment of a cell varies with developmental state.

Stem cells in the body exist in niches, a unique environment composed of basement membrane proteins and supporting cells that secrete soluble factors and provide cell-cell contact [69, 82]. Once activated, these cells migrate from the niches into somatic tissue and mature into adult phenotype. Their microenvironment inside and later outside the niche directs their behavior. Maturation of neonatal rat cardiomyocytes is likely matrix-dependent, as the degree of spreading varies with matrix protein with the greatest spreading observed on fibronectin [83]. Furthermore cardiomyocyte adhesion to fibronectin, as compared to collagen I, stimulates higher expression of n-cadherin and

connexin 43, suggesting maturation [84]. Culture of embryonic stem cells with laminin or collagen I did not induce their differentiation. However, when cultured with a complex, naturally-derived ECM Matrigel the embryonic stem cells adopted a mesenchymal stem cell phenotype or formed epithelial-like structures. These effects were ECM specific as decellularized cartilage (Cartrigel) produce cartilage-like nodules from embryonic stem cells [85]. In a separate study, collagen IV and laminin were both shown to increase the expression of the endothelial marker fetal liver kinase 1 in embryonic stem cells, whereas expression of the cardiomyocyte marker alpha myosin heavy chain was induced on fibronectin [86]. The differentiation of embryoid bodies cultured in a three-dimensional environment, was matrix specific. Fibronectin induced formation of endothelial-like structures, whereas laminin induced spontaneous beating [87]. In addition to structural ECM proteins, matricellular proteins regulate cell-ECM interaction such as adhesion, signaling, proliferation, migration and survival [88].

While numerous studies evaluate differentiation of stem cells through soluble signals, it is beyond the scope of this work, except where those factors interact with the cellular microenvironment. Stem cells release cytokines during differentiation and proliferation. These may contribute to distant or neighboring paracrine signaling as well as autocrine regulation to increase their maturation [89]. ECM components have growth factor binding sites that position soluble growth factors near cells [90]. Laminin and fibronectin have known growth factor binding sites [90]. Indeed, in order to stimulate proliferation of human vascular endothelial cells co-activation of integrins and vascular endothelial growth factor (VEGF) is required [91]. Fibronectin may bind as many as 20 distinct growth factors [89]. The binding of growth factors to ECM may be interrupted by mechanical strain. Mechanical strain applied to ECM proteins can also expose cryptic binding sites for growth factors or adhesion molecules [90]. It is unclear if the matrix is acting as a scaffold to capture soluble growth factors and present them to the cells, or

sequestering soluble cells from binding receptors. This is likely dependent on the matrix protein and growth factor combination, increasing the complexity.

3.2.2 Biophysical Signals

Cells present in the myocardium experience a range of mechanical forces from the binding of individual integrins to their ligands (pN) to the active contraction of the myocardium (N) [92-96]. Additionally, physical cues such as extracellular matrix organization, topology and stiffness contribute to the biophysical aspects of the microenvironment and effect cell behavior. As discussed below, these signal direct differentiation and maturation of stem cells, whereas in adult cells they dictate function. In part, these responses are due to altered tension in the plasma membrane and cytoskeleton [97].

Myocyte form and function is dependent on substrate stiffness. On soft (1 kPa) substrates, neonatal rat ventricular myocytes (NRVM) have poorly defined striations. On substrates of intermediate stiffness and mimicking the stiffness of healthy myocardium (10 kPa), NRVM have nicely defined striations. On stiffer substrates mimicking infarct stiffness (50 kPa) the striations are unaligned and long stress fibers are observed [98]. Embryonic stem cell-derived cardiomyocytes demonstrate increased spreading and stress fiber formation with increasing substrate stiffness. In addition to cell spreading, substrate stiffness also dictated how well the NRVM were able to elongate, with the highest aspect ratio observed on substrates of 50 kPa [48]. The number of beating NRVM and the contraction force they generate is also dependent on substrate stiffness [48, 99]. Culturing quail chick embryonic cardiomyocytes at infarct stiffnesses prevented their contraction, which was restored at stiffnesses mimicking the healthy myocardium [100]. Contractility was dependent on cell spreading and myofibril structure. Furthermore, changes in contractility that are modulated by substrate stiffness and nanotopography can

direct differentiation of stem cells [89]. However, cells may actually be interpreting stiffness as ligand density [101]. In a landmark study, mesenchymal stem cells (MSCs) were seeded on collagen-coated polyacrylamide gels of increasing stiffness that mimicked various tissues. When cultured in the appropriate media, lineage commitment was stiffness dependent: soft for neurogenesis (<1 kPa), intermediate for myogenesis (13 kPa) and stiff for osteogenesis (32 kPa) [102]. In following studies, stiffness did not affect attachment of embryonic stem cells, but increases from 41 kPa to 3 MPa led to increased proliferation and early mesendoderm differentiation [103]. Mouse embryoid bodies cultured on tissue-culture polystyrene increased troponin T expression; however more beating cells were observed on softer (12 kPa) polydimethylsiloxane substrates [104]. The authors also observed that rigidity could control whether stem cells mature into atrial or ventricular-like myocytes. Studies in mesenchymal stem cells demonstrate that long-term culture of cells on stiff substrate can lead to irreversible changes [105].

Cell spreading and shape is dependent on substrate stiffness and ligand density. Cells spread more on stiffer substrates and increasing the ligand density on soft substrates is insufficient to induce spreading [97]. MSC differentiation can be controlled by micropatterning. Culturing MSCs on small islands, maintaining a rounded phenotype, induces adipogenesis. Conversely, osteogenesis occurs in MSC seeded on larger patterns that allowed for spreading. These results were dependent on changes in cytoskeletal structure [106]. More relevant to myogenesis, patterning of surfaces induced durotaxis, alignment and fusion of adipose-derived stem cells into myotubes [107]. In a separate study, micropatterning induced MSC elongation and alignment, leading to increased cardiomyogenic gene expression [108]. Alignment of MSCs is sufficient to induce connexin 43 expression, a cardiomyocyte marker [109]. Similar effects were observed for NRVM cultured on micropatterned strips. The cells aligned and elongated dependent on strip width. Alignment induced end-to-end expression of N-cadherin and connexin 43

[110]. Additionally, alignment of NRVM alters the expression and activity of their ion channels, potentially leading to the functional changes observed on varying substrate stiffnesses [111].

In addition to these passive physical signals, the active beating of the heart exposes the myocardium to cyclic strain. All major cardiac cell types elongate and align perpendicular to an applied strain [112]. However, the effect of strain varies by cell type, the strain regimen (magnitude, frequency and duration) and culture conditions [113]. Within minutes of applied strain cells begin to remodel their cytoskeleton [114]. Cytoskeletal stiffness increases proportional to applied stress [115]. After the removal of mechanical strain, cytoskeletal tension drops below baseline, with more drastic effects for larger strains. Mechanical strain induces anisotropic increases in cytoskeletal tension in the direction of the long axis of the cell [116]. As discussed below, mechanical strain regulates proliferation, hypertrophy, differentiation and paracrine signaling in part through cytoskeletal changes.

Cyclic mechanical strain of embryonic chick cardiomyocytes induced proliferation, with a demonstrated activation of p38MAPK and Akt [117, 118]. Proliferation of non-cardiomyocytes was not increased. Strain also increased proliferation of MSCs [119]. In this study, MSCs were seeded on micro-patterned surfaces in line with the direction of strain, which reduced their reorganization and alignment perpendicular to strain. This suggests that surface topography might be more influential on cell phenotype than tensile strain. In the myocardium strains are anisotropic and biaxial with the primary axis of strain in line with cells [120, 121]. This is in contrast to in vitro strain experiments where cells tend to align perpendicular to the primary axis of strain. By aligning NRVM on micropatterned surfaces, the effect of strain direction on phenotype is evaluated. Transverse strain resulted in loss of striations and expression of hypertrophic factors

[122]. This response is typical of adult cardiomyocytes, which increase in size and resort to increases in embryonic gene program under stress [123, 124]. Strain also dictates calcium dynamics. In isolated rabbit sinoatrial node cells, stretch increased spontaneous beating, potentially through activation of stretch-mediated ion channels [124].

Straining NRVM lead to a more mature phenotype as demonstrated by increases in mechanical junction proteins plakoglobin, desmoplakin and N-cadherin [125]. Strain of embryoid bodies resulted in increased angiogenesis or cardiogenesis depending on strain magnitude [126]. These effects were mediated by reactive oxygen species, which may contribute to changes in cytoskeletal tension and the calcium sensitivity of myofibrils. In MSCs, higher strain magnitudes paired with grooved micropatterns induced smooth muscle cell differentiation. Conversely, at lower strains on flat surfaces osteoblast differentiation was induced [119]. Strain induced alignment of human cardiosphere-derived cells perpendicular to the direction of strain and increased the expression of cardiac troponin I [127]. Furthermore, strain induced secretion of vascular endothelial growth factor, basic fibroblast growth factor and interleukins -6 and 1b. No changes in insulin-like growth factor, hepatocyte growth factor, stromal cell-derived factor or transforming growth factor beta were observed. Strain of NRVM also induced vascular endothelial growth factor secretion [125]. In adult cardiomyocytes, strain induced release of transforming growth factor beta, angiotensin II and other factors involved in hypertrophy [128, 129].

Our understanding of the role that mechanical forces play in cell proliferation, maturation and survival, has led to improved tissue engineering strategies. Mechanical strain was applied to tissue engineered grafts constructed of gelfoam and a mixed population of human pediatric cardiac cells [130]. Strain doubled the number of cells and improved migration of cells into the scaffold. Increased ECM deposition was also observed. In

addition to the effects that mechanical strain has directly on cells, stretch of a three-dimensional construct may alter pore size and diffusion through the scaffold. Similarly, mechanical strain was applied to constructs of human embryonic stem cell-derived cardiomyocytes on gelatin scaffolds. Strained constructs showed greater cell elongation and cardiac troponin T, L-type calcium channel and connexin 43 expression. Implantation of the constructs into a rat heart showed improved cell survival and recruitment as compared to static controls [131]. As survival and engraftment of cells transplanted to the myocardium is a hurdle, Kurazumi et al. evaluated the effects of haemodynamic unloading on stem cell engraftment through a heterotopic cardiac transplantation mouse model. They observed a significant improvement in the survival and proliferation of the delivered stem cells [132]. In comparison, 50% of injected cells were lost in haemodynamically loaded hearts within three days. Loading also had an effect on differentiation as higher levels of smooth-muscle actin were observed in loaded cells as compared to higher levels of sarcomeric alpha actin in cells in unloaded hearts.

3.2.3 Combined Biochemical and Biophysical Signals

In the tissue microenvironment, a number of cues are provided simultaneously. It is difficult to distinguish between signals such as stiffness and ligand density, cell shape or ligand identity, as they are inextricably linked. In order to better recapitulate the microenvironment and direct cell behavior an increasing number of studies evaluate multiple cues simultaneously. Although this combinatorial approach sacrifices the understanding of the effect of specific cues, it is more biomimetic.

To evaluate the combined effect of substrate stiffness and matrix coating, human MSCs were grown on substrates with stiffness's ranging from 25-80 kPa and coated with collagen I, collagen IV, fibronectin or laminin. The cells were more rounded on softer substrates and spindly in shape when cultured on laminin. Proliferation appeared to be

dependent only on stiffness, while myoD1 gene expression increased on 25 kPa fibronectin gels and 80 kPa collagen gels indicating maturation may require an integration of signaling cues [133]. In a similar study, the authors recreated cardiac microenvironments with various decellularized cardiac ECMs covalently attached to polyacrylamide gels with stiffness to match various stages of the myocardium, 9 kPa (fetal), 25 kPa (neonatal and adult), 49 kPa (infarcted adult). MSC spreading on these gels was dependent only on stiffness. However the traction forces generated by the cells were dependent on the stiffness and the developmental stage of the ECM. Maximal traction forces were observed on neonatal and adult ECM at low stiffness and were maintained with increasing stiffness. However, on fetal ECM, MSCs generated higher traction forces with increasing stiffness. Differentiation was also stiffness and ECM dependent. On fetal ECM, increasing substrate stiffness reduced Nkx2.5 expression; however Nkx2.5 expression was increased with stiffness on neonatal and adult ECM [41]. Cell shape in combination with matrix protein also dictates MSC fate [134]. MSCs seeded on small round micropatterns had a tendency to adopt an adipogenic fate dependent on the matrix protein present, whereas spread cells always adopted a neurogenic fate.

Similar studies have evaluated the application of mechanical force in combination with matrix components or soluble factors. MSC were cultured on collagen I or laminin and strained 10%. While similar degrees of cell spreading were observed for all conditions, myogenic gene expression decreased in MSC cultured on collagen. Secretion of growth factors and inflammatory cytokines was also lower on collagen than laminin. Overall, the authors concluded that MSC are more sensitive to matrix than mechanical strain [135]. In contrast, smooth muscle cells and cardiac fibroblast exhibit integrin-dependent matrix specific effects of static strain [136]. Culture of MSCs on aligned nanofibers increased their proliferation more than mechanical loading. Aligned nanofibers and

mechanical loading both induced cell alignment, but MSC differentiation required the input of both signals [137]. In addition to matrix composition and mechanical stretch, two studies also evaluated the role of soluble factors on MSC differentiation and showed interaction between the treatments [138, 139]. Taken together, these studies demonstrate the complexity of cell response to signals in the microenvironment.

3.3 Mechanotransduction

Mechanotransduction is the activation of a biochemical signaling cascade opposite the cell membrane from the occurrence of a mechanical event and the integration of these signals into a cellular response. [47, 113, 140-143]. Cells sense nano- and micro-scale topographies, geometric cues and stiffness of their environments by pulling on their surroundings [113, 144]. In addition to ligand identity, the presentation of extracellular signals through spacing, density and stiffness integrate into the signal received by the cell [90, 145, 146]. These signals, mediated by attachment and intracellular changes, integrate across force and length scales to influence cell behavior such as migration, survival, proliferation and differentiation [47, 113, 145, 147, 148]. Initial cellular responses to the microenvironment occur within seconds to minutes and increase over time through feedback mechanisms [148]. Furthermore, many intracellular signaling pathways interact to produce a given functional outcome. These effects are cell type specific and change with developmental state and disease [149]. Complete mechanisms of how cells sense their microenvironment remain elusive, but integrins, as discussed below, play an important role.

Mechanotransduction is bidirectional and occurs largely through integrins, transmembrane heterodimeric proteins composed of an alpha and beta subunit [142, 150]. Integrins bind specific extracellular matrix proteins, depending on the combination of the alpha and beta subunit present [142]. Adult cardiomyocytes express the alpha1, alpha3,

alpha5, alpha6, alpha7, alpha9 and alpha10 integrin subunits along with the beta1, beta3 and beta5 subunits [124, 151]. Integrin expression on cardiomyocytes varies with developmental and disease state, but the beta1 subunit is almost ubiquitously expressed [152]. Specifically, alpha1 and alpha5 are expressed in embryonic cardiomyocytes, are downregulated postnatally and upregulated by mechanical load, mimicking disease [124]. While integrin heterodimers are known to preferentially bind to a single matrix protein, the binding kinetics of integrins and their competition for binding site on ECM may contribute to mechanotransduction [149]. Additionally, sub-cellular localization of integrins through clustering affects their activity [153].

The beta1 integrin subunit is one of the most well studied in the myocardium. The beta1 integrin contributes to regulation of the cell cycle in cardiomyocytes in development and hypertrophy in disease [154, 155]. In NRVM, overexpression of the beta1 integrin increased cell size and markers of hypertrophy [151, 156]. The effects were reduced in cells that overexpressed the free cytoplasmic domain of the integrin. In mice, adult cardiac knockout of the beta1 integrin did not alter basal function. However, when the mice where challenged with transverse aortic constriction, hypertrophy of myocytes was reduced [157]. In a model of development, embryonic stem cells lacking the beta1 integrin have impaired cardiomyogenic differentiation. Knockout mice were viable, but had defective cardiomyocyte maturation [158]. Additionally, integrins likely play a role in the proliferation of cardiosphere-derived stem cells [159]. Rounded cells had lower integrin expression, but higher c-kit expression. This was reversed as the cells spread.

Forces at the cell-ECM interface are heterogeneous as attachment occurs through integrins, which cluster in response to mechanical stimuli [47]. This leads to the formation of focal adhesions and focal complexes that increase in size with increasing mechanical stimuli [128, 144, 145, 160, 161]. Focal adhesions form around the

cytoplasmic domain of integrins and are composed of focal adhesion kinase (FAK), talin, paxillin, vinculin, Src, and potentially as many as 200 additional proteins [47, 89, 102, 140, 162]. The role of FAK in mechanotransduction is not fully understood [89]. FAK has multiple phosphorylation sites (Y397, Y576, Y577, Y861 and Y925) that contribute to its activity when phosphorylated [162, 163]. Binding of FAK to the cytoplasmic domain of integrins induces phosphorylation at Y397, potentially through scaffolding kinases in the focal adhesion [162]. Activation of FAK can lead to downstream signaling through phosphoinositide 3-kinase, mitogen-activated protein kinase, RhoA, Rho-associated coiled-coil containing protein kinase 1, extracellular signal-regulated kinase, and c-Jun N-terminal kinases [98, 162-166]. In addition to signaling cascades that are activated by phosphorylation events, mechanotransduction may occur through exposure of cryptic peptide sites, conformational changes that alter enzyme activity, altering state of ion channels, altered bond strengthening or dissociation of binding partners [89, 148].

In addition to these traditional views of mechanotransduction, the theory of cellular tensegrity considers the cell to be a mechanical unit rather than a biochemical unit [145]. FAK is tethered to the actin cytoskeleton [145, 162]. This allows for the propagation of force from adhesions to the nucleus. Changes in nuclear shape may alter the transcriptional state of chromatin, facilitating transcription [89, 145]. In theory, mechanically transmitted signals would propagate faster than diffusion based biochemical signals. However, as mechanotransduction is complex, a cell likely integrates biochemically and mechanically transduced signals. In regards to transcription, FAK can translocate from focal adhesions to the nucleus, where it acts as a transcription co-regulator with Gata-4 [145]. Additionally, mechanical stretch regulates the expression and localization of chromatin remodeling enzymes called tension-induced proteins [113].

CHAPTER 4 Naturally-Derived Cardiac Extracellular Matrix Enhances Cardiac Progenitor Cell Behavior in Vitro

Myocardial infarction (MI) produces a collagen scar, altering the local microenvironment and impeding cardiac function. Cell therapy is a promising therapeutic option to replace the billions of myocytes lost following MI. Despite early successes, chronic function remains impaired and is likely a result of poor cellular retention, proliferation, and differentiation/maturation. While some efforts to deliver cells with scaffolds attempt to address these shortcomings, they lack the natural cues required for optimal cell function. The goal of this study was to determine whether a naturally-derived cardiac extracellular matrix (cECM) could enhance cardiac progenitor cell (CPC) function in vitro. CPCs were isolated via magnetic sorting of c-kit+ cells and were grown on plates coated with either cECM or collagen I (COL). Our results show an increase in early cardiomyocyte markers on cECM compared to COL, as well as corresponding protein expression later. CPCs show stronger serum-induced proliferation on cECM as compared to COL, as well as increased resistance to apoptosis following serum-starvation. Finally, a microfluidic adhesion assay demonstrated stronger adhesion of CPCs to cECM compared with COL. These data suggest that cECM may be optimal for CPC therapeutic delivery, as well as provide potential mechanisms for the shortcomings in naked cell therapy.

4.1 Introduction

4.1.1 Cardiac Progenitor Cells

Cardiac stem/progenitor cells that express the receptor c-kit have been identified in mice, rats, dogs and humans [59-63]. Previous work indicates that isolated populations of cardiac stem cells, while being >90% positive for c-kit and negative for markers of myeloid, lymphoid and erythroid lineages, do not express alpha-sarcomeric actin, cardiac myosin, desmin, alpha-cardiac actinin, connexin 43, von Willebrand factor, platelet

endothelial cell adhesion molecule, vimentin, alpha-smooth muscle actin and only 7-10% express Nkx2.5, Gata-4 or MEF2C [60]. This is distinct from cells isolated and cloned in our laboratory, which are >90% positive for c-kit and negative for haematopoetic markers, but also express significant levels of Nkx2.5, Gata-4 and platelet endothelial cell adhesion molecule [unpublished data and [167]][2]. Thus we refer to our cells as cardiac progenitor cells (CPCs) instead of cardiac stem cells, but will use the notation CPC throughout this work for all c-kit positive cardiac stem/progenitor cells. Characterization of CPCs isolated in our lab are shown in Figure 39. Regardless of nomenclature, c-kit has been shown to be required for the differentiation of CPCs and its dysfunction leads to increased proliferation without commitment of the cells [168, 169]. In various adult animal models, CPCs have been estimated to exist at a rate of <0.01-0.5% total cardiac cells [59, 61, 119]. The number of c-kit positive cells is higher during development, increases post-MI, but decreases with aging [59, 62]. These cells can be maintained in culture >40 passages [170]. Although lower amounts of clonogenic cells with time suggest that might commit to a lineage over long cultures.

These cells reside endogenously in niches in the myocardium [171]. The niches are distributed throughout both ventricular and atrial myocardium, but more exist in regions of lower wall strain, such as the atria and ventricular apex [60, 64]. While not completely characterized, these niches have been shown to contain the matrix components laminin and fibronectin [62, 63]. Additionally, further work is needed to identify factors that

---

[2] French KM and Davis ME. 2014. Isolation and Expansion of C-Kit-Positive Cardiac Progenitor Cells by Magnetic Cell Sorting. In: M Radisic and LD Black (Eds.), Cardiac Tissue Engineering: Methods and Protocols (39-50). New York: Springer.

activate CPCs to induce migration out of the niche. It is known that matrix metalloproteinases 2 and 9 are required for CPC migration and that they migrate in response to hepatocyte growth factor [61, 172]. Furthermore, when treated with hepatocyte growth factor or insulin-like growth factor, CPCs respond by releasing more of the same growth factors [61]. Insulin-like growth factor positively influences survival and proliferation of CPCs [172]. CPCs also interact with their microenvironment through integrins. While the full integrin expression profile has not been investigated, CPCs have been shown to express beta1 and alpha4 integrin subunits [63]. In culture, induction media or co-culture with cardiomyocytes can induce differentiation of CPCs [59]. Induction media is more effective for this purpose and leads to differentiation into all four cardiac cell types within 7-10 days. About 35% of these cells express myocyte markers, 25% endothelial markers, 20% smooth muscle markers and 12% fibroblast [60]. The majority of these cells are clonogenic [61]. Unfortunately, older CPCs found in heart failure patients have shorter telomeres and are less regenerative [62, 173]. Thus there is an interest in evaluating the regenerative potential of younger CPC populations [174].

As discussed earlier, CPCs are insufficient at regenerating the myocardium after an infarct and they are presumed to have evolved for maintenance of healthy tissue during aging [32]. Recent work has also questioned whether endogenous CPCs reconstitute lost myocytes [169]. With intervention, CPCs are a good candidate for repairing the myocardium due to their regenerative potential and lack of teratoma formation. Intramyocardial injections of CPCs have shown improvements in cardiac function after injury, potentially through myocardial regeneration [60, 61, 64]. In the Phase I safety trial SCIPIO, 2 million CPCs were delivered through intracoronary infusion about 4 months after coronary artery bypass grafting surgery in patients with aged infarcts [68]. There were no adverse effects to CPC infusion. A year after cell infusion, increases in ejection fraction and reduction in scar mass were observed. Although these

improvements are positive, treated patients still had an average ejection fraction of 43%, indicative of heart failure and leaving room for improvement.

4.1.2 Naturally-derived Cardiac Extracellular Matrix

Decellularized ventricular myocardium was digested to generate a naturally-derived cardiac extracellular matrix (cECM) [175-177]. When isolated from porcine left ventricular tissue, cECM is free of cellular debris and contains collagens I-VI, elastin, fibrinogen, fibronectin, laminin, fibrilin-1, lumican, fibulin-3 and -5. Its matrix composition is unique from porcine skeletal muscle [176]. Additionally, cECM has a glycosaminoglycan content of 23 ug/mg [175]. When gelled at concentrations of 6 mg/mL, nanofibers of 40-100 nm in diameter were observed [175]. Because it is digested rather than in a patch form, it can be used as an injectable hydrogel that self-assembles into a porous and fibrous scaffold in vivo, opening up the possibility for minimally invasive delivery [175, 178, 179]. When injected into the rat myocardium, cECM has shown an immune response comparable to implanted decellularized small intestine submucosa and syngeneic muscle implants [178]. Moreover, there were more surviving myocytes in matrix-injected hearts and presence of troponin, Ki67 double-positive cells and low numbers of c-kit positive cells were observed, suggesting cECM may support myocardial regeneration. The material also supports NRVM culture and the migration of endothelial and smooth muscle cells [175]. Human embryonic stem cell-derived cardiomyocytes showed improved multi-cellular organization in long-term cultures on cECM as compared to gelatin [176]. As a potentially autologous source for decellularized matrix, human pericardial matrix was compared to porcine pericardial decellularized matrix [180]. Pericardial matrix has a higher glycosaminoglycan content and distinct matrix composition, lacking laminin and fibronectin, when compared to ventricular matrix. However, it was injectable and gelled in the myocardium, promoting neovascularization and recruitment of c-kit positive cells [180]. Human cadaveric

decellularized ventricular ECM has also been considered for therapy [177]. More than half of human cECM samples did not self-assemble, possibly due to age-related matrix changes including higher crosslinking and the deposition of adipose and fibrotic tissues. Human cECM had a similar matrix composition to porcine, but lower glycosaminoglycan content. The authors concluded that porcine cECM was superior for therapy since it is compositionally similar to human cECM, but easier to source and more consistent [177]. While not applicable to MI therapy at this time, decellularization of rat myocardium at various stages of development showed that fetal cECM better supports NRVM proliferation [40]. To optimize cell therapy it is important to evaluate the effects of matrix composition on cell behavior. Developmental stage effected protein content as a decrease in fibronectin, collagen IV and periostin, with an increase in collagens I and III and laminin was observed with increasing age. Fetal cECM had a smaller fiber diameter and less collagen organization [40].

The use of naturally derived biomaterials for MI therapy has been limited by their mechanical properties. To increase the stiffness of cECM, it can be crosslinked with glutaraldehyde [181]. This slows degradation and increases the storage modulus 25-fold, but even-crosslinked cECM is still much softer than native myocardium. Additionally, crosslinking agents should be avoided to reduce the likelihood of triggering an immune response [182]. Alternatively, cECM can be tethered to poly-(ethylene glycol) to tune its stiffness, degradation kinetics and nanofiber dimensions [183]. In a pre-clinical porcine model, cECM was injected into the border zone two weeks post-MI [184]. This timepoint is clinically relevant as it allows time to identify patients and the myocardium is less susceptible to rupture. Additionally, there are fewer matrix metalloproteinases present, contributing to longer lifetime of the material before degradation. cECM remained in the myocardium for about 1 week and was undetectable by 4 weeks. Three months post-injection, the ejection fraction of animals that received matrix was

significantly higher and both end diastolic and systolic volumes were lower. Viable muscle was detected in the cECM injected regions [184]. This study demonstrated safety and led to the initiation of clinical trials.

4.1.3 Cell Therapy

Cellular therapy has shown early success as a potential treatment for improving acute cardiac function post-MI [2, 26, 185, 186]. MSC injection into the infarcted myocardium shows decreased fibrosis and improvement in certain heart function parameters [26, 52]. While exciting, this finding was not due to reconstitution of the myocardium, but attributed to increased angiogenesis [2]. In 2003, the heart was found to have a population of stem/progenitor cells capable of cardiac differentiation, termed cardiac progenitor cells (CPCs) [60]. These cells are clonogenic, self-renewing, and capable of differentiation into the 4 major cardiac cell types (cardiomyocyte, endothelial, smooth muscle, fibroblast), [61, 64]. For these reasons, and because CPCs do not form teratomas in cell therapies, they are a good candidate for repairing the myocardium. Intramyocardial injections of CPCs have shown improvements in cardiac function after injury, potentially through myocardial regeneration [60-62, 64]. Phase 1 clinical trials are underway with injection of autologous CPCs and are promising [102]. However, while many cell therapy trials show acute success, improvements in chronic function remain a challenge. This is most likely due to the fact that local delivery of cells faces several shortcomings such as poor retention of the cells in the myocardium, reduced survival, and poor differentiation and maturation of implanted cells [187]. Due to these issues, the mechanisms by which positive effects have been seen are controversial (i.e. paracrine factors vs. regeneration) [52, 187].

Cellular phenotypes are influenced by their microenvironment. Matrix stiffness [102, 188, 189], organization [Hynes 2009], and biochemistry [87, 90, 190] have been shown

to influence cell fate. These signals are transduced intracellularly through receptor-ligand interactions, mainly integrins [191]. It is important to consider that these trends are likely to be matrix and cell type specific. By providing cells with an ideal microenvironment, it is plausible that the cells will have a more favorable outcome (i.e. improved survival, proliferation, differentiation). This is achieved either in vitro by culturing cells on a matrix or in vivo by administering cells within a matrix that can assemble into a three-dimensional scaffold. Injectable biomaterials are attractive as potential cell delivery vehicles as they can provide a suitable microenvironment and can potentially be delivered via minimally invasive catheters [70]. Cellular therapies have been combined with various matrices to treat MI [71, 73-77]. The major disadvantage of the currently used biomaterials for myocardial regeneration is that they lack the complexity and specificity of the native myocardial extracellular matrix [79].

In this study, a naturally-derived, porcine cardiac extracellular matrix (cECM) was examined for the ability to improve CPC function. Our hypothesis was centered on the fact that this would mimic the biochemical cues of a healthy myocardium, while collagen would represent both the diseased area and a commonly used cell delivery vehicle [77]. Our results demonstrate that CPCs prefer the naturally-derived cECM over collagen as measured by cardiomyogenic gene expression, cell survival, proliferation, and adhesion.

4.2 Results

4.2.1 Gene expression analysis of CPC differentiation

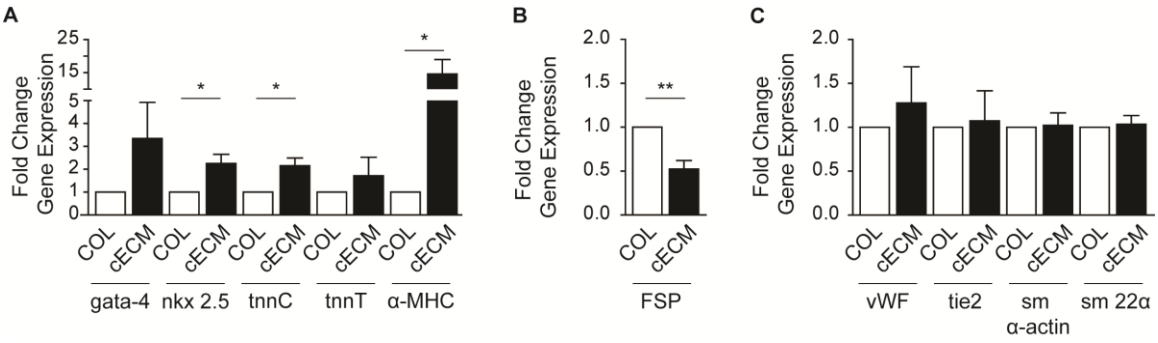

Figure 1. Cardiogenic gene expression of CPCs cultured on cECM and COL. CPCs were cultured on cECM (black bars) or COL (white bars) for 2 days and cardiomyocyte (A), fibroblast (B) and endothelial and smooth muscle (C) lineage markers evaluated by qPCR. Results were normalized to GAPDH and expressed as a fold change for cECM over COL (ΔΔCt) and reported as a mean ± SEM. Unpaired student's t-test; *p<0.05, **p<0.01, n=4-6. COL = collagen, cECM = cardiac decellularized extracellular matrix, tnn = troponin, mhc = myosin heavy chain, FSP = fibroblast specific protein, vwf = von Willebrand factor, sm = smooth muscle, GAPDH = glyceraldehyde-3-phosphate dehydrogenase.

In order to measure the effects of cECM on CPCs cardiogenic differentiation, real-time quantitative PCR was performed. CPCs were analyzed for each potential lineage: gata-4, nkx-2.5, α-myosin heavy chain (α-mhc), troponinC, troponinT (tnn; cardiomyocyte); smooth muscle (sm) α-actin, sm22α (smooth muscle); von Willbrand Factor (vwf), tie2 (endothelial); and fibroblast-specific protein 1 (FSP; fibroblast). As shown in Figure 1, culture of CPCs on cECM significantly ($p<0.05$) increased the expression of early cardiomyocyte markers, nkx-2.5 (2.3 ± 0.4-fold), α -mhc (14.6 ± 4.4-fold), and troponinC (2.4 ± 0.2-fold) as compared with cells cultured on collagen I (COL). While there was a

trend for increased gata-4 and troponinT, they did not reach significance. In addition, there was a significant decrease in the expression of the fibroblastic marker FSP (0.5 ± 0.1-fold) in cells cultured on cECM compared with COL ($p<0.01$). No significant differences were seen for the selected endothelial and smooth muscle markers. When extended to day 7, there was still no increase in smooth muscle or fibroblastic markers (data not shown). Further, to determine whether this response was tissue-specific, we examined gene expression changes in cells cultured on adipose-derived ECM as described in [192]. In contrast to cECM, there was no significant increase in any cardiac marker expression in cells cultured on adipose ECM compared with collagen (Figure 2). Additionally, the decrease seen in FSP in cells cultured on cECM was not seen in cells cultured on adipose ECM. These data suggest that cells seeded on cECM demonstrate enhanced differentiation or maturation toward the cardiac lineage and decreased maturation toward the fibroblastic lineage as compared to COL.

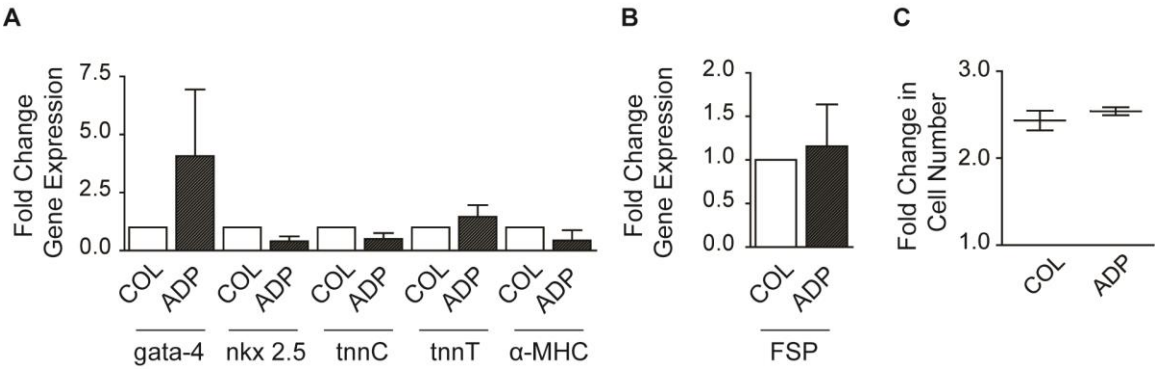

Figure 2. Cardiogenic gene expression of CPCs cultured on ADP and COL. CPCs were cultured on cECM (black bars) or COL (white bars) for 2 days and cardiomyocyte (A), fibroblast (B) and endothelial and smooth muscle (C) Proliferation of CPCs by Coulter Counter. Results were normalized to GAPDH and expressed as a fold change for cECM over COL ($\Delta\Delta$Ct) and reported as a mean ± SEM. Unpaired student's t-test; *$p<0.05$, **$p<0.01$, n=4-6. COL = collagen, ADP = adipose-derived decellularized extracellular

matrix, tnn = troponin, mhc = myosin heavy chain, FSP = fibroblast specific protein, vwf = von Willebrand factor, sm = smooth muscle, GAPDH = glyceraldehyde-3-phosphate dehydrogenase.

4.2.2 Western analysis of CPC cardiomyogenesis

To determine if gene expression changes were followed by protein changes, Western blot analysis was performed on protein samples collected from CPCs cultured on either cECM or COL for 7 days. Figure 3 shows representative blots (b) probed for the cardiomyocyte markers Gata-4 and Nkx2.5 along with grouped data (a). CPCs cultured on cECM had significantly higher ($p<0.001$) levels of Gata-4 as compared to COL (1.8 ± 0.1-fold) after normalization to GAPDH. A similar increase was seen for Nkx2.5 (1.6 ± 0.2-fold; $p<0.05$) in cells cultured on cECM compared to COL. These data demonstrate that significant changes in cardiomyogenic gene expression lead to subsequent increases in protein levels.

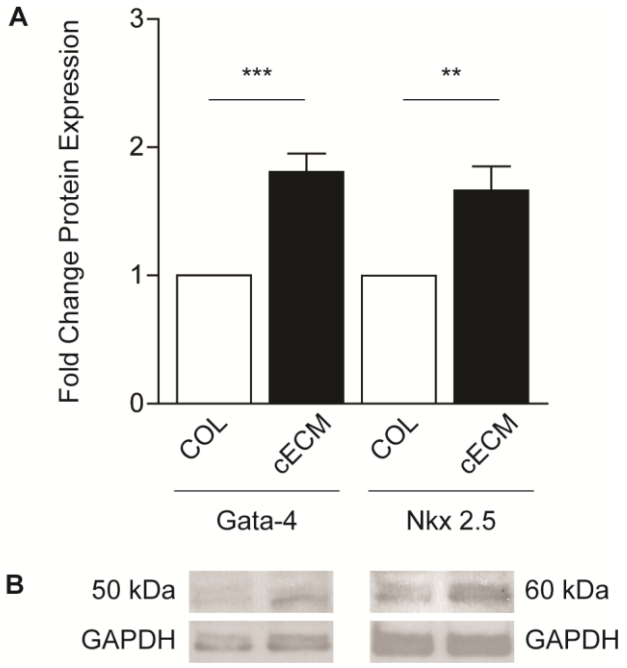

Figure 3. Western analysis of cardiac protein expression. Protein was isolated from cardiac progenitor cells cultured on cECM (black bars) or COL (white bars) for 7 days. Grouped data (A) and representative blots (B) are shown as mean ± SEM. Images were

quantified with ImageJ and protein expression was normalized to GAPDH. Unpaired student's t-test; **p<0.01, ***p<0.001; n=4-6. COL = collagen, cECM = cardiac decellularized extracellular matrix, GAPDH = glyceraldehyde-3-phosphate dehydrogenase..

4.2.3 Proliferation of CPCs

In order to determine the effect of cECM on CPC proliferation, cells were cultured on cECM or COL in the presence of serum and cell count was measured 48 hours later. As the grouped data in Figure 4 demonstrate, there was a significant ($p<0.05$) 35% increase in proliferation of CPCs on cECM when compared to those seeded on COL (cECM = 2.9-fold over initial seeding, COL = 2.3-fold). In addition, we examined this response using adipose ECM to determine the role of tissue-specificity. As the data in Figure 2 demonstrate, there was no significant increase in proliferation in cells cultured on adipose ECM compared with collagen. These data show that cECM is a better substrate for CPC proliferation as compared to COL.

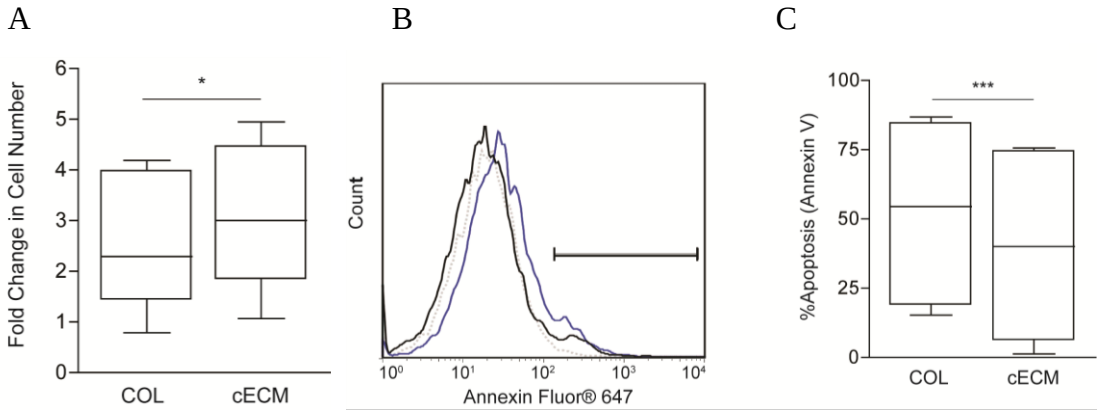

Figure 4. Improved CPC cell number on cECM and COL. (A) Cardiac progenitor cells (CPCs) seeded on cECM or COL were cultured for 48 hours. Fold change in cell number was calculated as the final cell count divided by the number of cells seeded as determine by Coulter counting. (B-C) CPCs cultured on cECM or COL were serum-deprived for 12 hours, then harvested for Annexin V staining. Representative histograms of Annexin V

staining for CPCs cultured on cECM (black) and COL (blue) are shown (B). Gating was based on CPCs that were not serum-deprived (dotted line). Box and whisker plots (C) show mean, quartile ± SEM for grouped data. Paired student's t-test; *p<0.05, ***p<0.001; n=6-7. COL = collagen, cECM = cardiac decellularized extracellular matrix.

4.2.4 Survival of CPCs

To evaluate the effects of cECM on CPC survival, Annexin V staining was performed after CPCs seeded on either cECM or COL were serum-starved for 12 hours. Figure 4 shows a representative histogram of Annexin V staining, illustrating decreased apoptosis for CPCs cultured on cECM as compared to COL. Grouped data demonstrate a significant reduction in percent apoptosis for cells cultured on cECM (40% ± 14%), as compared to COL (53% ± 14%; p<0.001). These data show a significant improvement in survival for cells cultured on cECM as compared to COL.

4.2.5 Adhesion of CPCs

To determine if CPCs adhered more strongly to cECM or COL, microfluidic adhesion assays were performed under increasing levels of shear stress. The grouped data in Figure 5 show that CPCs cultured on cECM adhere more strongly as compared to CPCs cultured on COL as represented by the higher fraction of adherent cells over increasing shear stresses. The force at which 50% of the cells were removed was 120 dynes/cm^2 for cells cultured on cECM compared with 60 dynes/cm^2 for COL. CPCs cultured on fibronectin and laminin adhere to their substrate with a similar strength to CPCs cultured on COL (data not shown). These data provide evidence that CPCs adhere more tightly to cECM as compared to COL.

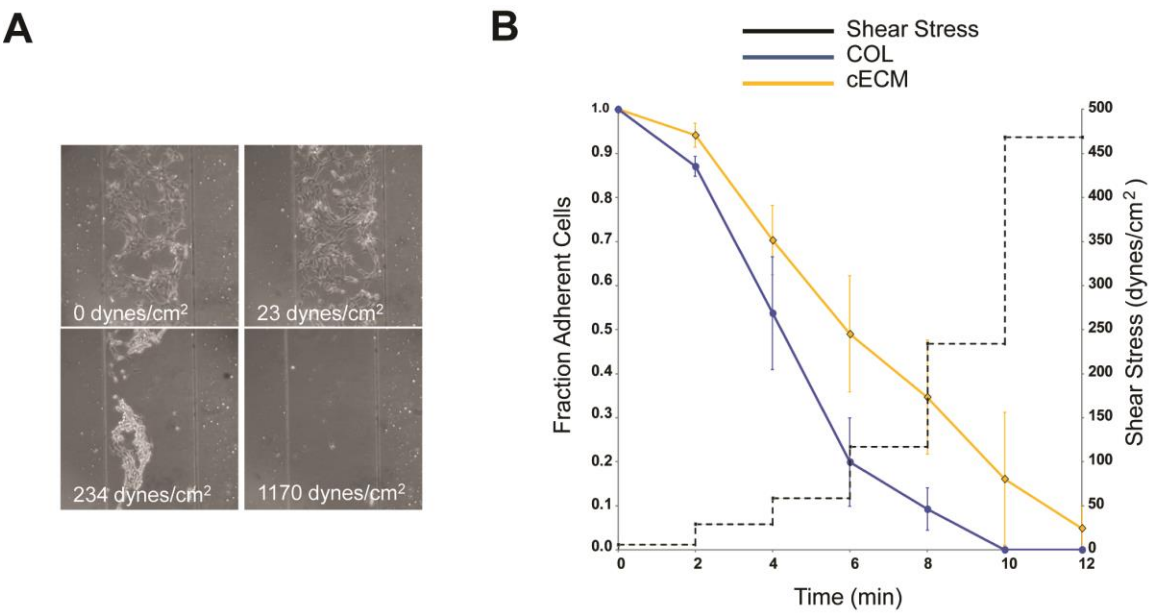

Figure 5. CPC adhesion to cECM and COL. CPC adherence to cECM (yellow) and COL (blue) was determined by microfluidic adhesion assay where cells were subjected to increasing shear stresses. (A) Representative images of microfluidic assay. (B) Grouped data shows mean ± SEM fraction of adherent cells (left-axis) over time with increasing shear stresses (dotted line, right-axis). CPC adherence to fibronectin and laminin were similar to COL (data not shown).

4.2.6 PCR-array data

In order to investigate the global regulation of extracellular-matrix related proteins in CPCs, cells were cultured on cECM or COL for 48 hours and samples were pooled from 3 experiments for gene array analysis and presented in Figure 6. Extracted data demonstrated >2.5-fold increases in lama3 (laminin 5; 3.55-fold), mmp3 (3.20-fold), mmp10 (2.46-fold), mmp13 (11.79-fold), mmp16 (3.25-fold), timp3 (4.17-fold), and tnc (tenascinC; 4.92-fold). Interestingly, col1a1 was detected in COL cultured CPCs but not in cECM-cultured cells. CD44, a receptor for hyaluronic acid was also increased in cECM compared to COL (4.63-fold). These data demonstrate that cells cultured on

cECM display enhanced expression of collagenases, as well as increased expression of laminin, suggesting extensive remodeling of the extracellular environment.

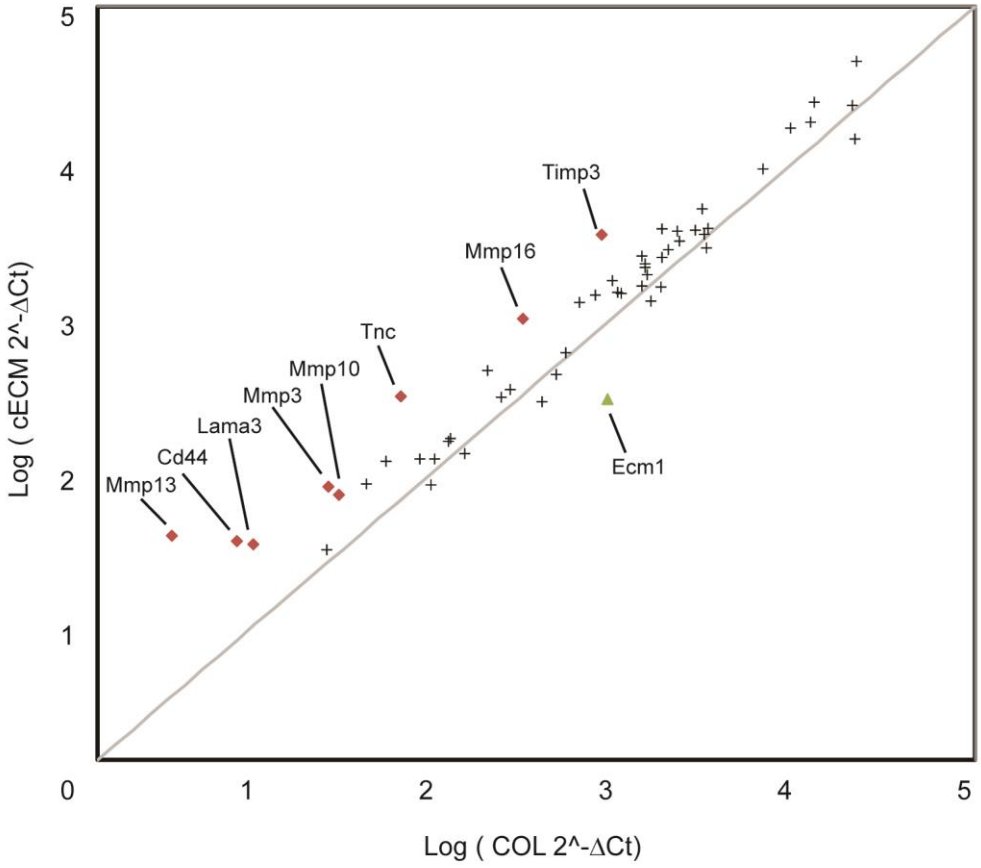

Figure 6. Extracellular matrix and adhesion molecule PCR array.CPCs were cultured on either cECM (y-axis) or COL (x-axis) for 2 days and 3 samples from each condition were pooled for a total of 1 mg cDNA. PCR array plates were purchased from Qiagen (SABiosciences). Results are presented as logddCt and considered significantly up- (red diamonds) or down- (green triangle) regulated for ± 2.5-fold changes for cECM compared to COL. Gray line represents no change in gene expression between conditions.

4.3 Discussion

Adult stem cell delivery is a promising therapy that has shown improvements in early clinical trials. Despite these exciting preliminary trials, problems still exist in the retention, survival, and maturation of implanted cells [187]. While natural and synthetic materials may have the potential to improve some of these parameters, great care must be taken to ensure that the implanted cells receive the proper signals to support their function. In this report, we identify a naturally-derived, decellularized cardiac extracellular matrix (cECM) that is capable of enhancing cardiac progenitor cell (CPC) adhesion, growth, survival, and maturation as compared with the commonly used matrix collagen I (COL). While the original three-dimensional structure is lost when preparing the liquid form of cECM, the liquid matrix still retains ECM proteins and peptide fragments, and thus many of the original biochemical cues, providing a mimic of the adult heart ECM [175, 176].

In order to repair the infarcted myocardium, it is expected that new cardiomyocytes must be generated and that the continued deposition of a collagen scar must be slowed. CPCs are capable of differentiating into all cardiac cell types [61, 64], though their function can be enhanced by soluble factors and genetic manipulation. Here, we show that culture of CPCs on cECM increases the expression of early cardiac markers after 2 days of treatment [193]. Of these markers, two (Gata-4 and Nkx2.5) were chosen for examination at the protein level after 7 days of treatment. A significant increase in Gata-4 and Nkx2.5 protein levels was demonstrated through Western blot. While we do not present evidence of functional cardiomyogenesis, we show cECM increases the propensity of CPCs to become cardiomyocyte precursors. It is unlikely that this short time period would show significant differences in cardiomyogenesis. Longer periods of genetic analysis were not performed as the initial matrix is likely replaced after 3 days [15, 18]. In fact, our PCR array data suggest that CPCs cultured on cECM may actively

replace extracellular matrix proteins via upregulation of collagenases such as mmp3, 10, 13 and 16. Additionally, there was a >3.5-fold increase in laminin, as well as smaller increases in collagen IV and fibronectin (~1.5-2-fold) suggesting the deposition of a more complex extracellular matrix. Increases in these cardiac markers, specifically the more mature α-MHC and troponins, are well associated with increased maturation of progenitor cells [194, 195]. MHC and troponin expression is known to follow Nkx2.5 and Gata-4 in development, and cells with increased expression of these markers demonstrate improved regenerative capacity. In agreement with these results, we previously demonstrated enhanced maturation of human embryonic stem cell derived cardiomyocytes when plated on cECM compared to gelatin, as indicated by increased multi-cellular organization and desmosome formation [176]. While this is an exciting result, human embryonic stem cells have the disadvantage of potentially forming teratomas in vivo.

No statistically significant differences in the expression of smooth muscle and early endothelial genes were observed, suggesting that cECM treatment is not more or less likely to push CPCs toward these lineages than COL. Lack of maturation to the endothelial and smooth muscle lineage may affect implanted cardiomyocyte function as endothelial cells play a critical role in cardiomyocyte survival. While this may be a concern, recent studies from our laboratory and others demonstrate robust endothelial and smooth muscle cell population of implanted matrices, and thus implanted cells may still receive the signals they require [87, 175, 196]. Additionally, a lack of increase in endothelial and smooth muscle markers does not necessarily mean CPCs do not differentiate/mature to these lineages, as our comparisons are to COL. Of significant note in our study, is the reduction in fibroblast specific protein 1 (FSP), a fibroblastic marker, after two days of culture on cECM compared to COL. Fibroblasts are largely responsible for depositing collagens in the myocardium following MI, and a reduction in

FSP may correlate to a reduction in collagen production; however this was outside the scope of this study. Once again, our PCR data confirms this potential phenotype through upregulation of collagenases and deposition of more contractile collagen isoforms (collagen III and IV).

Our studies also demonstrate cECM to be a better substrate for proliferation of CPCs than COL. This may be important for cell transplantation, when many cells are lost or diffuse away from the site of injection [187]. While most matrices would inhibit this loss, enhanced proliferation is an added benefit as it may increase the likelihood for tissue repair by brute numbers. Unlike embryonic stem cells, CPCs have not been shown to induce tumor formation upon injection making their enhanced proliferation less of a concern [197]. Aside from cECM's conceivable use as a delivery vehicle, another potential use for cECM is for the expansion of these cells in vitro following tissue harvest. Current clinical protocols for autologous CPC therapy call for the removal of patient tissue biopsies, followed by isolation and expansion of the c-kit+ fraction. This now takes up to 3 months for patients to receive their own cells back, and tissue damage/loss is still occurring in this time [67, 68]. Culture of cells on cECM during expansion could lead to faster implantation times for patients and improve functional recovery. In conjunction with enhanced proliferation, cECM provides protection to CPCs under stress from serum-starvation. A 12% reduction in apoptosis as seen in our studies on cECM compared to COL is quite significant. In a clinical setting, this could translate to more than 100,000 additional viable cells as a patient receives a dose of 1 million cells [68]. These results show promise for future work, as CPCs injected within a cECM hydrogel into the infarcted myocardium may be better primed to survive the harsh conditions than cells injected with COL.

This study compares cECM to COL and does not include other matrix components, or the use of tissue culture plastic as a control. COL was chosen due to its abundance in both the myocardium following infarction, as well as its use as a cell delivery vehicle. In future work, it would be relevant to examine the effects of other single protein matrix components on CPC differentiation, proliferation, and survival. Collagen IV and laminin are present in CPC niches, while collagen III and fibronectin are also present in the myocardium post-MI [21]. Additionally, how cells respond on tissue culture plastic was not examined in this study as the response would be largely irrelevant for the reason discussed above. We did not examine how these cells respond in three-dimensional culture, and it is possible that behaviors do not mimic results seen in two-dimensional coating experiments. While this may mimic the conditions under which CPCs would be cultured if cECM is used for pre-conditioning, it does not adequately address the proposed in vivo model in which CPCs are injected with cECM to form a three-dimensional hydrogel in vivo. Moreover, there is also a possibility that CPCs may be cultured in three-dimension using this material and may behave quite differently than seen in our study.

As noted previously, one of the limitations of stem cell injection in the infarcted myocardium is the lack of retention of the cells [187]. Microfluidic adhesion assay shows that CPCs adhere more strongly to cECM than COL. Additionally, other single protein ECM components were tested (laminin and fibronectin) and similar adhesion as COL was seen (data not shown). These results suggest that CPCs may interact more tightly with the more complex cECM than single matrix proteins like COL, which may play a role in the other findings in this study. It is unclear if the forces used in this study represent the post-infarct tissue environment as the assay is merely intended to demonstrate cell-material interaction strength. Tighter adhesion to ECM is shown to improve survival, proliferation, and growth of cells as this may lead to enhanced integrin

activation [113]. While this study does not determine mechanistic pathways, integrins such as the β1 integrin are critical for cardiac development. Modulation of the β1 integrin negatively affects cardiomyocyte function, post-injury healing, and stem cell differentiation [158, 198]. Additionally, in mesenchymal stem cells, while β1 regulates adhesion to the ECM, βvα3 may regulate differentiation [199, 200]. Cardiac progenitor cells exist in niches that are rich in laminin, and thus a more complex mix of integrins may regulate different functions [63]. Full compositional characterization of the cECM has not yet been achieved, though initial mass spectrometry studies determined the presence of collagens I-VI, elastin, fibrinogen, fibronectin, laminin, fibrillin-1, lumican, and fibulin-3 and -5 [176]. These components are not surprising given that the myocardium is known to contain collagens I and III, laminin, fibronectin, and elastin [19, 201]. Finally, our array data demonstrates a substantial (>4-fold) increase in tenascinC gene expression. While the role of tenascin in CPCs is unstudied, it plays an important role in the adhesion and mitogen responses of hematopoetic progenitors and this study identifies a potential role for its involvement in the cECM response [202].

Previously, the successful use of cECM as an injectable biomaterial has been established [175, 178]. When injected into the rat myocardium, cECM has shown an immune response comparable to implanted decellularized small intestine submucosa and syngeneic muscle implants [178]. Numerous xenogeneic decellularized ECMs have been cleared by the FDA, are considered biocompatible, and are in clinical use [203]. Appropriate processing however needs to be performed to avoid significant residual DNA and detergents, and xenogeneic antigens are always of concern. Our decellularized cardiac matrix, however, appears to have excellent biocompatibility though further antigenicity and biocompatibility tests are underway prior to clinical translation. Because it is digested rather than in a patch form, it can be used as an injectable hydrogel that self-assembles into a porous and fibrous scaffold in vivo, opening up the possibility of

minimally invasive delivery [179]. In fact, recent studies demonstrate the cECM hydrogel can be delivered as a liquid to the myocardium of pigs through a minimally invasive, transendocardial catheter injection, and subsequently form a scaffold in vivo [178]. This liquid form requires the use of pepsin, which does remain in the material, although it is inactivated in the process of the pH adjustment and has previously been used in other FDA approved products. Interestingly, when delivered intramyocardially in rats, cECM demonstrated improved function compared with untreated animals, with an observed increase in cardiomyocytes [178]. The source of the myocytes was not determined, though taken together with our studies it may suggest the mechanism of enhanced endogenous CPC proliferation and differentiation. While not done in this study, stem cells have been delivered to patients via intramyocardial catheters and thus this approach may have great clinical significance. For the myocardium, small intestine submucosa (SIS) and urinary bladder matrix have been examined for treating cardiac wall defects and MI. Although SIS and bladder matrix patches, and a SIS emulsion have resulted in cell infiltration, [204-206] they have also caused undesirable tissue formation such as adipose and even cartilaginous tissue, [205] potentially due to inappropriate cell-matrix interactions. While the ECM contains similar components across tissues, each tissue does have its own distinct combination of ECM components. Our data with cECM and preliminary results with adipose ECM demonstrate the importance of tissue-specific ECM cues in regulating progenitor cell growth, survival, differentiation, and adhesion.

CHAPTER 5 EFFECTS OF CYCLIC STRAIN ON CPC BEHAVIOR ARE EXTRACELLULAR MATRIX-DEPENDENT

The myocardium is a dynamic heterogeneous tissue that changes in matrix composition and mechanical properties from development, through aging and disease. Endogenous cells are exposed to a variety of microenvironments during these changes. The biochemical or biomechanical cues necessary to activate an endogenous cardiac progenitor cell (CPC) response or to best precondition or deliver CPCs for cell therapy is unknown. We aim to assess the effect of matrix composition and strain magnitude on CPC behavior by mimicking microenvironments from the myocardium. For this, laminin (LN, niche), fibronectin (FN, infarct), collagen I (COL, infarct), a naturally-derived cardiac extracellular matrix (cECM, healthy myocardium) and poly-l-lysine (PLL, negative control) were evaluated as ECM conditions. Simultaneously, 0 (negative control), 5 (infarct), 10 (literature condition) and 15% (healthy) strain were evaluated. Our results show that CPCs align in response to cyclic strain when cultured on a matrix protein. Cell division is higher at lower strain magnitudes and on fibronectin. These culture conditions are summarized in Figure 7. CPCs cultured on FN, COL or cECM oscillate calcium. Strain increases vascular endothelial growth factor concentration in conditioned media from CPCs on LN and cECM; basal concentrations are high for FN, COL and PLL. Connexin 43 expression was increased in unstrained CPCs on FN and COL and decreased with increasing strain magnitude on COL and cECM. Activation of focal adhesion kinase was observed upon cell attachment and was maintained by the application of 15 minutes of cyclic strain. FN further maintained this activation for 24 hours of cyclic strain. Activation of extracellular signal-regulated kinase was increased at 15 minutes of cyclic strain on cECM for higher strain magnitudes and COL and PLL at lower strain magnitudes. Results for Aim 2 are summarized in **Error! Reference source**

not found.. These data suggest that CPCs integrate complex signals from the microenvironment into their behavior.

<table>
<tr><th></th><th>Static</th><th>5% Strain, 1 Hz</th><th>10% Strain, 1 Hz</th><th>15% Strain, 1 Hz</th></tr>
<tr><td>PLL</td><td colspan="4">Negative Biological Control</td></tr>
<tr><td>LN</td><td>Control</td><td>Niche</td><td rowspan="4">Typical, published in vitro strain conditions</td><td>Niche</td></tr>
<tr><td>FN</td><td>Control</td><td>Infarct</td><td>Healthy</td></tr>
<tr><td>COL</td><td>Control</td><td>Infarct</td><td>Healthy</td></tr>
<tr><td>cECM</td><td>Control</td><td>Biomaterial Therapy- ?</td><td>Healthy</td></tr>
</table>

Figure 7. Microenvironments Mimicked in Experimental Design.

5.1 Introduction

5.1.1 Extracellular Matrix Components in the Myocardium

The distinct microenvironments of the myocardium during development, adulthood and disease were discussed in the background. Briefly, after MI there is an increase in collagen and fibronectin content and a decrease in laminin content [21]. A distinct environment, the stem cell niche is a local collection of stem cells surrounded by ECM and supporting cells. Niches control stem cell self-renewal. Loss of contact with the niche leads to differentiation of a stem cell [207]. The expression and localization of ECM proteins in the CPCs niche is unknown; but the niche is speculated to maintain

CPCs in a quiescent state [82]. Fibronectin is present, although not exclusively expressed, in cardiac niches [62]. Laminin is also present in cardiac niches and surrounds CPCs more closely [63]. Collagen IV, osteopontin, tenascinC, chondroitin sulfate and heparin sulfate play roles in development and may also be involved in CPC niches [82]. Niches for cardiac progenitor cells identified by the insulin gene enhancer protein contain collagen IV and laminin in close proximity to the progenitor cells, with fibronectin and collagen I found outside of niche [86]. Differentiating cardiac progenitors migrate away from the niche and it is important to identify signals from the microenvironment that are responsible for activating CPCs for regeneration after MI. In this section, distinct characteristics of individual matrix proteins will be discussed.

The molecular weight of fibronectin (440 kDa) and collagen I (390 kDa) are fairly similar, but laminin (850 kDa) is much larger. Fibronectin plays a role in cell adhesion, migration, growth and differentiation. Its dimer has 6 distinct integrin binding sites, as well as binding domains for heparin, collagen and fibrin [208]. Some of these binding domains are buried in cryptic sites. The bond strength between fibronectin and an integrin, estimated to be 30-100 pN, is 10-fold higher than the force required to unfold cryptic subdomains [47]. Fibronectin expression correlates with increase in CPC presence in the myocardium and the two are found in close proximity in development and disease. In global knockouts of fibronectin, CPC expansion and survival were impaired, reducing the number of newly formed myocytes [209]. Fibronectin may play a crucial role in CPC expansion and maturation. The primary role of collagen I is to provide structural support and force transmission [17]. Collagen I has 3 distinct integrin binding sites [210]. The binding of integrins to collagen I is dependent on its quaternary structures [211]. Laminin directs development, migration and differentiation [45, 212]. The gamma-1 chain of laminin has 7 distinct adhesion domains [213]. In its trimeric form, laminin as 19 distinct integrin binding site [214]. Poly-l-lysine is often used a

negative control in cell culture since it should not activate integrins. Instead cells adhere to poly-l-lysine through electrostatics [215].

5.1.2 Mechanical Strain for Cell Stimulation

The active contracting of the myocardium exposes cardiac cells to a cyclic strain. The response of strain on cardiomyocytes in vitro is to elongate and align perpendicular to the direction of strain [112]. Neonatal cardiomyocytes are more proliferative and increase protein production when exposed to strain [117, 123, 129, 216]. Furthermore, cyclically straining NRVM increased their connexin 43 (Cnx43) expression 2-fold. Interestingly, the same effect could be achieved by incubating unstrained cells with soluble vascular endothelial growth factor (VEGF) [217]. The release of VEGF from strained cardiomyocytes is dependent on focal adhesion kinase (FAK). In return, VEGF activates extracellular signal-regulated kinase (ERK) and leads to the expression of Cnx43 [218]. In stem cell populations, cyclic strain has been demonstrated to increase cardiomyogenic gene expression [20, 139, 219]. In mesenchymal stem cells, this effect is dependent on the matrix conditions [139]. Strain is also used to condition three-dimensional engineered cardiac tissue into constructs that beat spontaneously and resemble the neonatal myocardium [220]. In tissue engineered constructs containing embryonic stem cells, mechanical strain after implantation in the MI border zone reduced fibrosis and apoptosis and improved neovascularization over strain resistant constructs [219].

Mechanotransduction pathways are activated by mechanical strain. The beta1 integrin plays various roles in stem cell maintenance, differentiation and proliferation depending on cell type and the alpha subunit present in the heterodimer [146, 221]. FAK activation occurs downstream of outside-in integrin signaling. Adhesion to collagen, laminin and fibronectin, but not poly-l-lysine triggered FAK phosphorylation within 20 minutes [222]. Phosphorylation of FAK was lower in cells seeded on fibronectin-coated

polyacrylamide gels than those seeded on fibronectin-coated tissue culture plates, indicating its activation may be dependent on substrate stiffness [103]. Additionally, strain induced FAK phosphorylation in various cell types within minutes and was maintained for hours [152, 164, 165, 223-226]. NRVM, this signaling was dependent on the beta1 integrin subunit [163]. Following FAK activation with cyclic strain, ERK phosphorylation transiently increased [165, 223, 224, 226]. ERK activation could be suppressed by mutating FAK [223]. As another signaling mechanism, cyclic strain dissociates RhoA from FAK [164]. In addition to activation, mechanical strain can also increase the expression of FAK and the beta1 integrin subunit [127]. The effect of cyclic strain on cardiac progenitor cells is unknown. Strain magnitudes in this proposal will be based on physiological conditions (healthy myocardium = 15%, infarcted myocardium = 5% [31]) and in vitro optimization assays (improved cardiomyogenesis = 10% [227]).

5.1.3 Calcium Handling in Cardiac Cells

The contractile force of adult cardiomyocytes is regulated by the size and duration of their calcium transients [98]. Not only is calcium cycling regulated by mechanical load, but because the mechanical properties of cardiomyocytes are dependent on cytoplasmic calcium, mechanotransduction is coupled to calcium signaling pathways in a cyclic fashion [228]. As cardiomyocytes mature, they increase expression of the ryanodine receptor and sarcoendoplasmic reticulum calcium transport ATPase (SERCA) [98]. This shifts the source of calcium for transient from the extracellular space in immature cells to the sarcoplasmic reticulum in mature cells [99]. Expression of SERCA, but not L-type calcium channels, is stiffness dependent [98]. However, alignment of NRVM increases L-type calcium channel expression [111]. Cell shape, membrane rigidity and the activation of mechanosensitive ion channels through the application of mechanical strain all influence intracellular calcium [229-232]. Integrins may also be involved in regulating calcium handling. Beta3 integrin knockout in mice reduced SERCA transcript

levels [233]. SERCA levels are also reduced in cardiac hypertrophy [233]. Regenerative medicine may be able to restore SERCA levels [234].

Human CPCs express SERCA, inositol trisphosphate receptor, sodium calcium exchanger and low expression of the L-type calcium channel [235]. Ryanodine receptor is not detected in these cells. Spontaneous calcium oscillations were observed in 20% of CPCs and they averaged 2 oscillations, with an average duration of 80 seconds, in 33 minutes. The percent of active cells increased after 2 hours in Tyrode solution. Oscillations were mediated primarily through the inositol trisphosphate receptor and SERCA and were independent of gap junctions. Interestingly, calcium oscillations correlated with increased entry of CPCs into the cell cycle. Stimulating calcium oscillations in CPCs before intramyocardial infusion in infarcted mice improved their engraftment and expansion [235]. Further work from the same group showed that the number of cycling CPCs could be increased by stimulating the inositol trisphosphate receptor in the cells with adenosine triphosphate and that this lead to increased bromodeoxyuridine incorporation [236]. Only 10% of the CPCs had spontaneous calcium oscillations in Tyrodes solutions, but this increased to 70% with adenosine triphosphate stimulation. Induction of calcium oscillations also led to an increase in asymmetrical division [236]. Manipulation of CPCs through engineered expression of the human serine/threonine kinase Pim-1 and co-culture with neonatal rat cardiomyocytes produces CPCs with cardiomyocyte-like calcium transients [237].

Connexin 43 (Cnx43) expression is diffuse in endogenous CPCs, but these cells can form gap junctions with mature cardiomyocytes [63, 235]. In addition to electrically coupling cells, Cnx43 is protective in cardiomyocytes and regulates proliferation in the H9C2 cardiomyocyte cell line [238, 239]. Hypoxia, present in disease states, induces dysregulation of Cnx43 [240]. However, Cnx43 expression can be restored through

cyclic strain [99]. Culture of NRVM in the presence of strain with fibronectin increased their expression of Cnx43 as compared to culture on COL [84]. Additionally, autocrine and paracrine signaling through VEGF, released by strained myocytes, increased Cnx43 expression [217].

This aim takes a combinatorial approach to evaluate the response of CPCs to extracellular matrix proteins and mechanical strain. We sought to determine if a single stimuli was sufficient to induce CPC cardiomyogenic maturation or if a complex set of signals is necessary. We aimed to identify the signal(s) necessary for CPC activation, and in comparison CPC maintenance. The response of CPCs to microenvironmental stimuli is dependent on extracellular matrix and strain conditions.

5.2 Results

5.2.1 Statistics

For all data sets, two-way ANOVAs were performed to establish overall effects of matrix and strain on a given endpoint. No post-test results are reported for the two-way ANOVA as we cannot compare between all relevant groups simultaneously. Instead the same data was analyzed by one-way ANOVAs to establish specific effects of matrix or strain, except where noted. All one-way ANOVA post-tests are Tukey's multiple comparison test allowing for the comparison of all groups to each other. Ultimately, this does not allow for direct comparisons of all culture conditions, but does allow conclusions to be drawn regarding the effect of strain for CPCs cultured on a given matrix and the effect of matrix conditions for a given strain. GraphPad Prism 5 was used for all statistical analysis.

5.2.2 Alignment

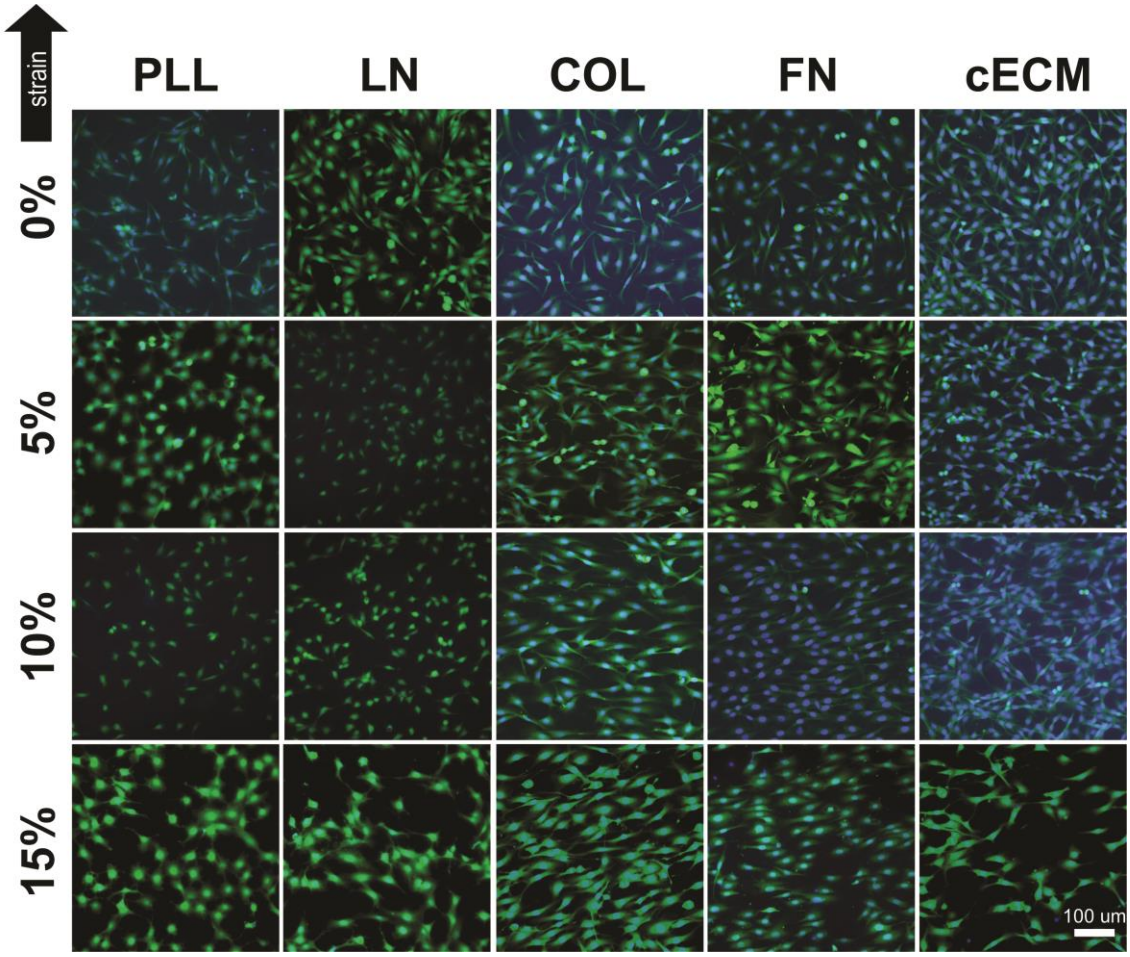

Figure 8. Representative Strain Images. CPCs were seeded on the appropriate matrix for 6 hours and then cyclic strain was applied for 24 hours. Blue = DAPI, Green = FITC-maleimide; arrow indicates principle direction of strain; 0-15%: strain magnitude; PLL = poly-l-lysine, LN = laminin, COL = collagen I, FN = fibronectin, cECM = naturally-derived cardiac extracellular matrix.

To determine if CPCs align in response to mechanical strain and if potential alignment was matrix-dependent, CPCs were seeded as described in the methods and evaluated by immunocytochemistry. Representative images are shown in Figure 8. By two-way ANOVA, there is an overall effect of matrix ($p<0.0001$) and strain ($p<0.0001$) on CPC alignment, with an observed interaction ($p<0.0001$). To further examine these effects,

Kruskal-Wallis tests with Dunn's multiple comparison tests were chosen due to unequal variances between data sets and performed for each strain group (0-15%) and each matrix group. For unstrained cells, there was an overall effect of matrix condition, but with no significant difference by post-tests. With the application of 5% strain, more CPCs align on COL (58%) than PLL (18%; $p<0.01$). At 10% strain, CPCs aligned better on COL (60%) than PLL (22%; <0.01), LN (22%; <0.05). At 15%, CPCs aligned better on FN (42%; $p<0.001$) and COL (54%; $p<0.001$) as compared to PLL (15%). Alignment quantification is reported in Figure 9.

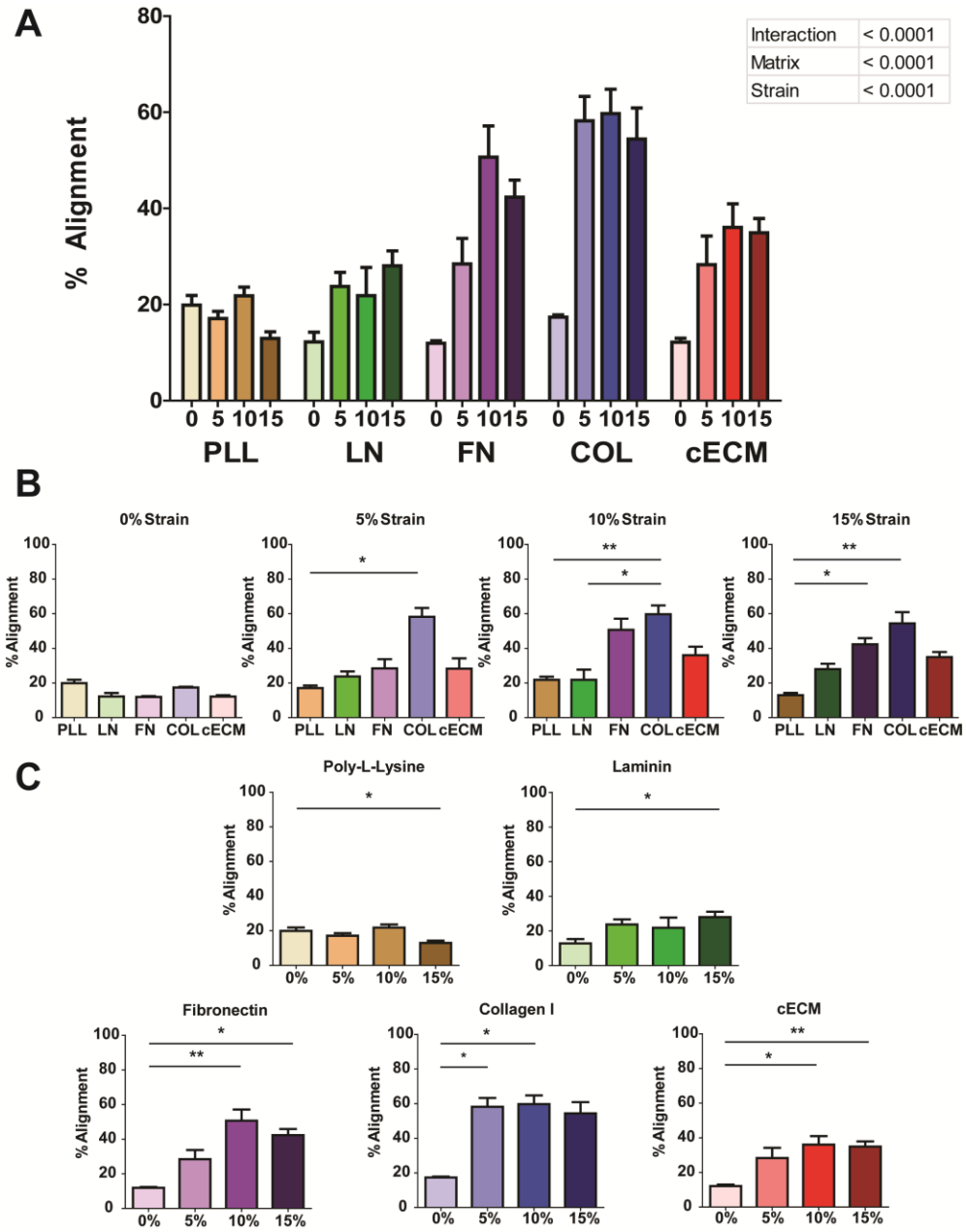

Figure 9. Quantification of Alignment. CPCs were seeded on the appropriate matrix for 6 hours and then cyclic strain was applied for 24 hours. (A) Analysis by two-way ANOVA. (B) Matrix effects. (C) Strain magnitude effects. (B-C) Kruskal-Wallis one-way ANOVA with Dunn's multiple comparison tests, bars represent mean + SEM, *p<0.05, **p<0.01; n =4-7; 0-15: strain magnitude; PLL = poly-l-lysine, LN = laminin, COL = collagen I, FN = fibronectin, cECM = naturally-derived cardiac extracellular matrix.

Within each matrix group, strain had an effect on alignment. For PLL, less alignment was observed at 15% than 10% ($p<0.05$), although this change was small (7% absolute). For CPCs cultured on LN a small increase in alignment was observed at 15% strain (28%) only as compared to 0% (12%; $p<0.05$). For CPCs cultured on FN, alignment was increased at 10 (51%; $p<0.01$) and 15% (42%; $p<0.05$) strains as compared to unstrained (12%) cells with no differences in alignment between 5, 10 or 15% strain. For CPCs cultured on COL, alignment was increased at 5 (58%; $p<0.05$) and 10% (60%; $p<0.05$) strains as compared to unstrained (17%) cells, with no differences in alignment between 5, 10 or 15% strain. Similarly, on cECM there was an increase in alignment at 10 (36%; $p<0.05$) and 15% (35%: $p<0.01$) strains as compared to unstrained (12%) CPCs, with no differences in alignment between 5, 10 or 15% strain.

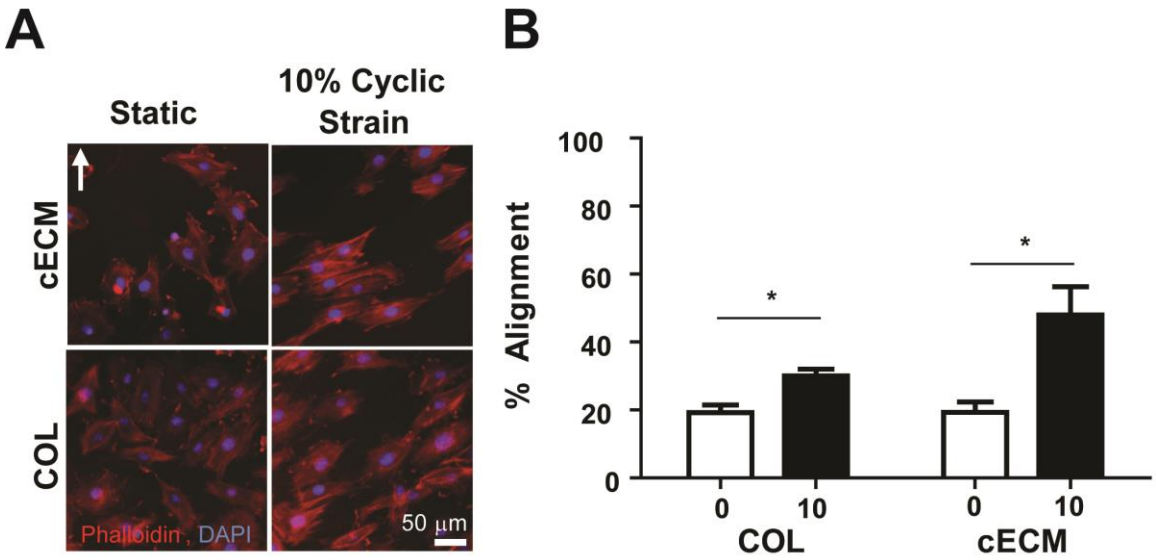

Figure 10. Preliminary Alignment. CPCs were seeded on the appropriate matrix (50 ug/cm^2) for 3 hours and then cyclic strain was applied for 24 hours. (A) Representative images; arrow indicates direction of principle strain, (B) Manual quantification, unpaired t-test, bars represent mean + SEM, *$p<0.05$; n =4; 0-10: strain magnitude; COL = collagen I, cECM = naturally-derived cardiac extracellular matrix.

While, these results may be dependent on matrix concentration and CPC seeding density, we observed similar effects in earlier studies (Figure 10). However, we cannot directly compare the results as we previously coated plates with 10-times the matrix and seeded them with half the number of cells to increase cell-matrix interactions and decrease cell-cell interactions. In that system, CPCs seeded on COL had a slight increase in alignment at 10% strain (30%) as compared to unstrained cells (19%; t-test: $p<0.05$). CPCs seeded on cECM aligned better at 10% strain (48%) as compared to unstrained CPCs on cECM (19%; t-test: $p<0.05$). There was no statistical difference in alignment at 0 or 10% for CPCs seeded on cECM as compared to COL. The remaining culture conditions were not examined.

5.2.3 Spread Area

In order to evaluate if seeding conditions or mechanical strain affect the spread area of CPCs, cells were seeded as described in the methods and immunocytochemistry was performed. The overall average spread area was 960 um^2. Representative images are shown in Figure 8. By two-way ANOVA, matrix had an overall effect ($p<0.0001$), strain did not have an overall effect and there was no interaction. Unstrained CPCs spread more on FN (1312 um^2) and COL (1284 um^2) as compared to PLL (683 um^2; $p<0.01$) and LN (804 um^2; $p<0.05$), as demonstrated by one-way ANOVA. With the application of 5% strain, CPCs on FN (1183 um^2) remained about as twice as spread than those on PLL (612 um^2; $p<0.05$). This effect remained at 10% strain, with cells on FN (1169 um^2) more spread than those on PLL (702 um^2; $p<0.01$) or LN (501 um^2; $p<0.001$) and cells on COL (1037 um^2; $p<0.05$) more spread than those on PLL. For these strain magnitudes, the spread area was intermediate for CPCs seeded on cECM. No difference in cell spreading with matrix condition was observed at 15% strain. Additionally, within each matrix group, no effect of strain magnitude was observed. Quantification of spread area is reported in Figure 11.

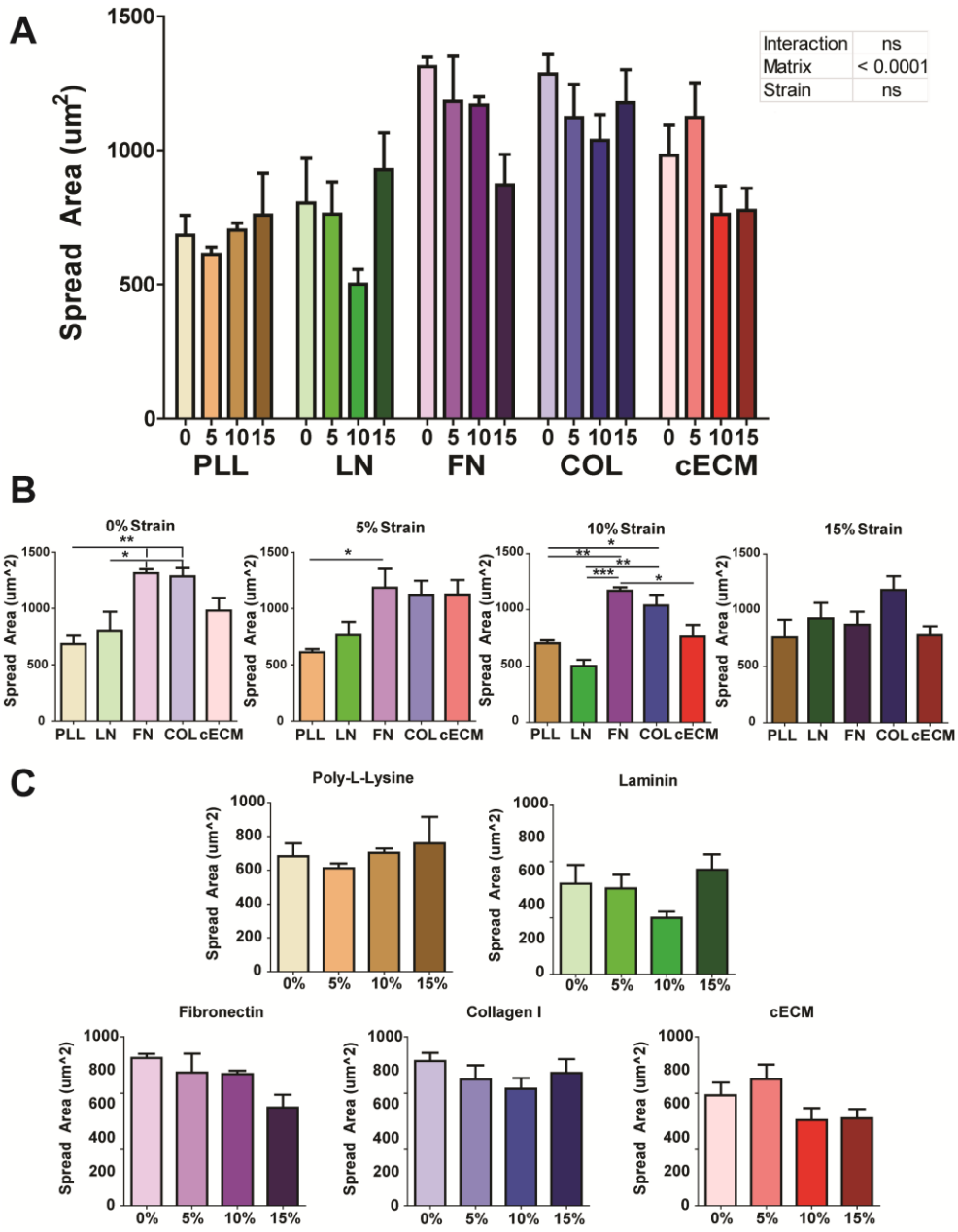

Figure 11. Quantification of Spread Area. CPCs were seeded on the appropriate matrix for 6 hours and then cyclic strain was applied for 24 hours. (A) Two-way ANOVAs. (B) Matrix effects. (C) Strain magnitude effects. (B-C) One-way ANOVA with Tukey's multiple comparison test, bars represent mean + SEM, *p<0.05, **p<0.01, ***p<0.001; n=4-6; 0-15: strain magnitude; PLL = poly-l-lysine, LN = laminin, COL = collagen I, FN = fibronectin, cECM = naturally-derived cardiac extracellular matrix.

5.2.4 Aspect Ratio

In order to evaluate if seeding conditions or mechanical strain affect the aspect ratio of CPCs, cells were seeded as described in the methods and immunocytochemistry was performed. Representative images are shown in Figure 8. The aspect ratio was determined by dividing the major axis by the minor axis of each cell. Although small changes in aspect ratio were observed, across all conditions CPCs maintain an aspect ratio of about 2:1. Results are reported in Figure 12.

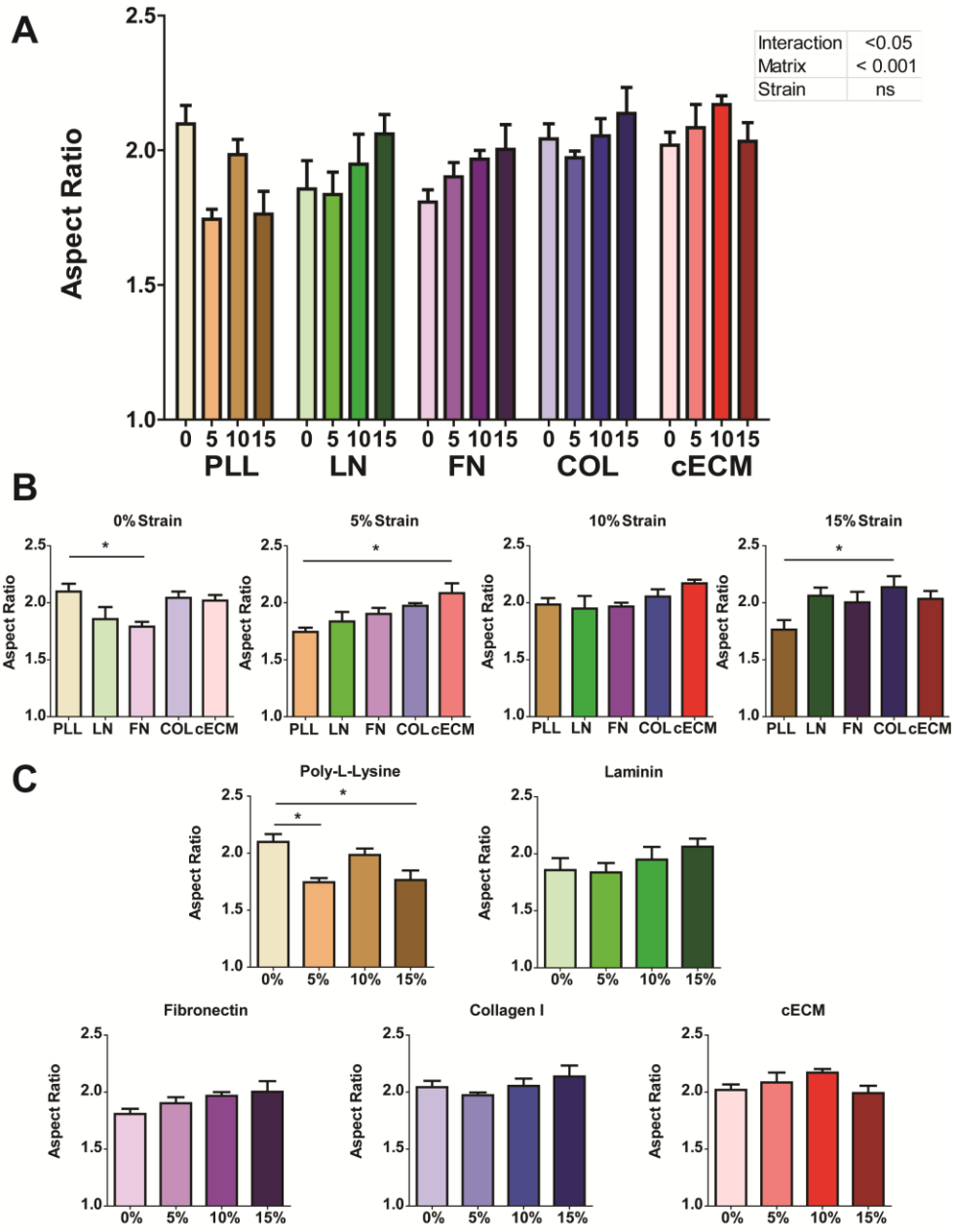

Figure 12. Quantification of Aspect Ratio. CPCs were seeded on the appropriate matrix for 6 hours and then cyclic strain was applied for 24 hours. (A) Two-way ANOVA. (B) Matrix effects. (C) Strain magnitude effects. (B-C) One-way ANOVA with Tukey's multiple comparison test, bars represent mean + SEM, *p<0.05; n=4-7; 0-15: strain magnitude; PLL = poly-l-lysine, LN = laminin, COL = collagen I, FN = fibronectin, cECM = naturally-derived cardiac extracellular matrix.

5.2.5 Proliferation of CPCs

As an estimate of proliferation, the number of visibly dividing cells was determined by immunocytochemistry for cells cultured under each condition. Sample images are shown in Figure 14 as examples of unique phenotypes. Asterisk indicates a dividing cell. Across all groups, <2% of the CPCs were undergoing cytokinesis in the acquired images as identified by nuclear condensation, division and cytoplasm shape. Dividing cells appeared more rounded than non-dividing cells. By two-way ANOVA, matrix had an overall effect ($p<0.0001$) and strain had an overall effect ($p<0.01$), without a significant interaction. Analysis by two-way ANOVA is shown in Figure 13. At 5 and 15% strains, CPCs seeded on FN were dividing more than those seeded on LN and PLL. One-way ANOVAs were performed to compare results within each strain magnitude group. Results by one-way ANOVA are reported in Figure 15. For unstrained CPCs, seeding on FN (1.2%), COL (1.0%) or cECM (0.9%) increased the number of dividing cells as compared to CPCs cultured on PLL (<0.01%; $p<0.05$ for COL and cECM, $p<0.001$ for FN). FN culture also increased the number of dividing cells relative to LN (0.5%; $p<0.01$). At 5% strain, significantly more CPCs were dividing on FN (2.7%) as compared to PLL (0.3%; $p<0.01$) and LN (0.9%; $p<0.05$). Matrix did not affect the number of dividing cells at 10% nor 15%, although there were trends for FN still inducing the highest number of dividing cells. No significant differences were observed between FN, COL and cECM for any strain magnitude.

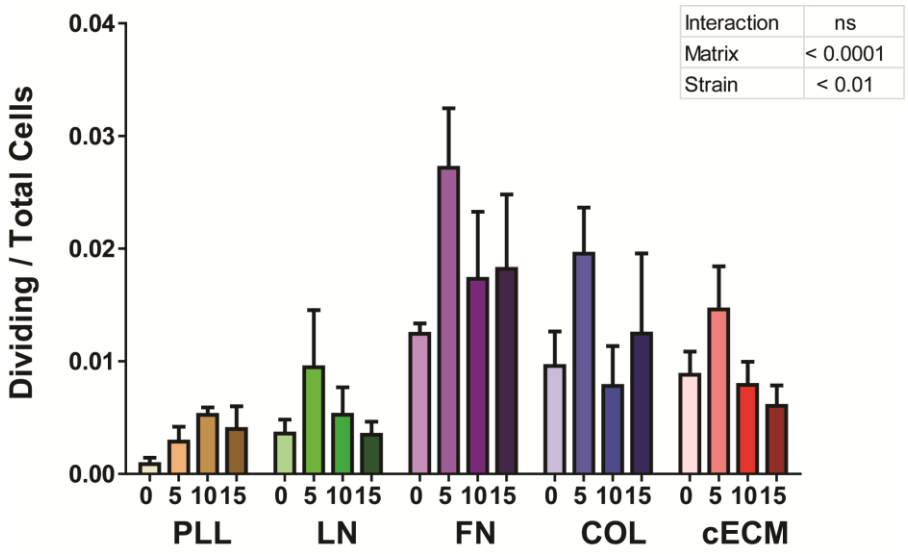

Figure 13. Quantification of Dividing CPCs. CPCs were seeded on the appropriate matrix for 6 hours and then cyclic strain was applied for 24 hours. Two-way ANOVA, bars represent mean + SEM; n=4-6; 0-15: strain magnitude; PLL = poly-l-lysine, LN = laminin, COL = collagen I, FN = fibronectin, cECM = naturally-derived cardiac extracellular matrix.

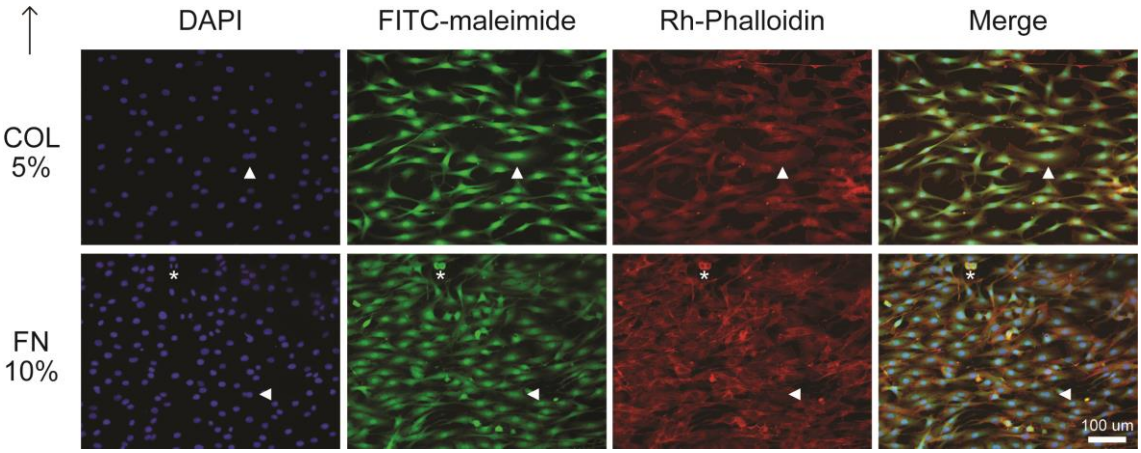

Figure 14. Representative Images of Unique CPC Phenotypes. CPCs were seeded on the appropriate matrix for 6 hours and then cyclic strain was applied for 24 hours. Arrow head shows example of cell with more than one nucleus and continuous cytoplasm; Asterisk shows a dividing cell; Black arrow indicates principle direction of strain; 5-10: strain magnitude; COL = collagen I, FN = fibronectin.

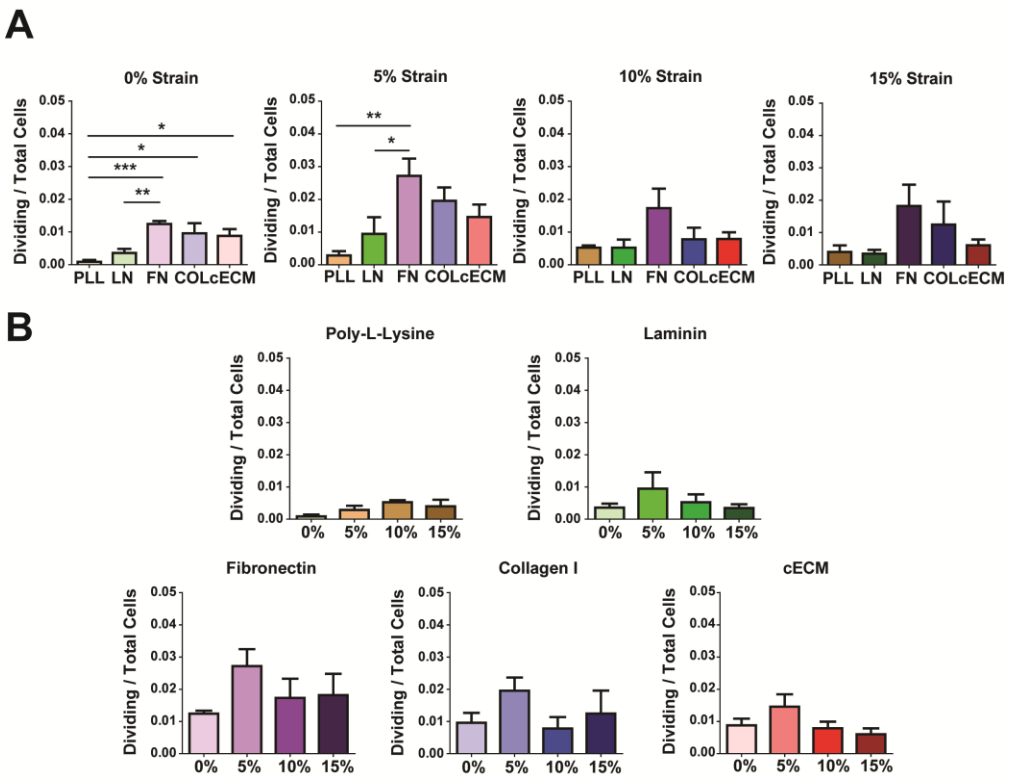

Figure 15. Quantification of Dividing Cells assessed by one-way ANOVA. CPCs were seeded on the appropriate matrix for 6 hours and then cyclic strain was applied for 24 hours. (A) Matrix effects, (B) Strain magnitude effects; (A-B) One-way ANOVA with Tukey's multiple comparison test, bars represent mean + SEM; *p<0.05, **p<0.01, ***p<0.001; n=4-6; 0-15: strain magnitude; PLL = poly-l-lysine, LN = laminin, COL = collagen I, FN = fibronectin, cECM = naturally-derived cardiac extracellular matrix.

5.2.6 Maturation of CPCs

To determine if matrix or strain conditions affect the differentiation and maturation of CPCs, cells were seeded as described in the methods and then harvested with either Trizol or NP-40 lysis buffer for qPCR and Western. Cardiac transcription factors gata-4 and nkx2.5, as well as the more mature cardiomyogenic markers troponinT1 and troponinT2 were detected in all culture conditions by qPCR. Data is summarized in Figure 16. While the qPCR results were promising, the sample size was too small to draw conclusions and further qPCR needs to be performed.

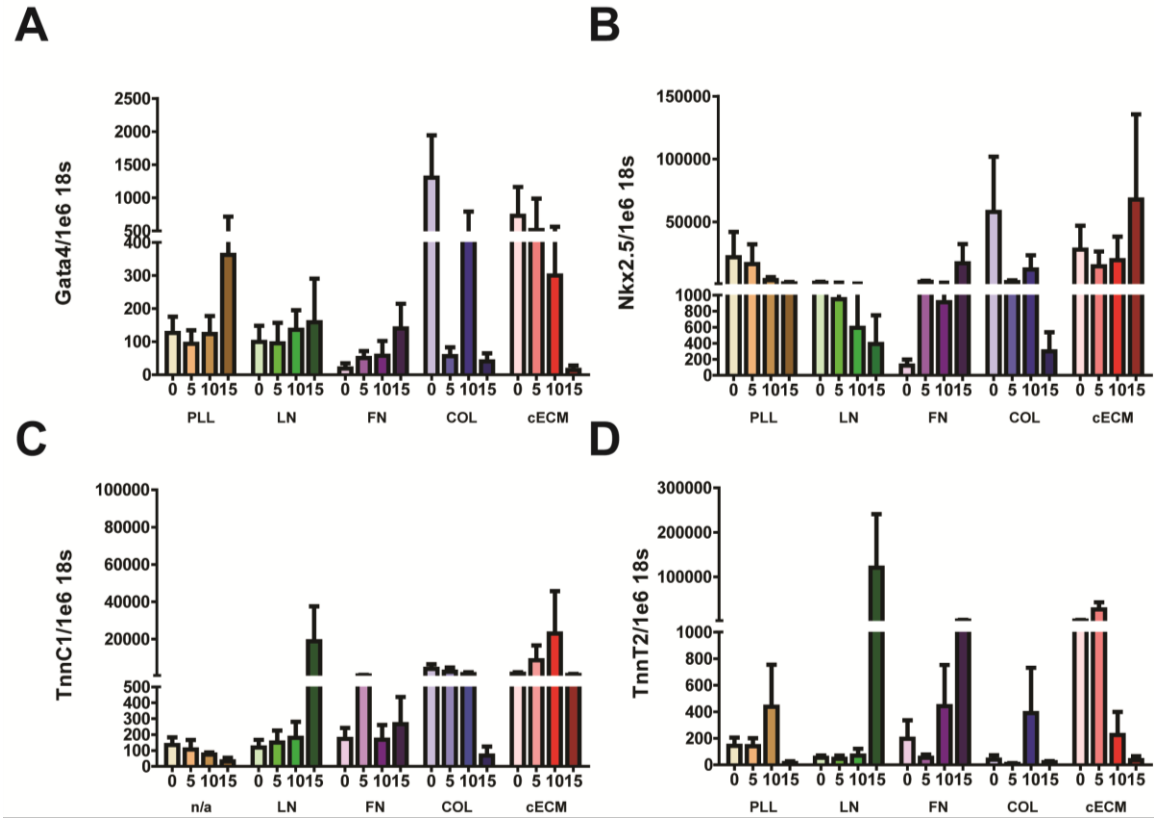

Figure 16. CPC cardiomyogenic differentiation by qPCR. CPCs were seeded on the appropriate matrix for 6 hours and then cyclic strain was applied for 24 hours. (A) Gata-4. (B) Nkx2.5. (C) TnnC1. (D) TnnT2. (A-D) Two-way ANOVA, bars represent mean + SEM; ns; n=2-5; 5-10: strain magnitude; PLL = poly-l-lysine, LN = laminin, COL = collagen I, FN = fibronectin, cECM = naturally-derived cardiac extracellular matrix; TnnC1 = troponin C1, TnnT2 = troponin T2.

5.2.6.1 Connexin 43 Expression

Connexin 43 (Cnx43), a component of gap junctions, was also detected by qPCR (Figure 40). Western blot analysis for Cnx43 revealed that Cnx43 expression had an overall dependency on matrix ($p<0.001$) and strain ($p<0.05$) conditions, without a significant interaction by two-way ANOVA. Representative blots and analysis by two-way ANOVA are shown in Figure 17. Analysis of individual strain magnitudes by one-way ANOVA shows that unstrained CPCs cultured on FN had more Cnx43 (1.4-fold over

GAPDH) than those cultured on PLL (1.0-fold; $p<0.05$), LN (0.9-fold; $p<0.05$) and cECM (1.0-fold; $p<0.05$). COL (1.3-fold) induced higher Cx43 expression as compared to LN only ($p<0.05$). At 5% strain, higher Cnx43 expression was maintained on FN (1.2-fold) as compared to PLL (0.6-fold; $p<0.05$). At 10 and 15% strains, Cnx43 expression was not-matrix dependent. Strain-dependent effects of Cnx43 expression were not observed for CPCs cultured on PLL, LN nor FN. However, Cnx43 expression decreased with increasing strain for CPCs on COL (0 v 5%: $p<0.01$, 0 v 15%: $p<0.01$) and cECM (0 v 10%: $p<0.01$, 0 v 15%: $p<0.01$, 5 v 15%: $p<0.05$). Analysis by one-way ANOVA is reported in Figure 18.

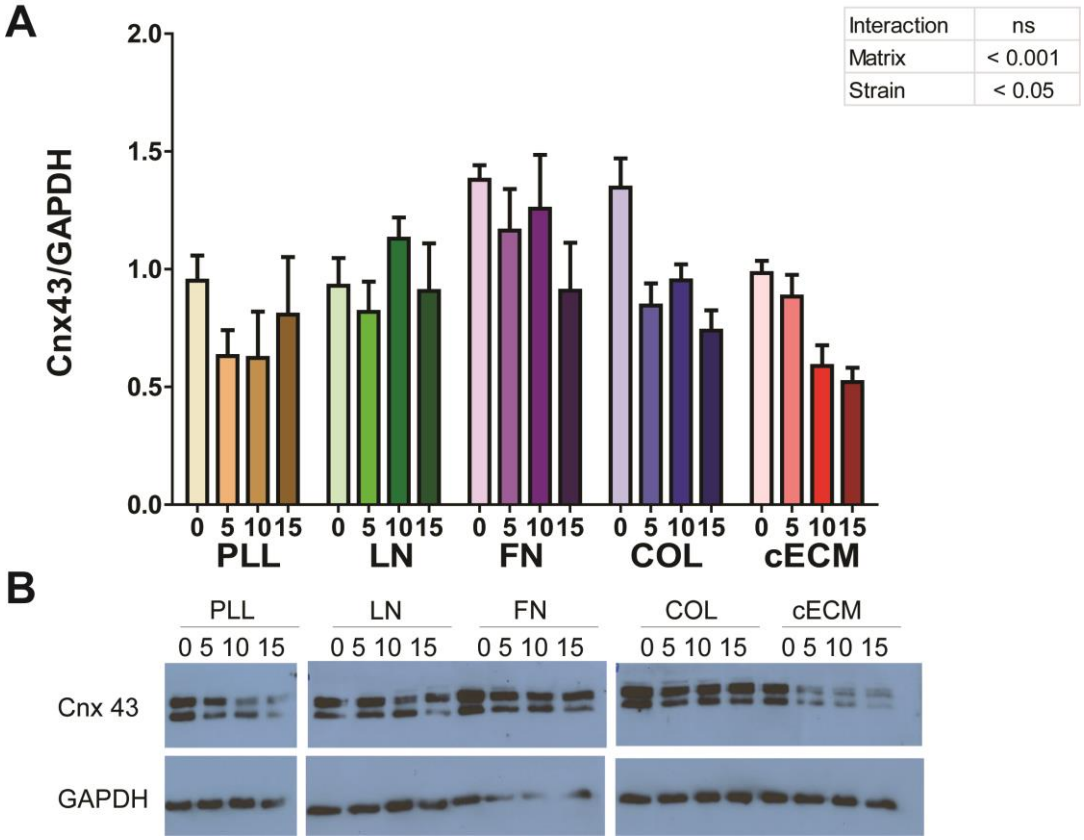

Figure 17. Cnx43 expression in CPCs. CPCs were seeded on the appropriate matrix for 6 hours and then cyclic strain was applied for 24 hours. Cell lysate was evaluated by Western. (A) Quantification by densitometry; Two-way ANOVA, bars represent mean + SEM; (B) Representative blots. n=4-7; 0-15: strain magnitude; Cnx43= connexin 43, PLL

= poly-l-lysine, LN = laminin, COL = collagen I, FN = fibronectin, cECM = naturally-derived cardiac extracellular matrix.

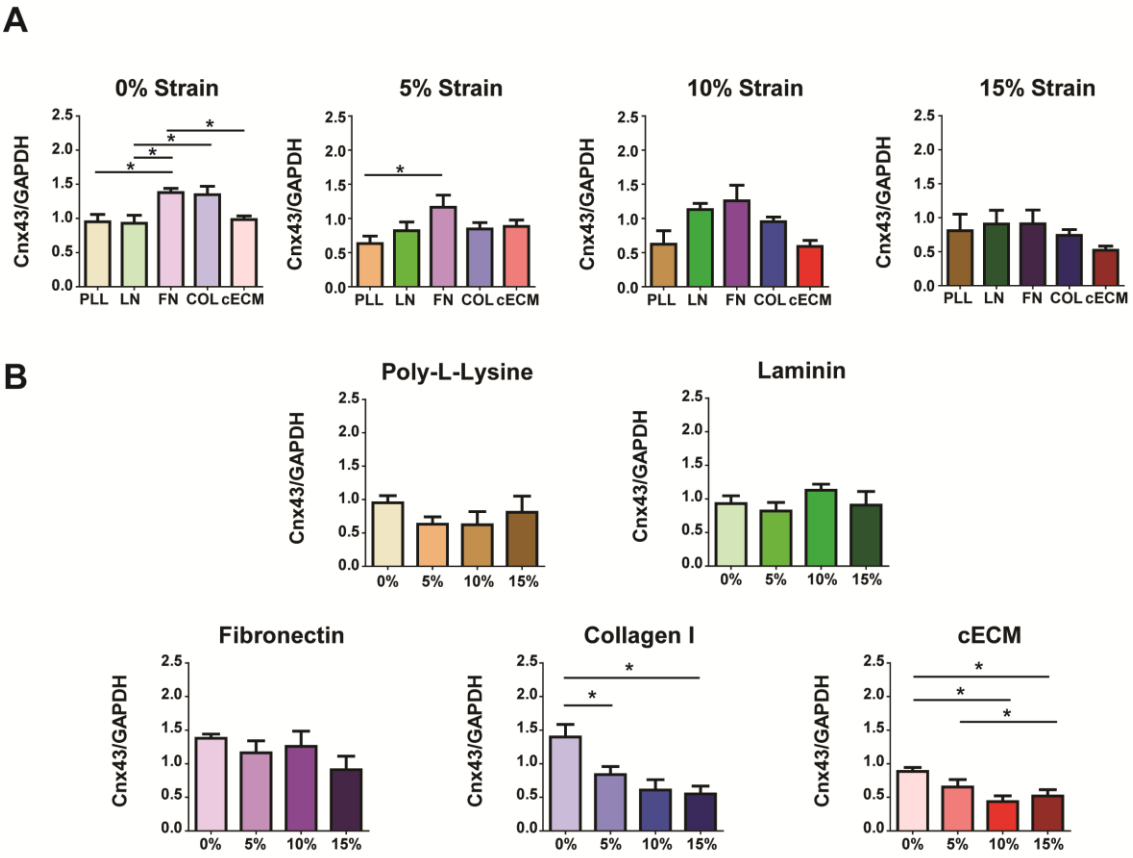

Figure 18. Cnx43 expression in CPCs assessed by one-way ANOVA. CPCs were seeded on the appropriate matrix for 6 hours and then cyclic strain was applied for 24 hours. (A) Matrix effects. (B) Strain magnitude effects. (A-B) One-way ANOVA with Tukey's multiple comparison test, bars represent mean + SEM; *p<0.05; n=4-7; 0-15: strain magnitude; Cnx43= connexin 43, PLL = poly-l-lysine, LN = laminin, COL = collagen I, FN = fibronectin, cECM = naturally-derived cardiac extracellular matrix.

5.2.6.2 Number of Nuclei

As a further way to identify the maturation of CPCs, cells with more than one nucleus where counted. These cells appeared distinct from dividing cells as the nuclei were

spread and the cytoplasm appeared continuous. Samples images are shown in Figure 14. Arrow head indicates cell with more than one nucleus. Less than 1% of all cells viewed contained more than one nucleus. Strain had an overall effect ($p<0.05$) by two-way ANOVA, the effect of matrix was not significant and no interaction was observed. Quantification and analysis by two-way ANOVA are shown in Figure 19. For CPCs seeded on FN, more cells with >1 nucleus were observed at 5% (1.2% cells >1 nucleus) than 15% (0.4% cells >1 nucleus) strain ($p<0.05$) by one-way ANOVA. Similarly, on COL 5% (1.0% cells >1 nucleus) strain groups showed more cells >1 nucleus than unstrained groups (0.4% cells >1 nucleus; $p<0.05$). Analysis by one-way ANOVA is reported in Figure 20. For cells that we observed to have more than one nucleus, the nuclei remain near each other, sometimes touching, and are sometimes oriented along the different axes.

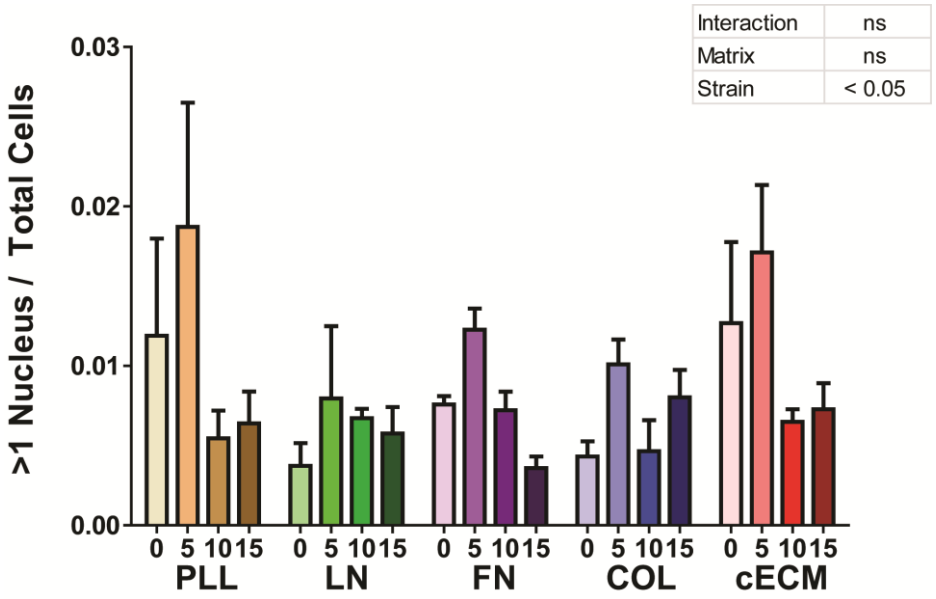

Figure 19. Quantification of CPCs with more than one nucleus. CPCs were seeded on the appropriate matrix for 6 hours and then cyclic strain was applied for 24 hours. Two-way ANOVA, bars represent mean + SEM; n=3-9; 0-15: strain magnitude; PLL = poly-l-lysine, LN = laminin, COL = collagen I, FN = fibronectin, cECM = naturally-derived cardiac extracellular matrix.

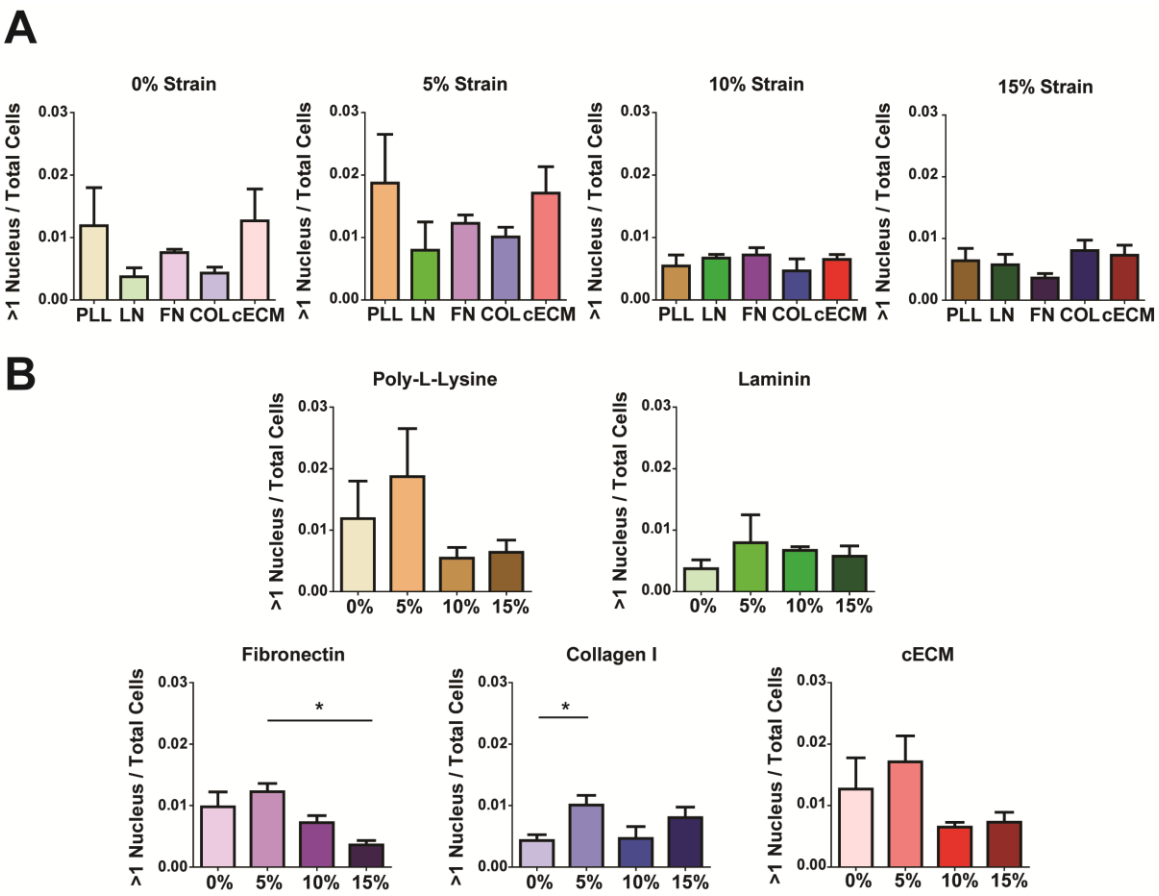

Figure 20. Quantification of CPCs with more than one nucleus by one-way ANOVA. CPCs were seeded on the appropriate matrix for 6 hours and then cyclic strain was applied for 24 hours. (A) Matrix effects. (B) Strain magnitude effects. (A-B) One-way ANOVA with Tukey's multiple comparison test , bars represent mean + SEM; *$p<0.05$; n=3-9; 0-15: strain magnitude; PLL = poly-l-lysine, LN = laminin, COL = collagen I, FN = fibronectin, cECM = naturally-derived cardiac extracellular matrix.

5.2.6.3 Calcium Oscillations

To determine if culture of CPCs on distinct extracellular matrices altered their calcium handling, cultured cells were loaded with Fluo-4, electrically stimulated (1 Hz) and viewed under epifluorescence. While rare, CPCs that paced with increasing stimulation frequency were observed as shown in Figure 44. Calcium handling is a useful endpoint

as it is a better functional representation of cardiomyogenic maturation than qPCR. Upon electrical stimulation, a marked increase in cytoplasmic calcium levels was observed on all matrices (data not shown). As shown in Figure 21, the percent of active CPCs (cells with calcium oscillations) and the number of oscillation per active cell in 90 seconds was quantified for videos acquired after initial stimulation. More active CPCs were observed after overnight culture on FN (54%; $p<0.05$), COL (60%; $p<0.01$) or cECM (55%; $p<0.05$) as compared to PLL (19%) by one-way ANOVA. Similarly, the number of oscillations per active cell was increased on FN (1.5 osc; $p<0.05$), COL (1.4 osc; $p<0.05$) and cECM (1.4 osc; $p<0.05$) as compared to PLL (0.6 osc). Intermediate levels of active CPCs (38%) and oscillations (1.1 osc) were observed on LN. CPCs that had been strained could not be assessed by this method without enzymatic disruption due to the thickness of the PDMS Bioflex membranes and the working distance of the objective used.

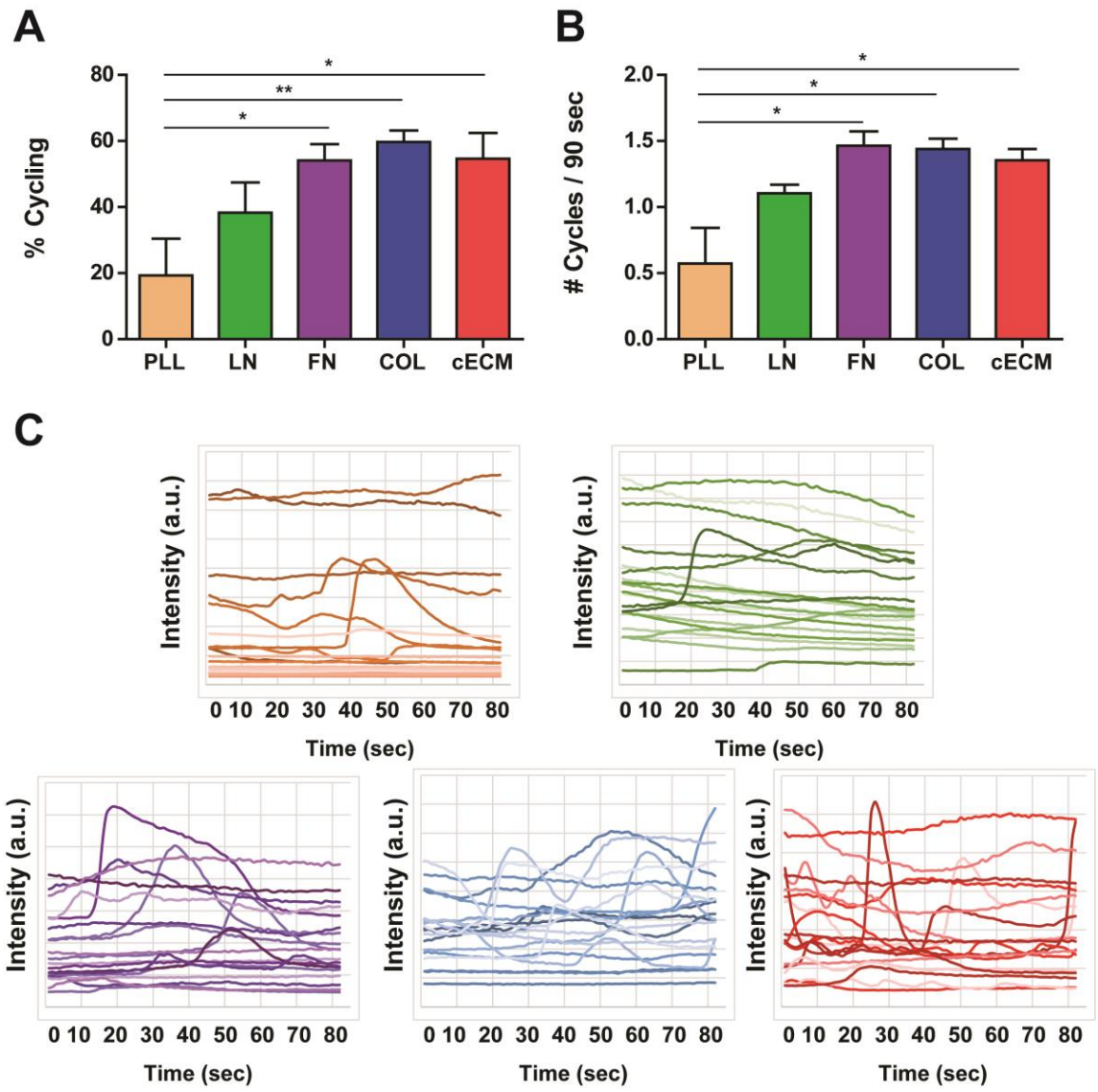

Figure 21. Calcium Oscillations in CPCs. CPCs were seeded on the appropriate matrix overnight. Calcium oscillations were evaluated by Fluo-4. (A) Percent of active cells. (B) Average number of oscillations in time period; (C) Representative traces of calcium oscillations: PLL (orange), LN (green), FN (purple), COL (blue), cECM (red); One-way ANOVA with Tukey's multiple comparison test, bars represent mean + SEM; *$p<0.05$, **$p<0.01$; n=5-6; PLL = poly-l-lysine, LN = laminin, COL = collagen I, FN = fibronectin, cECM = naturally-derived cardiac extracellular matrix.

5.2.7 Paracrine Signaling

To evaluate potential paracrine signaling, CPCs were seeded as described in the methods and conditioned media was collected after 24 hours. Commercial ELISAs were performed for vascular endothelial growth factor A (VEGF), platelet-derived growth factor BB (PDGF), hepatocyte growth factor (HGF) and stem cell factor (SCF). Neither PDGF nor SCF were detected in the conditioned media. VEGF was detected in conditioned media on the order of hundreds of pg/mL and is observed to be matrix ($p<0.05$) and strain ($p<0.001$) dependent, without an interaction by two-way ANOVA. However, by one-way ANOVA, no differences in VEGF were detected in the media of CPCs cultured on different matrices for a given strain magnitude. Summarized results are reported in Figure 22. Conditioned media from CPCs cultured on PLL contained more VEGF at 5 (955 pg/mL) and 10% (998 pg/mL) strains as compared to the matrix-matched unstrained group (515 pg/mL; $p<0.05$). There was a marked difference in the presence of VEGF in conditioned media from CPCs cultured on LN in the presence of 5, 10 and 15% (730, 729 and 699 pg/mL, respectively) strain as compared to unstrained groups (159 pg/mL; $p<0.01$). Conditioned media from CPCs strained 10% (1048 pg/mL) on cECM also showed higher VEGF than unstrained controls (420 pg/mL; $p<0.05$). VEGF was also detected by qPCR (Figure 40). As shown in Figure 23, HGF was detected in the conditioned media in smaller quantities (<10 ug/mL). By two-way ANOVA, the presence of HGF is not observed to be matrix nor strain dependent. However, by one-way ANOVA strain increased HGF presence in conditioned media for CPCs cultured on PLL (0 v 10%: 1.5 v 7.3 pg/mL; $p<0.01$, 5 v 10%: 2.4 v 7.3 pg/mL; $p<0.05$). The opposite was observed on FN (10 v 15%: 8.1 v 1.8 pg/mL; $p<0.05$) and COL (5 v 10%: 7.6 v 2.4 pg/mL; $p<0.05$), where increasing strain values demonstrated a drop in HGF in the media. No effects are observed between matrix conditions for individual strain magnitudes by one-way ANOVA.

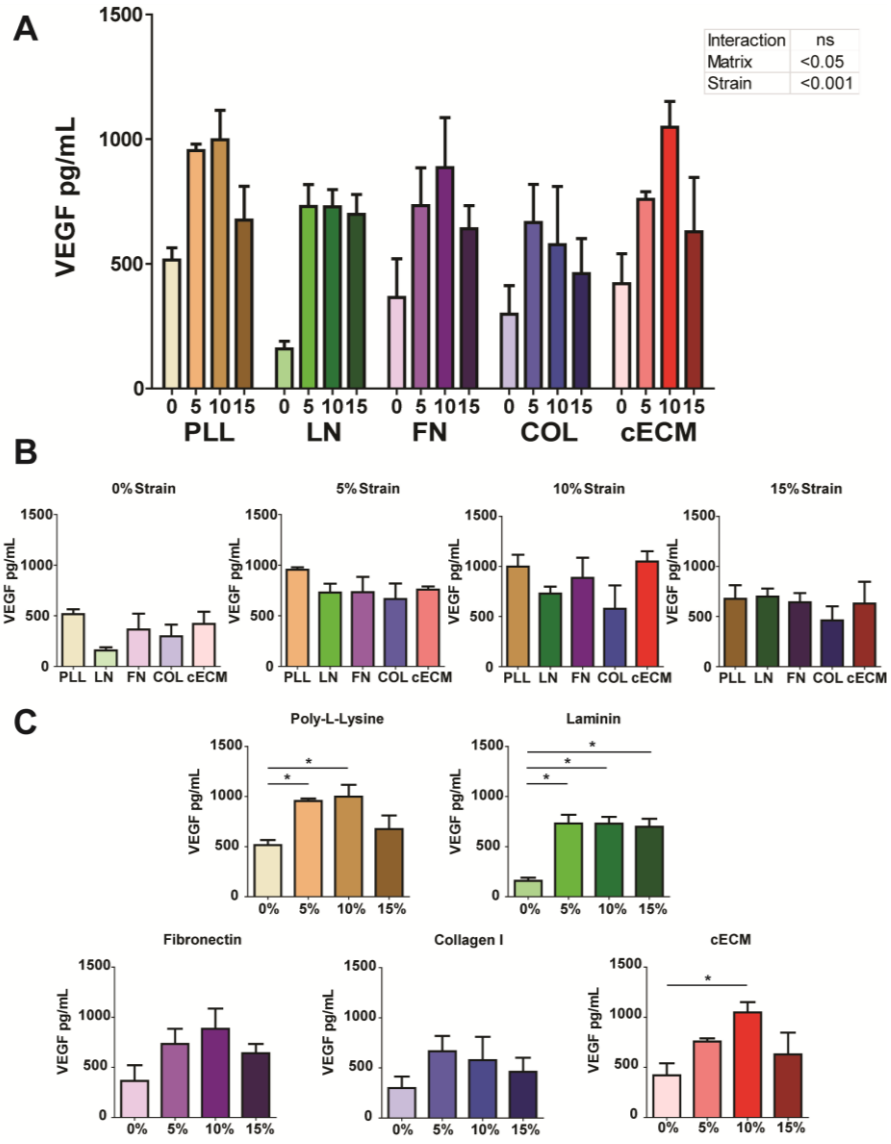

Figure 22. Concentration of VEGF in CPC conditioned media. CPCs were seeded on the appropriate matrix for 6 hours and then cyclic strain was applied for 24 hours. Conditioned media was evaluated by ELISA; (A) Two-way ANOVA. (B) Matrix effects. (C) Strain magnitude effects. (B-C) One-way ANOVA with Tukey's multiple comparison test, bars represent mean + SEM, *p<0.05; n=3-4; 0-15: strain magnitude; VEGF = vascular endothelial growth factor, PLL = poly-l-lysine, LN = laminin, COL = collagen I, FN = fibronectin, cECM = naturally-derived cardiac extracellular matrix.

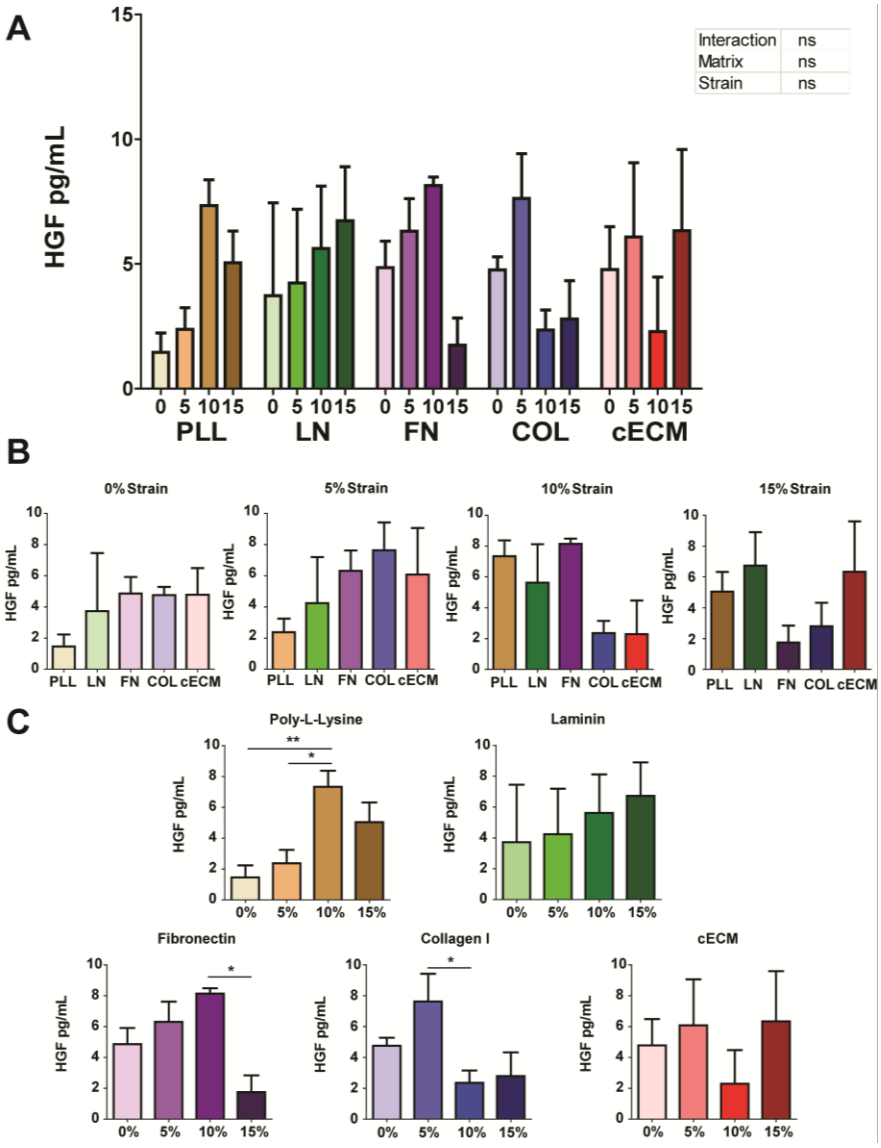

Figure 23. Concentration of HGF in CPC conditioned media. CPCs were seeded on the appropriate matrix for 6 hours and then cyclic strain was applied for 24 hours. Conditioned media was evaluated by ELISA. (A) Two-way ANOVA. (B) Matrix effects. (C) Strain magnitude effects. (B-C) One-way ANOVA with Tukey's multiple comparison test, bars represent mean + SEM, *p<0.05; n=2-4; 0-15: strain magnitude; HGF = hepatocyte growth factor, PLL = poly-l-lysine, LN = laminin, COL = collagen I, FN = fibronectin, cECM = naturally-derived cardiac extracellular matrix.

Additionally, the conditioned media was evaluated for the presence of inflammatory cytokines by luminex array for CPCs seeded on FN and cECM and strained either 5 or 15% (Figure 24). The sample size was too small to draw conclusions between groups, but the absence or presence of each cytokine was determined. Interleukin 1alpha, interferon gamma and tumor necrosis factor alpha were below the detectable limit. Small amounts (1-10 pg/mL) of interleukins -10, -6, -1b and -12 were detected. Interestingly, monocyte chemotactic protein 1 was highly present in the media (>75,000 pg/mL).

A

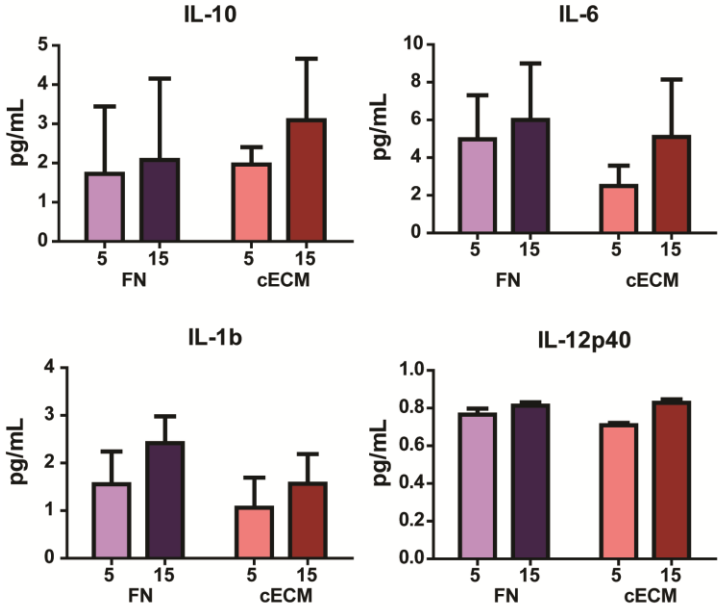

B

Analyte	Conc. Range (pg/mL)
IL-1alpha	0
IL-10	1-6
IL-6	1-10
IL-1b	1-4
IFN-y	0
IL-12p40	<1
TNF-alpha	0
MCP-1	Max intensity (75,000)

Figure 24. Luminex Panel Results. CPCs were seeded on the appropriate matrix for 6 hours and then cyclic strain was applied for 24 hours. Conditioned media was evaluated for cytokines. (A) Grouped data. (B) Analysis summary. Two-way ANOVA, bars represent mean + SEM; n=3; 5-15 = strain magnitude, IL = interleukin, MCP = monocyte chemoattractant protein, FN = fibronectin, cECM = naturally-derived cardiac extracellular matrix.

5.2.8 Cell Strain

To offer insight into the mechanism by which changes are induced in this setup, the composite strain experienced by single cells was evaluated by video microscopy. Schematics for experimental set-up and data analysis are shown in Figure 25. Unlike the Bioflex, the StageFlexer was unable to generate the programmed strains. For a 5% programmed strain, the Flexcell reported generation of 3.5% strain; for 10% programmed strain, 7.0% generated strain was reported and for 15% programmed strain, 8.4% generated strain was reported on the StageFlexer. These values are lower than the 4, 9 and 14% strains reported, respectively, in the 6-well Bioflex format. Cells oriented

parallel to the principle direction of strain were evaluated when possible to ensure a consistent and maximal strain was applied.

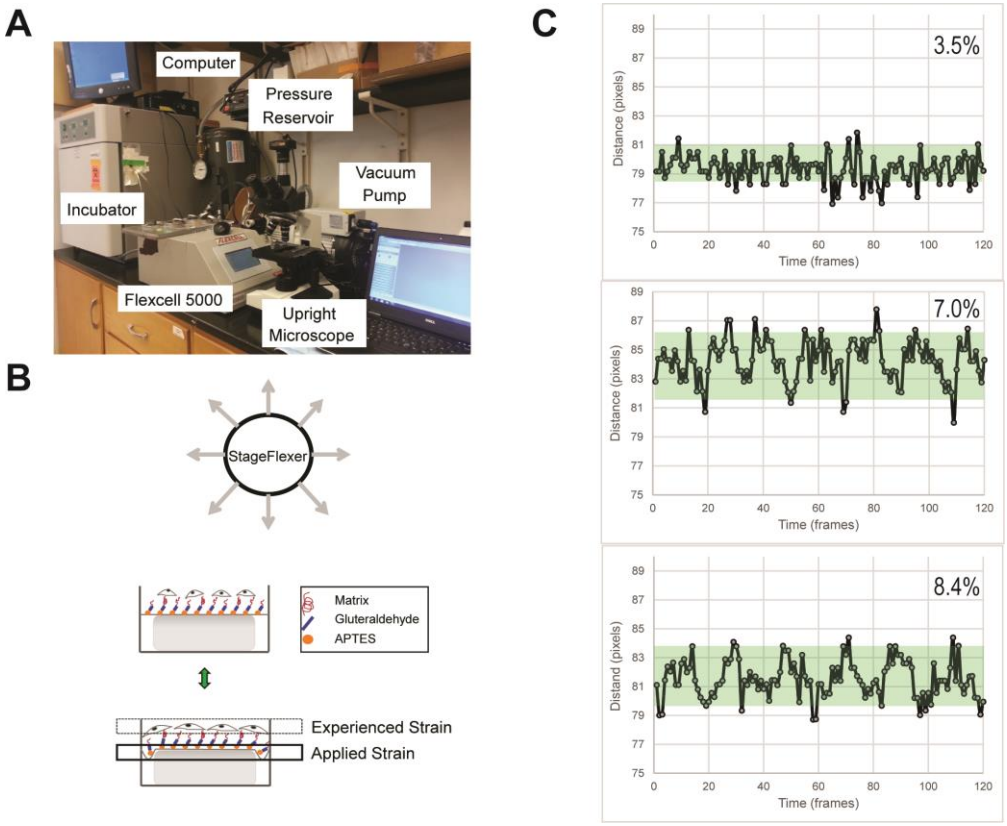

Figure 25. Cell Strain Experimental Set-up. (A) Workstation. (B) Schematic. (C) Representative tracings from CPCs cultured on cECM; programmed strain is reported on graph.

The slopes and y-intercepts for best-fit lines relating measured strain to reported strain were not different for matrix conditions. By two-way ANOVA, measured strains were not dependent on matrix, but were highly strain-dependent ($p<0.001$), with no interaction. One-way ANOVAs were performed to examine the effect of matrix at each strain magnitude and revealed that measured strain was independent of matrix condition. When each matrix condition was separately evaluated, the increase in measured strain was significant for LN (5 v 10% programmed: 4.0% v 7.7% measured; $p<0.01$), FN (5 v 10%

programmed: 3.8% v 7.7% measured; $p<0.001$) and cECM (5 v 10% programmed: 4.6% v 7.0% measured; $p<0.05$). Interestingly, while there was an increase in measured strain from 5 to 15% programmed strain (4.6% v 7.6% measured) for cECM ($p<0.01$), there was a decrease in measured strain on FN (10 v 15% programmed: 7.6% v 4.9% measured; $p<0.01$) and a similar trend on LN. For PLL, there was a trend toward increased measured strain at 10 and 15% relative to 5%. For COL, there was larger variability in the data than for other matrices; however, there was a trend for increased measured strain at 10% relative to 5%. Cell strain data is reported in Figure 26.

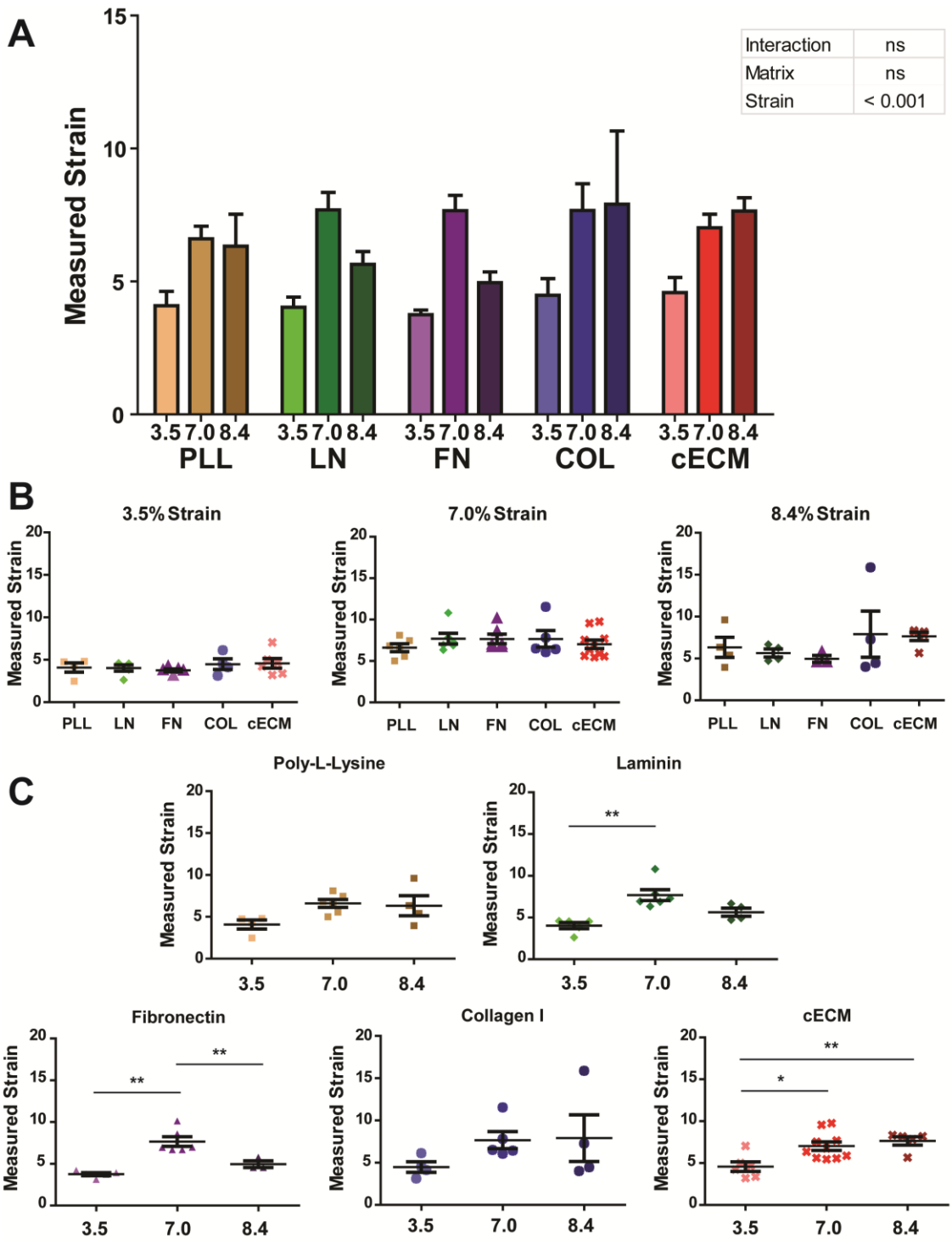

Figure 26. Cell Strain. CPCs were seeded on the appropriate matrix for 6 hours. Videomicroscopy captured the motion of beads tethered to CPCs under cyclic strain. (A) Two-way ANOVA. (B) Matrix effects. (C) Strain magnitude effects. (B-C) One-way

ANOVA with Tukey's multiple comparison test, bars represent mean + SEM, *$p<0.05$, $p<0.01$; n=3-10; 0-15: strain magnitude; PLL = poly-l-lysine, LN = laminin, COL = collagen I, FN = fibronectin, cECM = naturally-derived cardiac extracellular matrix.

5.2.9 Biochemical Mechanotransduction

To establish if the matrix and strain conditions alter biochemical signaling through focal adhesion kinase (FAK) and extracellular signal-regulated kinase (ERK) as a potential means of mechanotransduction, cells were seeded as described in the methods and lysed at varying time points with NP-40 lysis buffer for Western blot analysis. The presence of integrin beta1 was also evaluated by Western blot and qPCR.

CPCs were seeded on each of the matrices and allowed to adhere for 20 minutes before lysis to evaluate the initial role of FAK and ERK in cell attachment and spreading. In this time the cells were visibly adhered to the plates, but remained rounded. FAK and ERK were both activated at this timepoint as determined by presence of phosphorylated FAK (pFAK) and ERK (pERK), but the effects were not dependent on matrix. Cells in suspension were not evaluated, so it is unclear if the levels of pFAK and pERK observed indicate increased activation over basal conditions. Next, CPCs were seeded as described above, allowed to adhere for 6 hours and then mechanically strained for 15 minutes, to evaluate if strain would further activate FAK and ERK. By two-way ANOVA, the ratio of phosphorylated to total FAK was matrix ($p<0.05$), but not strain dependent and there was no observed interaction. Representative blots and quantification is shown in Figure 27. Including the initial adhesion data in this analysis, there were no significant changes observed for pFAK/FAK across matrices or strain magnitudes by one-way ANOVA. Analysis by one-way ANOVA is reported in Figure 28. This indicates that FAK signaling was maintained, but not increased by strain.

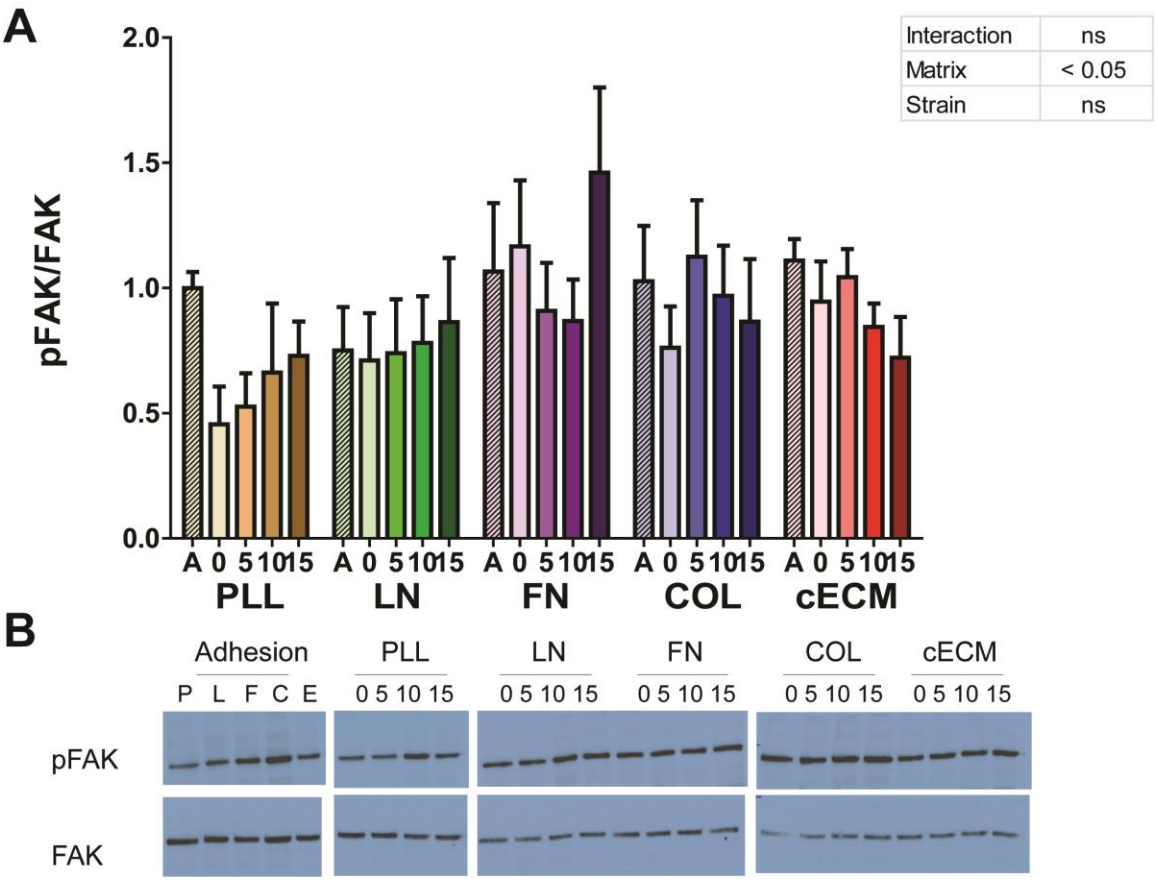

Figure 27. Acute FAK activation in CPCs. CPCs were seeded on the appropriate matrix for 20 minutes (hash bars) and lysed or 6 hours followed by 15 minutes of cyclic strain and lysed. Cell lysate was evaluated by Western. (A) Quantification by densitometry; Two-way ANOVA, bars represent mean + SEM; (B) Representative blots. n=4-5; 0-15: strain magnitude; FAK = focal adhesion kinase, PLL = poly-l-lysine, LN = laminin, COL = collagen I, FN = fibronectin, cECM = naturally-derived cardiac extracellular matrix.

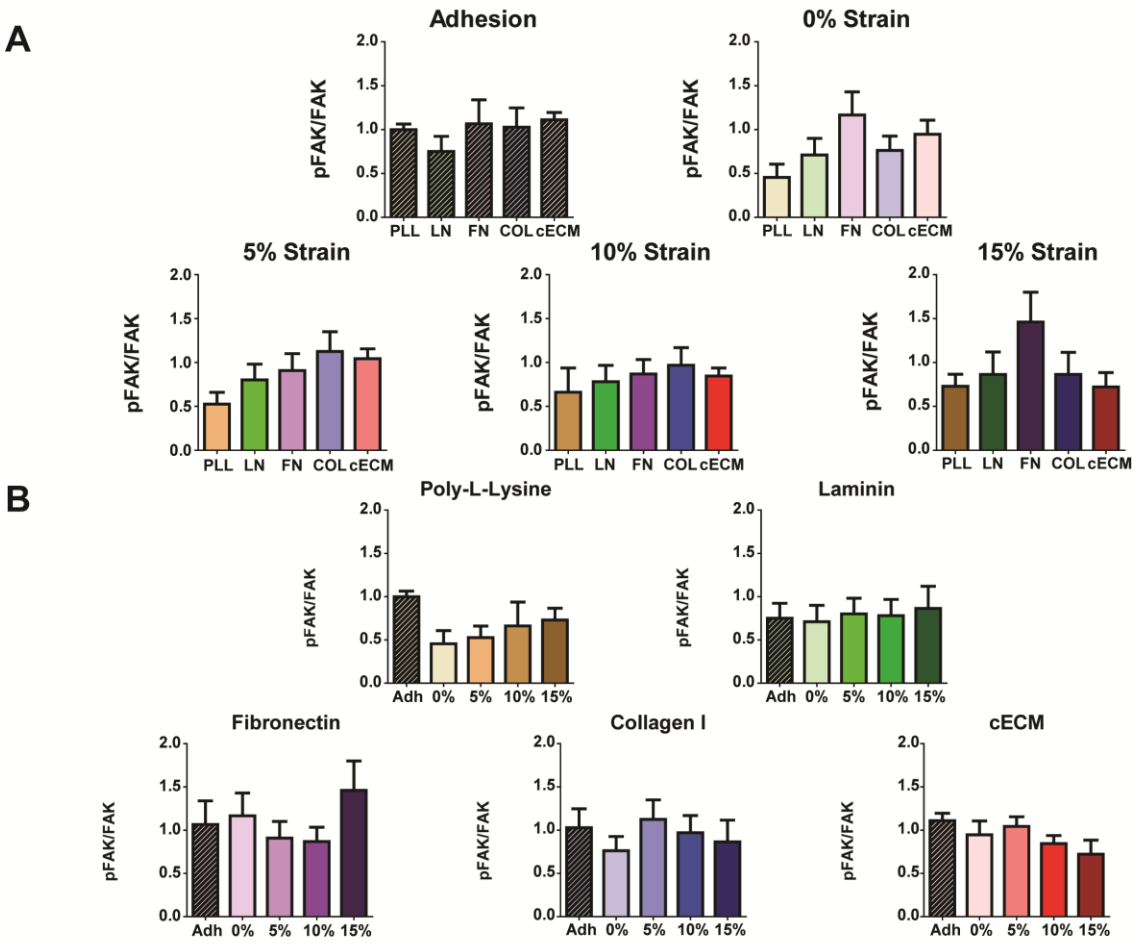

Figure 28. Acute FAK activation in CPCs assessed by one-way ANOVA. CPCs were seeded on the appropriate matrix for 20 minutes (hash bars) and lysed or 6 hours followed by 15 minutes of cyclic strain and lysed. Cell lysate was evaluated by Western. (A) Matrix effects. (B) Strain magnitude effects. (A-B) One-way ANOVA with Tukey's multiple comparison test, bars represent mean + SEM; n=4-5; 0-15: strain magnitude; FAK = focal adhesion kinase, PLL = poly-l-lysine, LN = laminin, COL = collagen I, FN = fibronectin, cECM = naturally-derived cardiac extracellular matrix.

Similarly as shown in Figure 29, by two-way ANOVA, the ratio of phosphorylated to total ERK was matrix (<0.001), but not strain dependent with an observed interaction

($p<0.05$). Further analysis by one-way ANOVA for individual strain or matrix groups showed matrix-dependent effects were more prominent for unstrained and 5% strain groups. Results are reported in Figure 30. For unstrained CPCs, pERK/ERK was greatest on PLL (1.8-fold) and COL (1.8-fold), although these groups were not statistically different from cECM (1.3-fold). Nearly twice the phosphorylation was observed for unstrained CPCs on PLL and COL as compared to LN (1.0-fold; $p<0.05$) or FN (0.8-fold; $p<0.05$). At 5% strain however, the highest pERK/ERK was observed for PLL (1.9-fold) and cECM (1.8-fold), although these groups again were not statistically different from COL (1.1-fold). Twice the phosphorylation was observed for PLL and cECM as compared to LN (0.9-fold; $p<0.05$) and FN (0.8-fold; $p<0.05$). The pERK/ERK ratio does not have a matrix-dependent effect at 10% and at 15% the phosphorylation observed for cECM (1.8-fold) only is 2.3-fold greater than FN (0.8-fold; $p<0.05$). Within each matrix, strain did not have a significant effect on ERK phosphorylation.

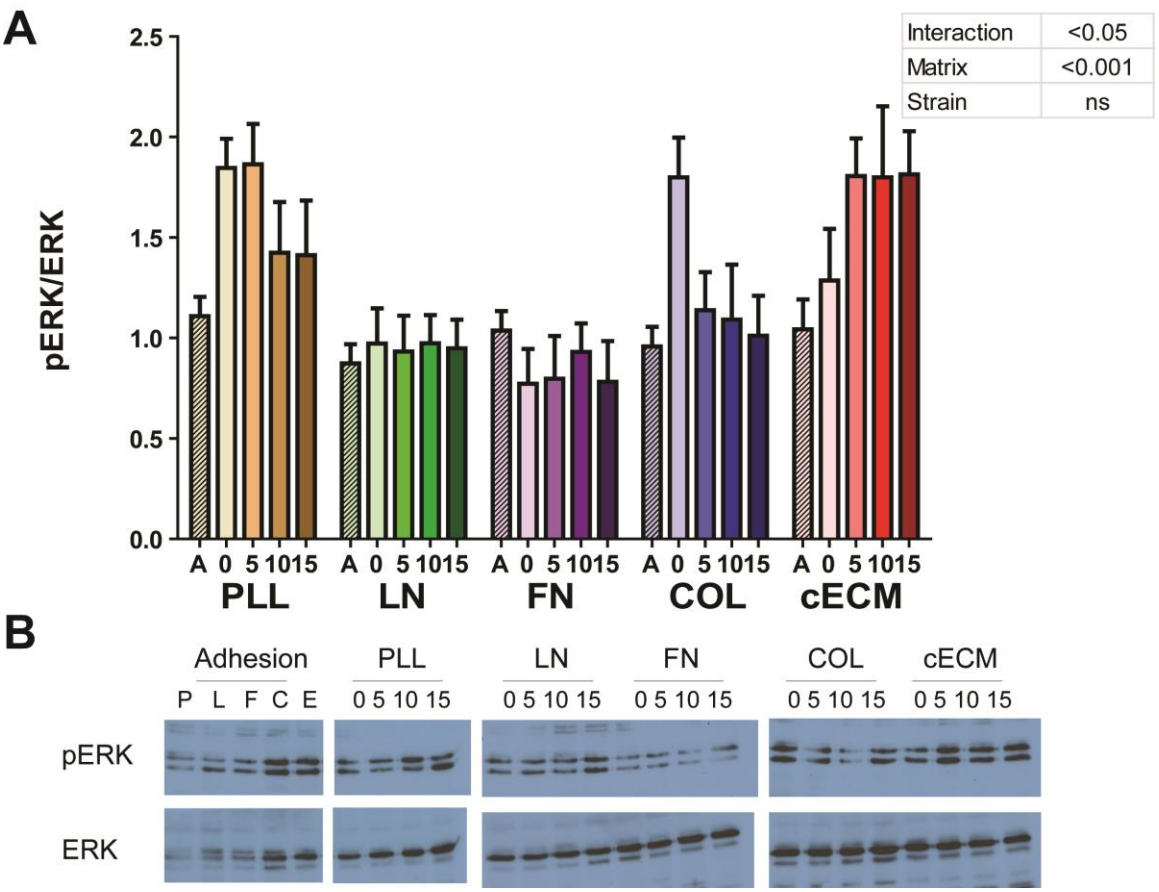

Figure 29. Acute ERK activation in CPCs. CPCs were seeded on the appropriate matrix for 20 minutes (hash bars) and lysed or 6 hours followed by 15 minutes of cyclic strain and lysed. Cell lysate was evaluated by Western. (A) Quantification by densitometry; Two-way ANOVA, bars represent mean + SEM; (B) Representative blots. n=4-5; 0-15: strain magnitude; ERK = extracellular signal-regulated kinase, PLL = poly-l-lysine, LN = laminin, COL = collagen I, FN = fibronectin, cECM = naturally-derived cardiac extracellular matrix.

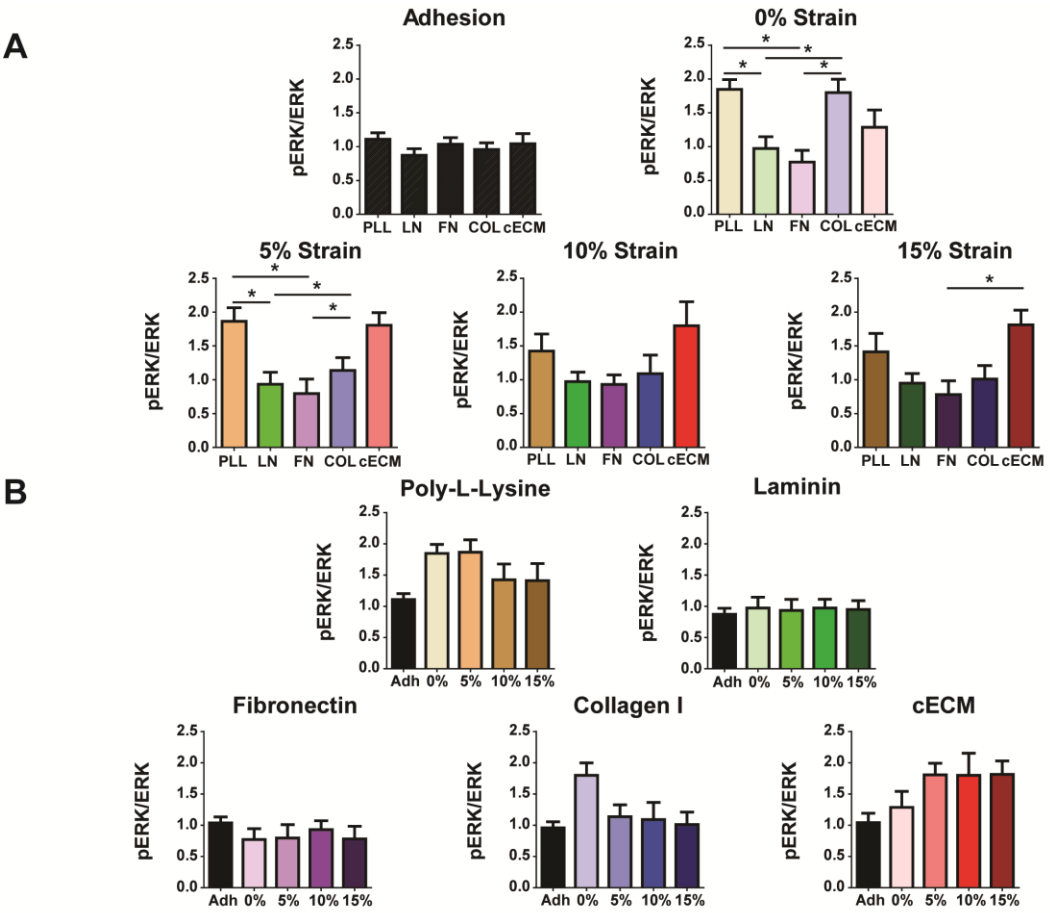

Figure 30. Acute ERK activation in CPCs assessed by one-way ANOVA. CPCs were seeded on the appropriate matrix for 20 minutes (hash bars) and lysed or 6 hours followed by 15 minutes of cyclic strain and lysed. Cell lysate was evaluated by Western. (A) Matrix effects. (B) Strain magnitude effects. (A-B) One-way ANOVA with Tukey's multiple comparison test, bars represent mean + SEM; *p<0.05; n=4-5; 0-15: strain magnitude; ERK = extracellular signal-regulated kinase, PLL = poly-l-lysine, LN = laminin, COL = collagen I, FN = fibronectin, cECM = naturally-derived cardiac extracellular matrix.

To determine if this signaling was transient or maintained throughout the length of this study, lysate was again collected at 24 hours. In line with the shorter time points, phosphorylation of FAK was matrix ($p<0.01$), but not strain dependent as determined by two-way ANOVA (no interaction). Representative blots and results are shown in Figure 31. For unstrained CPCs, the pFAK/FAK ratio was not affected by matrix condition. At 5% strain, there was twice as much pFAK/FAK for CPCs on FN (0.9-fold) as compared to cECM (0.4-fold; $p<0.05$). At 10% strain, pFAK/FAK was two-fold higher on FN (1.1-fold) than PLL (0.4-fold; $p<0.01$), LN (0.5-fold; $p<0.05$) and cECM (0.6-fold; $p<0.05$), but not different than COL (1.0-fold). COL had twice the pFAK/FAK as compared to PLL ($p<0.05$). These effects were diminished at 15% strain. Strain did not affect pFAK/FAK for any matrix conditions except for cECM, where there was a decrease at 5 and 15% (both 0.4-fold) strains as compared to unstrained CPCs (0.8-fold; $p<0.05$). Analysis by one-way ANOVA is reported in Figure 32. Phophorylation of ERK was not evaluated at this timepoint. As the amount of available FAK might affect its activation, total FAK protein levels were evaluated at 24 hours. The levels of FAK were unchanged across groups except for a spike in unstrained CPCs cultured on LN (0.9-fold over GAPDH) as compared to PLL (0.5-fold) and FN (0.5-fold; $p<0.05$). Analysis of FAK expression by two-way ANOVA and one-way ANOVA are reported in Figure 33 and Figure 34, respectively.

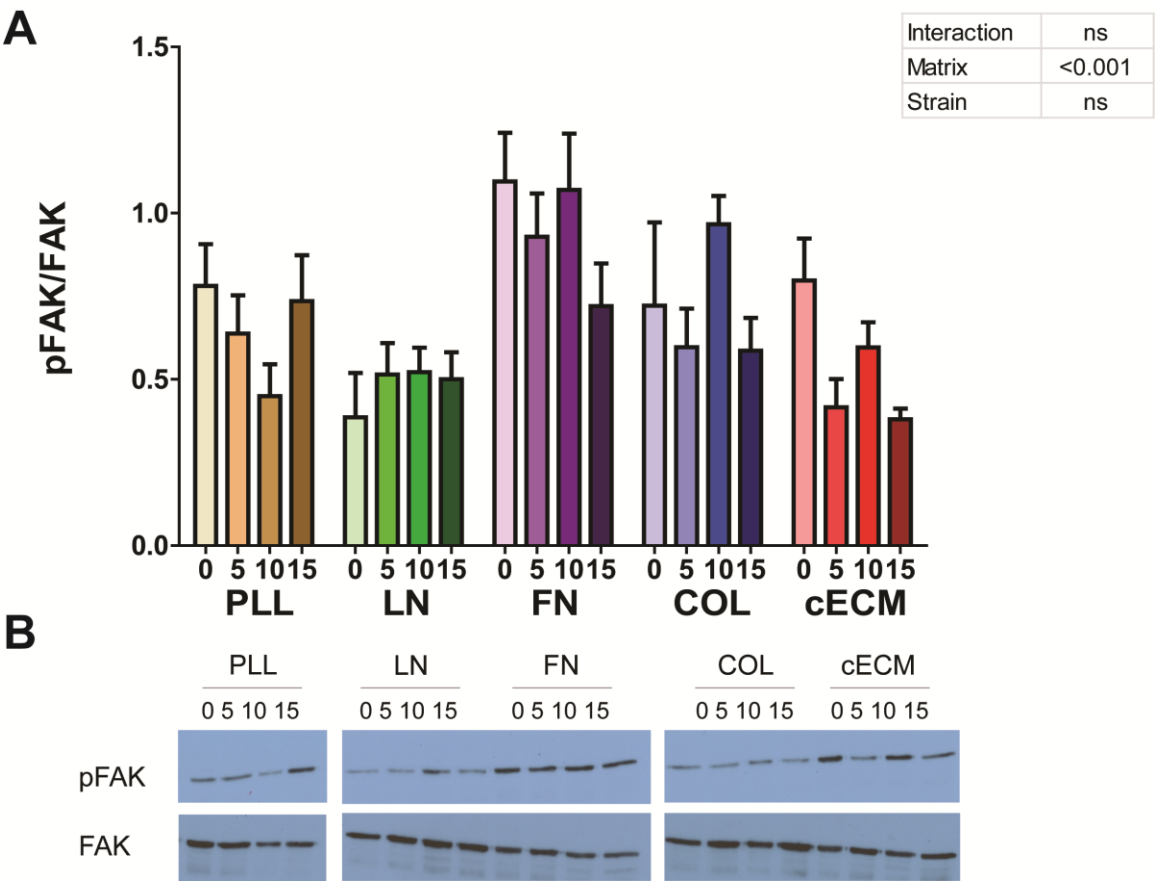

Figure 31. FAK activation in CPCs. CPCs were seeded on the appropriate matrix for 6 hours and then cyclic strain was applied for 24 hours. Cell lysate was evaluated by Western. (A) Quantification by densitometry; Two-way ANOVA, bars represent mean + SEM; (B) Representative blots. n=4-6; 0-15: strain magnitude; FAK = focal adhesion kinase, PLL = poly-l-lysine, LN = laminin, COL = collagen I, FN = fibronectin, cECM = naturally-derived cardiac extracellular matrix.

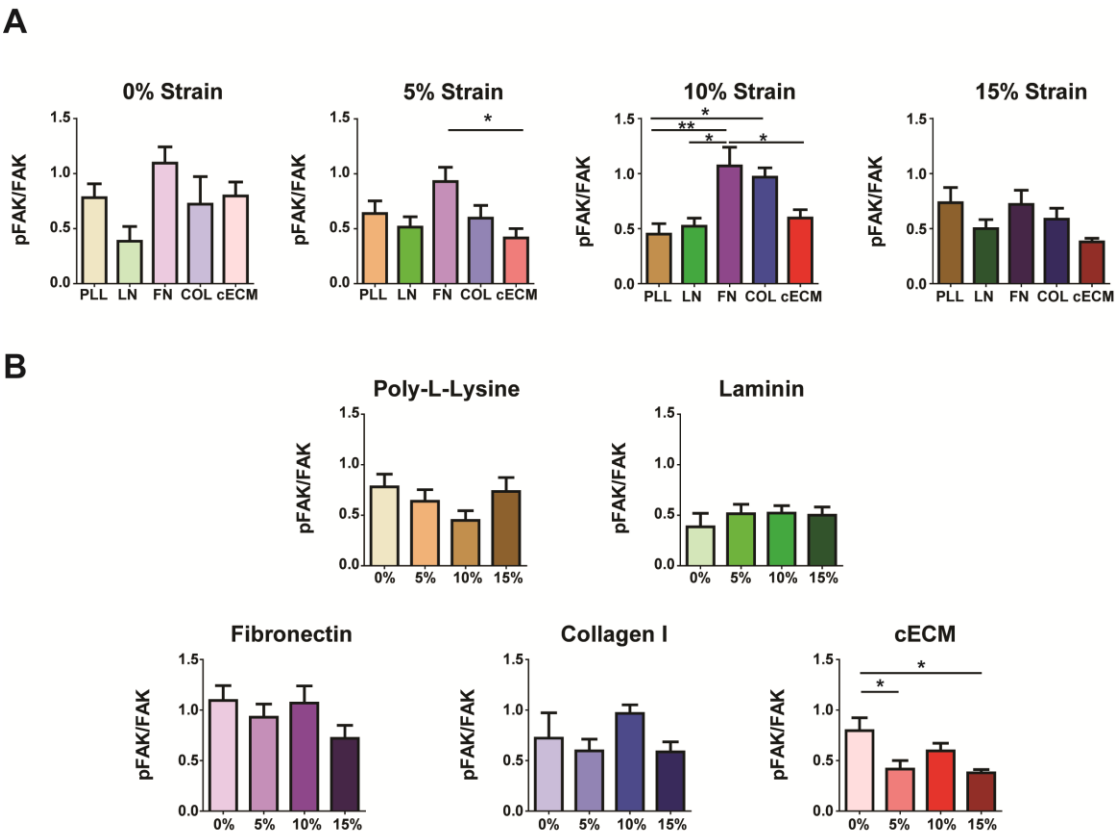

Figure 32. FAK activation in CPCs assessed by one-way ANOVA. CPCs were seeded on the appropriate matrix for 6 hours and then cyclic strain was applied for 24 hours. Cell lysate was evaluated by Western. (A) Matrix effects. (B) Strain magnitude effects. (A-B) One-way ANOVA with Tukey's multiple comparison test, bars represent mean + SEM; *p<0.05, **p<0.01; n=4-5; 0-15: strain magnitude; FAK = focal adhesion kinase, PLL = poly-l-lysine, LN = laminin, COL = collagen I, FN = fibronectin, cECM = naturally-derived cardiac extracellular matrix.

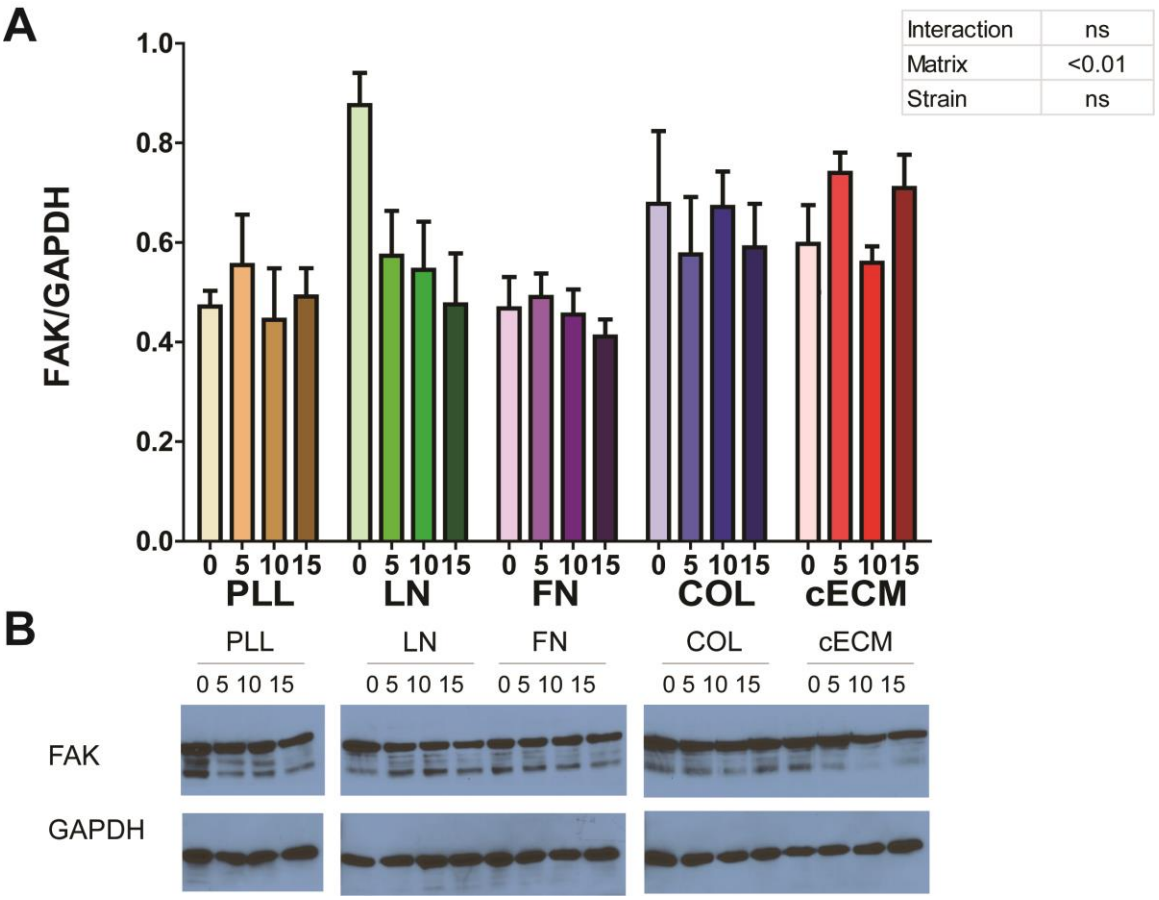

Figure 33. FAK expression in CPCs. CPCs were seeded on the appropriate matrix for 6 hours and then cyclic strain was applied for 24 hours. Cell lysate was evaluated by Western. (A) Quantification by densitometry; Two-way ANOVA, bars represent mean + SEM. (B) Representative blots. n=4-6; 0-15: strain magnitude; FAK = focal adhesion kinase, PLL = poly-l-lysine, LN = laminin, COL = collagen I, FN = fibronectin, cECM = naturally-derived cardiac extracellular matrix.

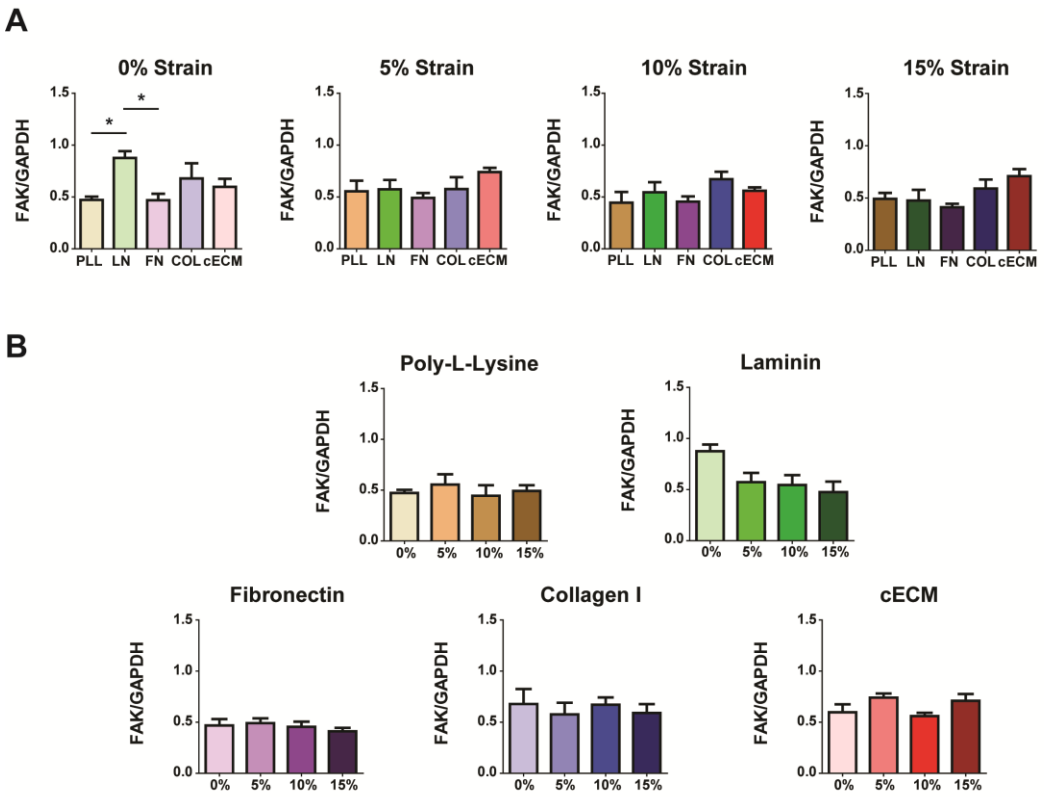

Figure 34. FAK expression in CPCs assessed by one-way ANOVA. CPCs were seeded on the appropriate matrix for 6 hours and then cyclic strain was applied for 24 hours. Cell lysate was evaluated by Western. (A) Matrix effects. (B) Strain magnitude effects. (A-B) One-way ANOVA with Tukey's multiple comparison test, bars represent mean + SEM; *p<0.05; n=4-6; 0-15: strain magnitude; FAK = focal adhesion kinase, PLL = poly-l-lysine, LN = laminin, COL = collagen I, FN = fibronectin, cECM = naturally-derived cardiac extracellular matrix.

As shown in Figure 35, flow cytometry showed that 99% of CPCs basally express the integrin beta1 subunit. By qPCR, the most prominent integrin subunits detected in CPCs in descending order are: beta1, alphaV, alpha5, alpha3, beta3, alphaE, alpha4, beta4 and alphaL. As FAK activity is linked to integrins, total levels of the beta1 integrin subunit were evaluated at 24 hours of cyclic strain. By two-way ANOVA, beta1 integrin expression as evaluated by Western was matrix ($p<0.001$), but not strain dependent, with no interaction. Results of the two-way ANOVA analysis are shown in Figure 36. At 10% strain, LN (1.9-fold over GAPDH) showed the highest integrin beta1 expression and had twice the levels of CPCs cultured on cECM (0.9-fold; $p<0.05$). No other significant changes were observed. Analysis by one-way ANOVA is shown in Figure 34. The sample size for qPCR data was too small to draw conclusions (Figure 40). Previously, in standard tissue polystyrene culture plates, we showed that the beta1 integrin subunit was equally activated on LN (1.5-fold over total beta1 integrin), FN (1.0-fold), COL (0.9-fold) and cECM (1.1-fold) and that this activation was significantly higher than CPCs in suspension (Ctrl, 0.4-fold). Activity on PLL was not evaluated. Beta1 integrin activity is reported in Figure 35. This antibody did not detect activity in strained signals, although it is difficult rule out the possibility of activation of the beta1 integrin.

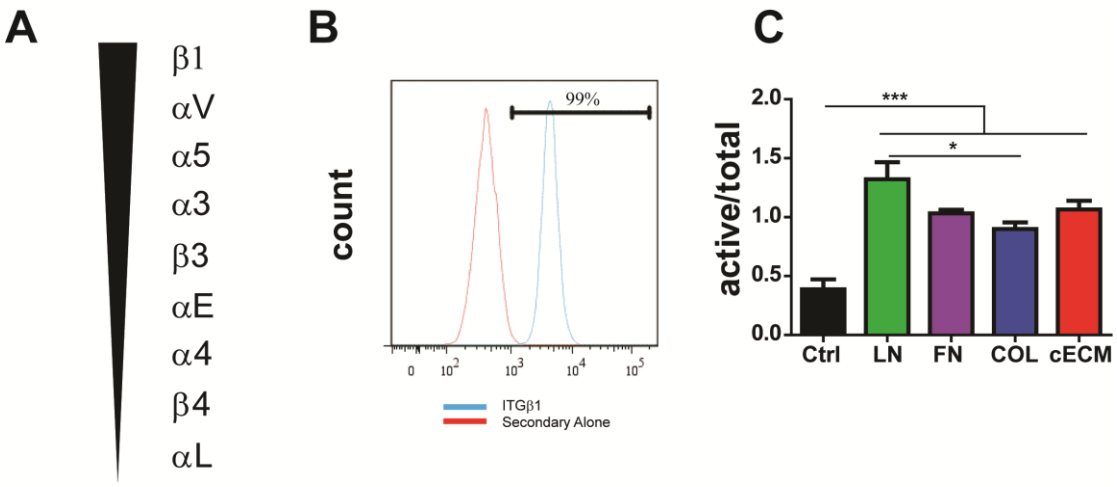

Figure 35. Integrins in CPCs. (A) Relative basal integrin subunit expression was determined by qPCR array. (B) flow cytrometric analysis of basal beta1 integrin expression in CPCs; red = control, blue = ITGβ1. (C) Activity of integrin beta1 subunit by Western blot; One-way ANOVA with Tukey's multiple comparison test, bars represent mean + SEM; *$p<0.05$, ***$p<0.001$; 0-15: strain magnitude; ITGb1= integrin beta1, LN = laminin, COL = collagen I, FN = fibronectin, cECM = naturally-derived cardiac extracellular matrix.

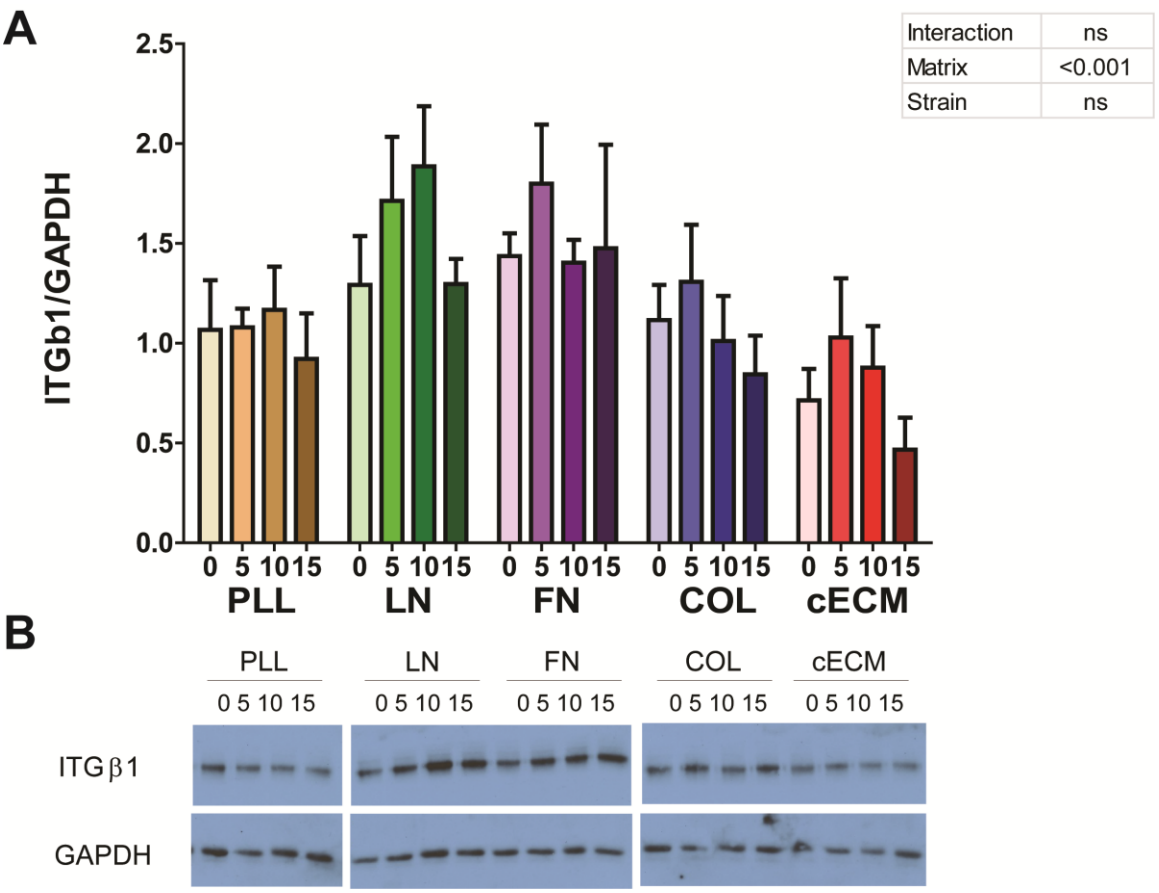

Figure 36. ITGβ1 expression in CPCs. CPCs were seeded on the appropriate matrix for 6 hours and then cyclic strain was applied for 24 hours. Cell lysate was evaluated by Western. (A) Quantification by densitometry; Two-way ANOVA, bars represent mean + SEM; (B) Representative blots. n=4-5; 0-15: strain magnitude; ITGb1= integrin beta1, GAPDH = Glyceraldehyde-3-phosphate dehydrogenase, PLL = poly-l-lysine, LN = laminin, COL = collagen I, FN = fibronectin, cECM = naturally-derived cardiac extracellular matrix.

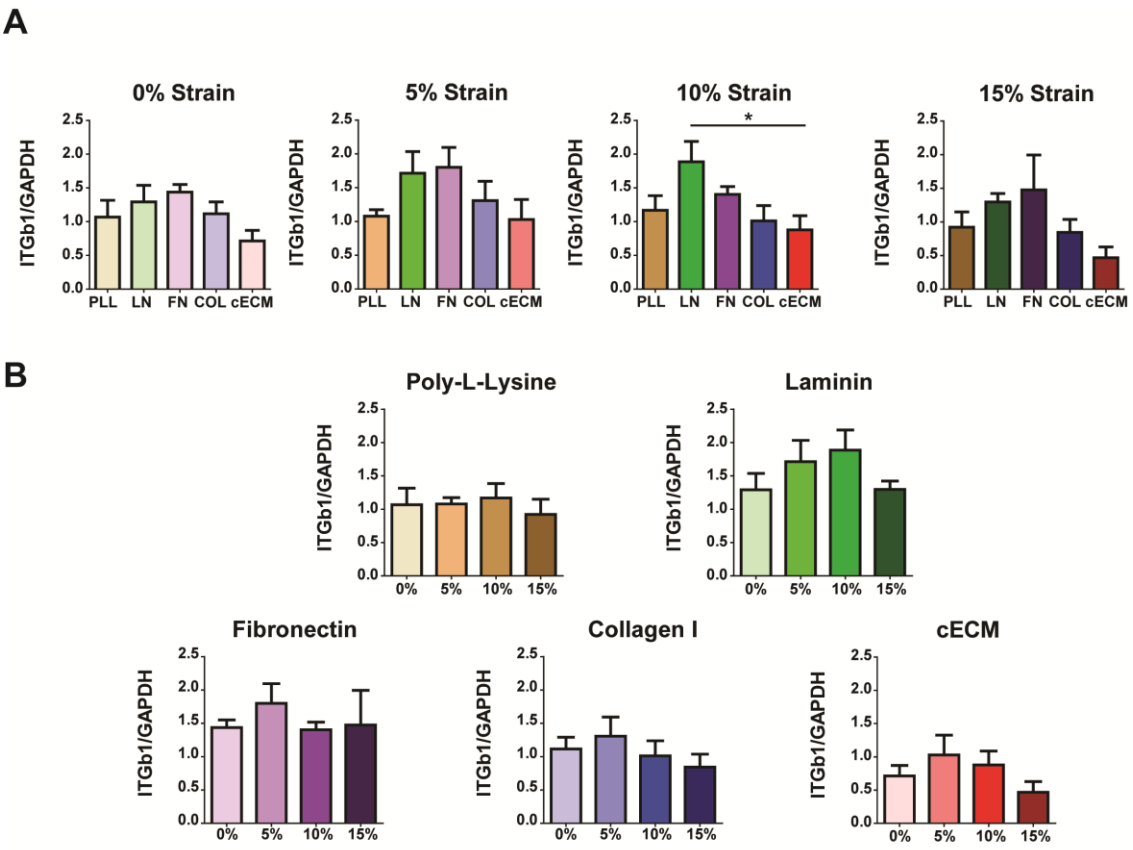

Figure 37. ITGb1 expression in CPCs assessed by one-way ANOVA. CPCs were seeded on the appropriate matrix for 6 hours and then cyclic strain was applied for 24 hours. Cell lysate was evaluated by Western. (A) Matrix effects. (B) Strain magnitude effects. (A-B) One-way ANOVA with Tukey's multiple comparison test, bars represent mean + SEM; *p<0.05; n=4-5; 0-15: strain magnitude; ITGb1= integrin beta1, GAPDH = Glyceraldehyde-3-phosphate dehydrogenase, PLL = poly-l-lysine, LN = laminin, COL = collagen I, FN = fibronectin, cECM = naturally-derived cardiac extracellular matrix.

5.3 Discussion

The myocardium is composed of a complex array of microenvironments that change throughout development, aging and disease progression. Young myocardium is composed of high amounts of laminin, collagen and fibronectin [21]. With increasing age, the matrix profile shifts, with increases in collagens I and III and laminin and

decreases in fibronectin. Myocardial infarction (MI) is the most prevalent form of coronary heart disease, a major contributor to the leading cause of death in the United States [1]. Post-MI, there is an acute decrease in collagen I, followed by increased in collagen I and fibronectin. This is an over-simplification as the myocardium also contains collagen II-VI, elastin, fibrinogen and many proteoglycans and glycoproteins [21]. Protein content alone insufficiently describes the myocardium as changes in crosslinking of the proteins also occur with age and disease [12, 16]. Furthermore, integrins expressed by cardiac cell types have been shown to change with age and disease indicating that the relationship between cells and their extracellular environment are dynamic [20]. Additionally, the stiffness of the myocardium and strain of endogenous cells is dependent on developmental and disease state. Strains in the developing and healthy adult hearts are globally 18% [32]. Strain decreases post-MI, due initially to loss of myocyte contractility and later to scar development. Stiffness of the myocardium is globally 15 kPa in healthy hearts and increases to 55-90 kPa after infarct formation [26]. This assessment of extracellular matrix components and biomechanical input treats the myocardium as a homogeneous tissue; however strain in the myocardium changes longitudinally, circumferentially and radially, with associated changes in matrix structure and likely composition. Furthermore, endogenous CPCs are known to exist in niches, particularly in areas of lower tissue strain [60, 64]. Matrix composition of these niches is believed to be high in laminin and fibronectin [62, 64, 172]. It is unknown how the mechanical forces of the myocardium are propagated throughout niches. Two large questions surround cardiac regeneration with CPCs. First, how can endogenous CPCs be activated? Second, what is the optimal microenvironment for CPC cardiomyogenic differentiation and maturation? Addressing these questions has the potential to inform studies aimed at activating endogeneous CPCs, understanding how to best expand and pre-condition CPCs before delivery and deciding on the choice of delivery vehicle. Thus, it is important to understand how CPC interact with their micronenvironment.

In order to improve myocardium regeneration an increase in the number of stem/progenitor cells available is an important first step, followed by either maturation of these cells into the desired cell types, increased paracrine signaling to salvage surviving cells, altering the immune response and remodeling, recruitment of endogenous stem/progenitor cells for repair or a combination of the above. In order to assess how culture conditions, specifically matrix composition and the application of mechanical strain, alter the proliferation and maturation of CPCs we examined these conditions in a combinatorial fashion. Strains of 5%, 10% and 15% were examined in addition to unstrained (0%) controls. Furthermore, five matrix conditions were evaluated: poly-L-lysine (PLL), laminin (LN), fibronectin (FN), collagen I (COL) and naturally-derived cardiac extracellular matrix (cECM). The results (summarized in **Error! Reference source not found.**) are discussed as phenotypic changes, proliferation and maturation, paracrine signaling and potential mechanisms for the effects observed.

	Static	5% Strain, 1 Hz	10% Strain, 1 Hz	15% Strain, 1 Hz	Overall
PLL	Control • ↑ 15 min pERK	Control • ↑ VEGF • ↑ 15 min pERK	Control • ↑ VEGF • ↑ HGF	Control	• CPCs rounded • Do not align • 15 min pFAK activation
LN	Control • ↓ VEGF • ↑ FAK	Niche	Control • ↑ ITGb1 expression	Niche	• Moderate alignment • 15 min pFAK activation • ITGb1 activation
FN	Control • ↑ Dividing cells • ↑ Cnx43	Infarct • ↑ Dividing cells • ↑ Cnx43	Control • ↑ 24 hr pFAK	Healthy • ↓ HGF	• Strong alignment • Calcium oscillations • 15 min pFAK activation • ITGb1 activation
COL	Control • ↑ Dividing cells • ↑ 15 min pERK	Infarct • ↑ Dividing cells • ↓ Cnx43	Control • ↓ HGF • ↑ 24 hr pFAK	Healthy • ↓ Cnx43	• Strong alignment • Calcium oscillations • 15 min pFAK activation • ITGb1 activation
cECM	Control • ↑ Dividing cells	Biomaterial Therapy • ↑ Dividing cells • ↑ 15 min pERK • ↓ 24 hr pFAK	Control • ↓ Cnx43 • ↑ VEGF	Healthy • ↓ Cnx43 • ↑ 15 min pERK • ↓ 24 hr pFAK	• Moderate alignment • Calcium oscillations • 15 min pFAK activation • ITGb1 activation
Overall	• No alignment • 15 min pFAK activation	• 15 min pFAK activation	• 15 min pFAK activation	• 15 min pFAK activation	

Figure 38 Aim 2 Results Summary

Alignment of cells within a tissue facilitates electrical and mechanical propagation. Strain has been shown to induce cell alignment in a variety of cell types [112, 127, 137, 161]. Although induced by strain, alignment alone-independent of mechanical strain- has also been shown to improve mesenchymal stem cells (MSCs) cardiomyogenic differentiation and the potential for cells to integrate in host myocardium [108-111]. To evaluate if strain induced alignment, cells from each culture condition were evaluated by immunocytochemistry. We observed CPC alignment with the application of mechanical strain. This effect was matrix specific, with COL aligning the cells more robustly with 3.0-fold more alignment as compared to PLL at 5, 10 and 15% strains. At 15% strain, CPCs also align 2.8-fold more robustly on FN than PLL. While not examined in this study, matrix-dependent changes in alignment may be due to differential binding of CPCs to extracellular matrix components and mechanotransduction through integrins.

Alignment of CPCs did not increase with the application of strain when cultured on PLL. When cultured on LN, strain induced a 2.3-fold increase in alignment for cells strained 15% as compared to unstrained cells. This effect was smaller than that observed on the other matrices, suggesting either a lack of mechanotransduction or differences in the mechanotranduction pathway that are activated. CPCs cultured on cECM, FN or COL had 3 to 4-fold increases in alignment with mechanical strain. Interestingly, alignment values did not differ with increasing magnitudes of strain within a single matrix group, suggesting the application of any strain >5% is enough to achieve alignment. In preliminary studies, we had seeded cells at approximately half the density and functionalize the surfaces with 10-fold more matrix. In those studies, we also observed an increase in alignment with the application of strain, which was not different between the two groups examined, COL and cECM, at 10%. We did not thoroughly evaluate if increasing the concentration of the matrix used to functionalize the plates actually resulted in increased matrix tethered to the surface and thus cannot comment specifically on ligand density differences. While we cannot directly compare results from these experiments, it appears as if there is less alignment on COL at this higher matrix concentration, while CPCs on cECM align similarly on each. It would be interesting to study the effect of ligand density on CPC phenotype in response to mechanical strain in future studies.

In the current study, spread area describes the interaction of CPCs with the underlying substrate. Increases in spread area are an indication that cells are interacting more with their environment and could lead to changes in cells shape. Cell shape is known to induce variable differentiation protocols [145, 241], while in MSCs roundness maintains multipotency [145]. The size, as evaluated by spread area, of the CPCs in our study mimics that of neonatal cardiomyocytes and embryonic stem cell-derived cardiomyocytes [100, 106]. The spreading of CPCs on each culture condition was matrix, but not strain,

dependent. At 0-10% strain, CPCs seeded on FN or COL were generally more spread than those on PLL. CPCs on LN were about as spread as those on PLL. Intermediate spreading of CPCs on cECM was observed. In mesenchymal stem cells, reduced adhesion improved maintenance of pluripotency, while still allowing for proliferation [145]. Spread area is not a direct measurement of adhesion, but suggests that CPCs on LN and PLL might have fewer cell-ECM contacts as they are more rounded. CPCs on these matrices also do not align as well, suggesting that they are less likely to contribute to CPC differentiation and maturation than FN, COL or cECM. In addition to spread area, cell shape was also evaluated by calculating the aspect ratio of the CPCs. While small changes were observed, primarily due to matrix conditions, the CPCs had aspect ratios of 1.5:1 to 2:1 for all culture conditions. This indicates that the cells are more round than neonatal rat ventricular myocytes and MSC-derived cardiomyocytes with aspect ratios of 4:1 and adult cardiomyocytes (7:1) [48, 98, 109, 242]. Given the size and shape of the CPCs alone, they phenotypically represent an immature cardiomyocyte. Culturing CPCs on a stiffer substrate or nanopatterned surface may help to increase their aspect ratio. This study does not directly link cell shape to differentiation or maturation; but these results do suggest that the CPCs phenotypically respond differently to each matrix, opening them to the possibility of further changes. Additionally, mechanical strain induces hypertrophy in more mature cardiomyocytes by effecting growth cycles. The size of the CPCs in our study mimics that of neonatal cardiomyocytes, while adult cardiomyocytes are typically larger. At longer timepoints, as CPCs differentiate toward cardiomyocytes, the application of mechanical strain may increase the size of CPCs and this could be considered in future work.

Proliferation of CPCs contributes to an increase in the number of available cells. We evaluate the number of dividing cells at the time of fixation. Dividing cells were detected even though the CPCs were cultured in the absence of serum for 30 hours. At maximum,

2.7% of CPCs were dividing for a given culture condition (FN, 5%). This is 270-fold greater than the minimum detected number of dividing cells, 0.01%, for PLL at 0%. Given that $4x10^5$ cells were initially seeded, and assuming that no cells were lost in culture and that each division event accounts for the formation of one new cell, this would account for 10,800 new cells formed on FN at 5% compared to 40 on PLL at 0%. Similarly, CPCs seeded on FN and strained 5%, were 5.4 times more proliferative than those seeded on LN and unstrained. For lower strains (0 and 5%) the matrix coating had a greater effect on proliferation. At higher strains (10 and 15%) proliferation was matrix-independent, suggesting that mechanical inputs may override the effect of the matrix. The proliferative capacity of CPCs is likely under estimated by this method since it only captures dividing cells at a single timepoint. Furthermore, we evaluate the number of dividing cells by phenotype alone. Immunocytochemistry for proliferation markers, such as Ki67 or aurora B kinase, are necessary for further confirmation. Alternatively, the total number of cells could be counted at a later timepoint as performed in Aim I. Population doubling times account for the total accumulation of proliferating cells in a given time period. Reported CPC doubling times in the presence of serum are ~31 hours [68]. Survival of CPCs was not evaluated in our study, but apoptosis would lead to decrease in the number of available cells.

There are two methods by which CPCs can effectively contribute to regeneration: direct differentiation and maturation or paracrine signaling. While CPCs can form endothelial cells, smooth muscle cells, cardiomyocytes or fibroblasts, here we examine the role of culture condition on cardiomyogenic differentiation. We assess cardiomyogenic differentiation by levels of early cardiac markers gata-4, nkx2.5, troponinC1 and troponinT2 by qPCR, and also evaluate gap junction component connexin 43 (Cnx43) by qPCR and Western, as well as phenotype. While there appear to be promising matrix-dependent differences in gata-4, troponinC1 and troponinT2 by qPCR, the sample size is

too small to draw conclusions and will be repeated. Literature shows that stretching cardiomyocytes increases Cnx43 expression [218]. Cnx43, aside from electrical propagation [125], has been linked to cell survival and proliferation [238] [239]. By Western, we show that for unstrained CPCs, Cnx43 expression is 40-50% higher on FN than PLL, LN or cECM. At 5% strain FN shows twice the Cnx43 expression as compared to PLL at 5%. At higher strains, Cnx43 is not matrix-dependent, suggesting that biomechanical inputs may supersede biochemical inputs. For CPCs cultured on COL and cECM, higher levels of strain resulted in 20-50% decrease in Cnx43 expression. The largest difference in Cnx43 expression is seen between unstrained CPCs on FN and CPCs cultured on cECM with 15% strain, resulting in 3-fold more Cnx43 on FN, 0% condition. This fits literature results that show Cnx43 expression is highest in neonatal rat ventricular myocytes cultured on fibronectin, although that particular study only compared FN to COL and we do not see significant changes between FN and COL in our cells [84]. Our qPCR results for Cnx43 expression do not show any differences in transcript levels, although are under powered and will be repeated. While expression alone is not proof of functional gap junction formation, increased Cnx43 expression suggests that the cells are better primed for functional gap junction formation and electrical propagation.

In vivo, maturation of myocytes is marked, in part, by their inability to undergo cytokinesis [99]. Myocytes that undergo karyokinesis that is not followed by cytokinesis result in multinucleated cells. In this study, CPCs that appear to have more than one nucleus were identified. While these cells do not phenotypically look like adult myocytes, their nucleation pattern is reminiscent of cultured neonatal rat ventricular myocytes [243, 244]. Less than 1% of all CPCs in our study had more than one nucleus, but significant strain-dependent changes were observed. On FN, 3-fold more cells (1.2%) with more than one nucleus at 5% strain than 15% strain (0.4%). The number of

CPCs with more than one nucleus was also 2.5-fold higher on COL at 5% as compared to 0%. Matrix conditions did not affect the number of cells containing more than one nucleus. To confirm that CPCs that appear to contain more than one nucleus are truly binucleated, further immunocytochemistry is necessary. For this, a four color stain is necessary to show total nuclei, actively dividing nuclei, cytoskeletal protein such as f-actin or beta-tubulin to show continuity or reorganization of the cytoskeleton and septins as a marker for karyokinesis. This would allow cells undergoing karyokinesis, without cytokinesis to be identified. Additionally, the number of CPCs with more than one nucleus could be evaluated in a long-term culture to establish if these binucleated cells accumulate over time, or if it is a transient phenotype.

CPCs spontaneously oscillate calcium [235, 236]. By genetically engineering CPCs, myocyte-like transients can be achieved [237]. Calcium oscillations serve as an indication of cardiomyogenic maturation and increase cell proliferation [235, 236]. Due to the constraints of our microscope, we were unable to evaluate calcium oscillations in strained CPCs without enzymatically disrupting them from the Bioflex plates. Instead, CPCs were cultured on each of the matrices overnight on glass coverslips and then assessed for calcium handling. Electrically-stimulating the CPCs increased the number of oscillations 25-fold over literature values, which observed 1.4 spontaneous oscillations (no electrical stimulation) per active cell in 33 minutes [236]. A 2.8-fold increase in the number of active CPCs and a 2.3-fold increase in the number of oscillations per active cells were observed for CPCs cultured on FN, COL or cECM as compared to PLL. This increase may be due to the morphology or clustering of CPCs on each matrix or changes in calcium handling proteins. Western blots analysis can be used to distinguish these mechanisms and to further evaluate the effects of strain on the expression of these proteins. CPCs cultured on LN had intermediate values of activity. By t-test of individual groups, the number of oscillations per cell was higher on FN, COL and cECM

than LN. LN was not statistically different than PLL. This suggests than LN, a niche protein, may maintain CPCs in a quiescent state. Activation of calcium oscillation leads to proliferation and asymmetric cells division, which may induce a CPC to migrate from the niche and mature [236].

Paracrine signaling of CPCs may also contribute to their regenerative potential, through recruitment of progenitor cells, differentiation of endogenous progenitor cells or survival of endogenous cells. To assess the potential for paracrine signaling, ELISAs were performed on conditioned media collected from CPCs in each of the culture conditions. No stem cell factor (SCF) or platelet-derived growth factor BB (PDGF) was detected in the conditioned media. SCF is a stem cell chemoattractant and is responsible for maintenance of haematopoietic stem cells [245-247]. Absence of SCF from the media might suggest that progenitor cells would not be recruited in an in vivo environment and present progenitor cells may be released from maintenance-protocols. PDGF has been shown to induce proliferation, migration and angiogenesis [248, 249]. Absence of PDGF from the media might suggest that the CPCs would not stimulate angiogenesis in an in vivo environment. Interestingly, both of these cytokines were previously detected in conditioned media collected from CPCs in our lab. Opposed to this study however, those CPCs were encapsulated in a three-dimensional hydrogel and cytokine levels were increased by Notch activation [250]. Interestingly, in the previously evaluated three-dimensional system vascular endothelial growth factor A (VEGF) was not detected, but it is robustly detected in the conditioned media in this study. In fact, VEGF presence in the media is matrix and strain dependent. Conditioned media from CPCs cultured on PLL contained 2-fold more VEGF for cells strained either 5 or 10% as compared to unstrained cells. The effect was similar for cells cultured on cECM, with 2.5-fold as much VEGF in the conditioned media for cells strained 10% as compared to unstrained cells. The effect was even larger on LN, with a 4.5-fold increase in VEGF for cells strained 5, 10 or 15%

as compared to unstrained controls. No effect of strain on VEGF concentration was observed for FN or COL. Strain induces VEGF secretion in a variety of cell types, including cardiomyoctytes, MSCs and embryonic stem cells [125-127, 138, 217-219, 234]. Studies that examined VEGF secretion from MSCs on various matrix proteins, showed no secretion on FN and less on COL relative LN, in line with our study [135, 138]. VEGF is known for its regulation of angiogenesis, but has also been shown to act through paracrine and autocrine effects to increase Cnx43 expression in myocytes to similar levels as achieved by strain [84, 217]. While beyond the scope of this study, it is possible that VEGF regulates CPC function in an autocrine fashion, as these cells contain low levels of VEGF receptor. Matrices that induce strain-dependent increases in VEGF concentration (PLL and LN) show maintained Cnx43 levels with increasing strain. On COL, there is no strain-induced VEGF increase in the media and Cnx43 levels are not maintained with increasing strain. These correlations do not extend to FN and cECM. However, FN is known to contain binding domains for both VEGF and HGF [90], so it is possible that VEGF is secreted by the CPCs, but sequestered by FN. This could further lead to positioning of the growth factor for CPC stimulation and Cnx43 expression, but this correlation is speculative. As the ELISA only measures current VEGF in the conditioned media, qPCR was performed to determine if the CPCs are producing new VEGF. However the results are inconclusive due to a small sample size and need to be repeated. Additionally, since CPCs express some level of VEGF receptor, the ELISA would not measure any VEGF bound to the cells, which may vary with strain condition. Hepatocyte growth factor (HGF) plays a role in cell proliferation, migration, survival and angiogenesis [172, 251]. HGF concentration in the conditioned media from CPCs cultured on PLL increased 4.9-fold on 10% strain as compared to 0% and 3-fold as compared to 5%. However on FN, there was a 75% decrease in HGF from 10 to 15% strain. The same occurred on COL, with a 68% decrease in HGF measured from 5 to 10% strain. Cardiac stem cells have previously been shown to secrete HGF, although at

an order to magnitude higher than that detected here [61, 62, 64]. Strain did not have an effect on HGF secretion from human cardiosphere-derived cells or MSCs [127, 135]. Even though statistical changes in HGF secretion are observed, it is unclear if it will have a biological effect at such low (<10 pg/mL) levels. Urbanek et al. evaluated HGF secretion within 2 hours of treatment, so it is possible that HGF secretion occurs early and that secreted HGF was degraded by extracellular protease by 24 hours [172]. For the evaluated inflammatory cytokines, levels were very low with the exception of monocyte chemoattractant 1 (MCP-1). Although the role of MCP-1 is not well studied in CPCs, it has been shown to also be secreted from cardiosphere-derived cells [234]. Additionally, in a murine model, overexpression of MCP-1 was cardioprotective after MI [252].

In order to further interpret the above results, we wanted to determine if CPCs seeded on each matrix were strained to the same degree for a given applied strain. It is important to note that a different device, the StageFlexer, was used in this experiment than the rest of experiments. This resulted in lower reported strains for each programmed strain and thus does not recapitulate the conditions used in the rest of the study. However, it does allow for comparison between strain and matrix groups on the same device. For programmed strains of 5%, a 3.5% strain was reported by the Flexcell and strains of 3.8-6.3% were measured. For programmed strains of 10%, a 7% strain was reported and strains of 6.6-7.6% were measured. For programmed strains of 15%, an 8.4% strain was reported and strains of 5.0-7.9% were measured. No differences were observed between matrix conditions for a given strain. For the lowest strain groups, some variability may be induced by measuring such small changes. At 10% programmed strain, the measured strains track well with reported values, supporting the validity of this method. However, for the highest strain group there is a wide range of reported strains, some lower than expected. For PLL (trend), LN, FN, COL (trend) and cECM the measured strain significantly increased at programmed 5 and 10% strains, suggesting that we are able to

achieve conditions of increasing strain. For CPCs seeded on FN, a lower strain is measured at 15% than 10% programmed strain. A similar trend is observed on LN. This is particularly interesting because the reported strain values differ by such a small amount (an absolute 1.4%). While it is possible that error was introduced at this strain magnitude by larger translation (and blurring) of the cells, given the distribution of measured strains it does not sufficiently explain the lower observed strain. Thus this effect may be due to increased cytoplasmic stiffening at short time scales or slippage of the CPCs from the matrix. Regardless of the effect, it is likely that it is exacerbated in our experiments where the change in reported strain is even larger between the 10 and 15% programmed strains (an absolute 5%).

Integrins link the cytoplasm to extracellular matrix components and are largely responsible for transducing mechanical signals from the microenvironment into biochemical intracellular signals. Focal adhesion kinase (FAK) associates with the cytoplasmic domain of integrins and is activated by phosphorylation. The extracellular signal-regulated kinase (ERK) is downstream of several signaling cascades including FAK and VEGF, and is also activated by phosphorylation [151, 253]. To establish activity of FAK and ERK by binding of CPCs to the extracellular matrix, Western blot was performed after allowing cells to adhere for 20 minutes. Phosphorylated FAK and ERK were both detected, suggesting adhesion alone is sufficient to activate this pathway. Mechanical stimulation may further activate FAK and ERK, as the application of strain to various cell types and culture conditions lead to increased pFAK and pERK within as little as 5 minutes of strain and is sustained for 1-4 hours [135, 222-226]. To determine if strain further activates FAK and ERK, CPCs were allowed to adhere to the appropriate matrix for 6 hours and then cyclic strain of 0-15% was applied for 15 minutes. No further activation of FAK was observed for any matrix or strain conditions. However, matrix-dependent changes in pERK were detected. In unstrained CPCs, PLL and COL

demonstrated 2-fold activation of ERK as compared to FN and LN, with moderate activation of ERK on cECM. Similarly, at 5% strain, CPCs on PLL and cECM showed 2-fold activation of ERK as compared to FN and LN, with moderate activation of ERK on COL. At 15% strain CPCs cultured on cECM had 2.3-fold ERK activation as compared to FN. These results are interesting because they do not parallel FAK activation, suggesting crosstalk between signaling pathways. Furthermore, ERK activation is required for VEGF production [254, 255]. In our study, pERK is typically highest on PLL, COL and cECM, while we also observed strain-dependent increases in VEGF in conditioned media of CPCs cultured on PLL, LN and cECM. While not a perfect correlation, it suggests that biochemical signaling within the cell is complex. We did not measure VEGF in the conditioned media at this timepoint, but through autocrine signaling, VEGF could also contribute to ERK activation.

Cell alignment is achieved by 24 hours, potentially through mechanotransduction pathways. To ascertain if FAK is still active at these time points, lysate was collected and evaluated by Western. Similar to the shorter time points, pFAK/FAK was dependent on matrix, but not strain. FAK activation on FN was maintained at 24 hours, with 2-fold higher pFAK/FAK at 5% for FN than cECM and at least 2-fold higher pFAK/FAK at 10% for FN than PLL, LN and cECM. For cECM alone, strain reduced the pFAK/FAK ratio 2-fold at 5 and 15% relative to unstrained CPCs. It is important to note that while the ratios of FAK activation vary, activation was still detected to some extent in all groups. This suggests that the CPCs are still engaging with the microenvironment and that further changes in cell phenotype may be observed at later timepoints, especially for CPCs cultured on FN. It has previously been shown that FAK was not activated in cells cultured on PLL as they adhere to PLL through ionic interactions instead of integrins [215, 222]. Surprisingly, we observe phosphorylation of FAK in CPCs cultured on PLL. This could be due to inside-out signaling, where FAK activation primes cells to bind to

extracellular matrix. Alternatively, we cannot rule out the accumulation of matrix proteins on the functionalized surface, and thus integrin activation, even though the PDMS is hydrophobic and the functionalization reaction was quenched. Activation of ERK was not evaluated at this timepoint as alignment has already been achieved and the presence of VEGF in the media would confound the results. In addition to FAK activation, total levels of FAK were evaluated and interestingly, there was a 1.8-fold increase in total FAK protein levels at 24 hours for CPCs cultured on LN as compared to PLL and FN. While different than our system, De Lisio et al. also observed matrix dependent changes in total FAK and pFAK levels [135]. This increase in total FAK, would contribute to lower pFAK/FAK ratios on LN and additionally could be a result of the CPCs on LN trying to probe their microenvironment. Localization of FAK was not evaluated in this study, but could be important to consider in future studies as FAK clusters in focal adhesion and binds other cytoplasmic proteins in response to mechanical stimulation [145, 164, 218]. To further evaluate if the CPCs are remodeling their mechanotransduction machinery, we evaluated total levels of the beta1 integrin subunit. As shown by qPCR and flow cytometry, CPCs basally express the beta1 integrin. At 10% strain, CPCs cultured on LN expressed 2-fold more beta1 integrin than on cECM. This further suggests that CPCs cultured on LN are probing for microenvironmental signals, perhaps because these pathways are not being stimulated. While the CPCs express the beta1 integrin subunit, individual alpha subunits were not evaluated in treated cells. We have shown that culture of CPCs on LN, FN, COL and cECM activates the beta1 integrin to similar levels over cells that were maintained in suspension. The pairing of an alpha subunit with a beta subunit determines the binding affinity for a particular extracellular matrix protein. To further elucidate the mechanotransduction pathways activated in CPCs, integrin alpha subunits would need to be evaluated.

CHAPTER 6 LIMITATIONS AND FUTURE DIRECTIONS

6.1 Cardiovascular Disease

Cardiovascular disease is the leading cause of death in the United States. There were an estimated 1.5 million cases of myocardial infarction (MI) in 2011 [256]. Following MI in animal models, there is a 40-60% reduction in myocyte number in the myocardium with billions of myocytes being lost within the first several days [8, 13]. These myocytes are not replaced and this results in extensive inflammation and fibrosis, leading to loss of contractility. Fibroblasts within the damaged tissue proliferate and secrete high levels of collagen to prevent the heart from rupturing, ultimately leading to heart failure. The only comprehensive cure for heart failure is cardiac transplant, which is greatly limited by the number of available donor hearts. This has forced clinicians to find new ways to improve chronic cardiac function such as the use of beta-blockers, angiotensin receptor blockers, and other pharmacological interventions [257]. While these therapies may sustain cardiac function, they do little to regenerate functional tissue.

6.2 Aim 1

6.2.1 Summary

In this study, a naturally-derived, porcine cardiac extracellular matrix (cECM) was examined for the ability to improve CPC function. Our hypothesis was centered on the fact that this would mimic the matrix composition of a healthy myocardium, while collagen would represent both the diseased area and a commonly used cell delivery vehicle [77]. Our results demonstrate that CPCs prefer the naturally-derived cECM over collagen in vitro. Culture of CPCs on cECM increases differentiation toward the cardiomyogenic lineage as shown by qPCR and western blot over collagen controls. Furthermore, culture of CPCs on cECM increases their proliferation rate and survival after serum deprivation as compared to COL. CPCs adhere more strongly to cECM than

COL and show greater potential for remodeling through the expression of matrix proteins and matrix degrading enzymes. These effects are believe to be tissue specific and are not observed when CPCs are cultured on adipose-derived ECM.

6.2.2 Limitations

While this work examines the specific effects of a naturally-derived cardiac ECM (cECM) on CPC behavior it does not recapitulate a true cardiac microenvironment for three reasons: 1) it is two-dimensional, 2) processing of cECM presents unnatural fragments to the CPCs and 3) other cell types are not present. Each of these points will be addressed individually. First, the three-dimensional microenvironment is complex and cells must integrate a variety of cues such as stiffness, nanotopography, biochemistry and soluble factor diffusion. Due to the multiple variables present it can make studying the single effect of one signal difficult. While it is possible to control for certain variable, i.e. stiffness, while modulating ECM composition then a single or few stiffness's have to be identified for evaluation. As discussed in the Background and Aim II, combinatorial design of microenvironmental signals often has complex results. Thus, a two-dimensional design was chosen for this first evaluation of cECM on CPC behavior in vitro. However, work in mouse embryonic stem cells, showed that their differentiation into cardiac progenitor stem cells was improved in three-dimensional environments over two-dimensional cultures [86]. Two-dimensional culture limits a cell's behavior (i.e. matrix degradation and compaction) and further work should be performed in three-dimensional hydrogels or animal models [147].

Next, in order to create an injectable material cECM undergoes detergent and pepsin processing. Detergents may reduce growth factor and glycosaminoglycan (GAG) content in decellularized ECMs and potentially cause collagen degradation [182]. GAGs provide non-structural roles to ECM, but may play a role in cell signaling and ECM organization.

GAGs were detected in cECM suggesting that the detergent does not lose all of its GAG content. However, it is unknown how this compares to endogenous GAG content. DNase treatment removes cellular material from decellularized ECMs, but may also reduce GAG and fibronectin content [182]. Fibronectin content is still detected in cECM [176]. Perhaps of larger concern is that pepsin degradation of cECM is required to acquire an injectable material. Cell adhesions sites on ECM proteins like fibronectin may require distinct protein configurations and proximal sub-domains in the same protein [208]. We do not know how pepsin digests cECM components. In vivo, peptide fragments may have distinct roles from whole proteins [8, 10]. That said RGD, an adhesive peptide from fibronectin, is commonly used as a cell adhesion site in synthetic hydrogel system in place of the full length protein. Additionally, culture of CPCs on cECM improves their behavior over the standard culture substrate collagen I. Thus cECM may not ideally mimic the native adult myocardium, but it is still an improvement over current culture conditions. Further, we show that CPCs may be remodeling their microenvironment. While in this study we limited our experiments to short timepoints to limit changes in the matrix composition, cECM may be sufficient to prime CPCs to create an ideal microenvironment of their own.

Finally, we did not evaluate cECM as a delivery vehicle for CPCs in an animal model of MI. As discussed above, the in vitro culture environment does not recapitulate the endogenous myocardium. To address the third point, the endogenous myocardium contains myocytes, smooth muscle, endothelial cells and fibroblasts. While these cell types were not the focus of this study, their behavior may also be influenced by cECM. Co-culture systems could be designed to evaluate how cECM alters fibroblast paracrine signaling (for example), which in turn could alter CPC behavior. This is beyond the scope of the current work. However, injection of CPCs with cECM into the myocardium would place other cell types in relevant proximity. Thus animal studies would best

incorporate the effect of a three-dimensional microenvironment with co-culture and establish the benefits of this therapy post-MI. While the cECM and CPCs are each individually in clinical trials, it is unknown whether they might provide a synergistic benefit to heart failure patients. It has been suggested that the initial properties of an implanted biomaterial are less important than its interaction with the host tissue and its eventual remodeling of the material into healthy tissue [182]. The remodeling of a biomaterial is best evaluated in an animal model.

Additionally, batch-to-batch variability may occur in decellularized matrix products. For the purposes of our study, a single batch of cECM was used. For scaling purposes, batches of cECM could be mixed from multiple subjects to ensure a more homogeneous supply before distribution. There is also some concern in sourcing cECM from porcine myocardium. However, this was concluded to be a better source than human cadaveric myocardium [177]. Removal of xenogeneic antigens and residual processing chemicals is required for biocompatibility. In a rodent model, cECM biocompatibility was comparable to currently used, FDA-approved decellularized matrices sourced from other tissue [178]. Pre-clinical studies were performed in an allogenic model, but did not raise any biocompatibility concerns and the material had been largely replaced one week post-injection [184]. Full characterization of cECM has not been performed and undefined components likely exist in this material. If the material continues to prove beneficial, then this may not be a concern. However, it is possible that the full material is not required to achieve beneficial effects. Identification of individual signaling components, such as a matrix protein, proteoglycan or tethered growth factor, would allow for a more controlled response and perhaps more consistent processing/manufacturing of that signal than the entire cECM.

Furthermore, the identification of a stem cell population based on the presence of a single biological marker may results in a homogeneous and inconsistent cell population [33]. Biological markers may change over time and after disease. The same marker may also be present on different cells types. Indeed, while all of the CPCs used in this study are clones that are >90% positive for c-kit, Gata-4 and Nkx2.5 there are notable differences between clones and their behaviors. For example, in proliferation studies cECM improved the proliferation of almost all clones, however due to differences in basal proliferation rates the final cell count varied between experiments with different clones.

6.2.3 Future Directions

Paracrine signaling is a major mechanism through which cell therapy is thought to achieve beneficial regeneration. Aside from qPCR results for matrix metalloproteinases, tissue inhibitors of matrix metalloproteinases and ECM proteins, we did not evaluate what the CPCs may be producing and secreting in response to culture on cECM as compared to COL. Many growth factors such as vascular endothelial growth factor, hepatocyte growth factor, platelet-derived growth factor, stem cell factor, insulin-like growth factor (as previously discussed in this work), among others play roles in cell recruitment, maturation and even neoangiogenesis. While less relevant in a two-dimensional environment, they would be active in cell therapy attempts. ELISAs could be performed to assess the concentration of each of these growth factors in conditioned media from CPCs cultured on cECM as compared to COL. Additionally, the same conditioned media could be used in migration assays to evaluate cell recruitment or for culture of adult myocytes or fibroblast to evaluate its effect on contractility and differentiation, respectively. Functional assays with conditioned media are important as we are only able to probe for a small number of growth factors in the conditioned media.

As discussed in the limitations section of this aim, two-dimensional culture does not recapitulate the cell microenvironment. As we have now shown that cECM improves CPC behavior over COL, it would be worth evaluating these effects in three-dimensional hydrogels. For this, cECM can form soft hydrogels at high concentrations (6mg/mL) or alternatively, poly-(ethylene glycol)-cECM hybrid hydrogels as described by Grover et al. could be utilized [183]. Hybrid hydrogels would allow for tunable stiffness without changing ECM composition. Similar endpoints should be evaluated in this study as compared to Aim 1: proliferation, survival, differentiation and paracrine signaling. Hybrid hydrogels could be compared to poly-(ethylene glycol)-RGD (fibronectin adhesion peptide) or GFOGER (collagen adhesion peptide) as a control. Hydrogels could be fixed and sectioned or viewed by confocal microscopy to assess proliferation (Ki67), survival (TUNEL) and differentiation (lineage markers). Conditioned media would need to be collected from the hydrogels for ELISA to evaluate the presence of growth factors.

A rat model of MI would allow for insight into cECM delivery of CPCs for cell therapy. Animals would undergo ischemia-reperfusion by ligation of the coronary artery for 20 minutes before restoration of blood flow. Following reperfusion, treatments (saline, cECM alone, CPCs alone, CPCs mixed with cECM) would be administered to the border zone through intramyocardial injection. Additionally, a group could be included for CPCs preconditioned by 48 hours of culture on cECM to evaluate preconditioning as a potential therapy. Functional cardiac assessment would be determined by echocardiography and invasive hemodynamics. To determine retention, CPCs would be labeled with a lipophilic tracer or virally transduced to express luciferase before injection. Fibrosis would be evaluated through Pico Sirius red staining of tissue sections. Immunohistochemistry would be used to evaluate vascularization. Engraftment could be determined through sex mismatching and immunocytochemistry. These studies could also be used to determine the lineage fate of engrafted CPCs.

6.3 Aim 2

6.3.1 Summary

The myocardial microenvironment is dynamic in development and disease states with changes in protein composition and mechanical strain. In cell therapy applications successful transplantation of cells requires survival, engraftment, paracrine signaling, differentiation and maturation of transplanted cells. Each of these endpoints may be affected by mechanical stimulation, motivating the study of mechanical strain on CPCs in vitro. Specifically, this study evaluates the matrix-dependent effects of mechanical strain on CPC behavior. Bioflex plates were functionalized with either poly-L-lysine (PLL), laminin (LN), fibronectin (FN), collagen I (COL) or cECM, seeded with CPCs and cyclically strained for 24 hours at 1 Hz and strain magnitudes of 0, 5, 10 or 15%. These conditions mimic the niche of endogenous CPCs (LN, 5 and 15%), physiological (COL, FN, cECM, 15%), pathophysiological (COL, FN, 5%) and therapeutic (cECM, 5%) conditions of the myocardium. The response of CPCs to signals from the microenvironment is complex, with more matrix-dependency observed at lower strains. Alignment, cell division and paracrine signaling are extracellular matrix and strain dependent. Extracellular matrix conditions affect CPC maturation and calcium signaling. Mechanotransduction pathways, including focal adhesion kinase are activated through adhesion and maintained under cyclic strain. In summary, this work demonstrates that fine control of the cardiac microenvironment is necessary for cardiac regeneration.

6.3.2 Limitations

While the results of Aim 1 and Aim 2 cannot be compared due to differences in matrix coatings and the stiffness of the underlying substrate, many of the same limitations from Aim 1 apply to Aim 2. In Aim 2, cECM and CPCs are used and carry the same critiques as described above. However, in Aim 2 a more complex combinatorial approach is taken to mimicking various microenvironments in the myocardium. This addresses a general

limitation of Aim 1, but still does not fully recapitulate endogenous microenvironments. Limitations to Aim 2 that will be addressed below include: 1) the two-dimensional culture, 2) presentation of ECM proteins, 3) in vitro application of mechanical strain, and 4) complexity of mechanotransduction.

As reviewed elsewhere, in vivo the ECM plays multiple roles by surrounding and orienting cells, allowing for transfer of mechanical forces, preventing over stretching of cells and providing mechanical support to the tissue [12, 15]. In addition to the limitations of two-dimensional culture discussed in Aim 1, the application of mechanical strain in Aim 2 does not permit the ECM to play its roles of force transmission and mechanical support as observed in vivo. Instead of a complex network, strain is transferred through what are likely single protein attachments to the underlying substrate. This is discussed further below. As discussed in the Aim1 limitations, multiple cell types are present in the myocardium. Fibroblasts are particularly influenced by strain and increase the secretion of matrix proteins, matrix metalloproteinases and cytokine and growth factor production in response to mechanical strain [258]. Thus the endogenous microenvironment is dynamic and would be influenced by the presence of other cell types. Mechanical loading of injected materials or the interaction of these materials with increased matrix metalloproteinases with strain application would affect their degradation in vivo [182]. Furthermore the three-dimensional environment would impose different passive stresses on cultured cells than the two-dimensional environments. In other cardiac progenitors, differentiation and maturation of the cells is dependent on stiffness [159]. Strain transmission through a three-dimensional hydrogel would be mediated by stiffness.

While we examined 20 different culture conditions, these do not fully span the possible microenvironments of the myocardium. For example, we did not evaluate elastin or

collagen IV as matrix conditions. Elastin is present in the myocardium and collagen IV has been suggested to exist in cardiac niches. It would have also been interesting to evaluate ECM obtained from an infarcted myocardium. In order to assess the effect of each matrix component in its purest form, single matrix proteins were used as culture conditions. Endogenously, the ratio of matrix proteins is likely to be as important as any single matrix component. While the cECM partially addresses this complexity, it is a single snapshot of the myocardial matrix as a whole. Endogenous ECM is heterogeneous and anisotropic [146]. We do not control for nanotopography differences in our matrix coatings and assume uniform coating across the entire plate by covalently attaching the matrix proteins. We do not know if or how the matrix proteins associate with each other in this format. Work by others has shown that the perceived stiffness of a peptide increases with the number of anchoring points and that this local stiffness is more relevant to cells than the bulk stiffness of a material [259]. Furthermore, we controlled protein content across all matrix conditions based on weight alone. Laminin is about twice as large as fibronectin and collagen I, so fewer laminin protein molecules were likely included. However, laminin has more known cell adhesive sites in its trimeric form than fibronectin or collagen, potentially compensating for the presence of fewer proteins. This would undoubtedly change the ligand density though. Finally, because the surfaces are quenched after functionalization and short time points are used in culture, we make the assumption that the covalently-attached matrix is the only matrix present. However, we do not know if the CPCs are secreting matrix and if so, if the newly formed matrix is soluble or can attach to the presented matrix proteins. For example, fibronectin has a known collagen binding site [208]. Moreover, we do not evaluate if the CPCs are remodeling their environment in this time period through the secretion of matrix metalloproteinases.

Endogenous strain is biaxial, anisotropic and heterogeneous [47]. Furthermore, cells are heterogeneous [114]. We apply a biaxial strain that is non-uniform across the culture dish as it is isotropic in the center of the well and anisotropic at the edges of the well. Thus the cell response is likely heterogeneous, but we largely consider the cell population as a whole. A uniaxial tension system is available by Flexcell, but even these do not fully represent the strain endogenously experienced by cells in a three-dimensional matrix. Moreover, we and others have shown that cultured cells orient perpendicular to an applied strain compared to endogenous cells that are oriented parallel to the strain and are actually responsible for strain generation. This may affect how cells interpret an applied strain [119]. Micropatterning the PDMS to align cells in the direction of strain may help to better mimic endogenous strain. We have chosen to evaluate cyclic strain magnitude instead of stress as our biomechanical stimuli, even though changes in both are observed post-MI. In the Bioflex system, stress and strain are proportional, whereas in the myocardium they are inversely proportional. However, it is easier to estimate cell strain than cell stress in the Bioflex system and endogenous biomechanics reflect the tissue as a whole and not necessarily what the cell experiences. While they should be consistent across all matrix conditions, it is worth noting that we do not know what fluid shear stresses are applied to cultured cells by the culture media at increasing strain magnitudes. Finally, we assess only one frequency (1 Hz) of cyclic strain. This mimics the beating frequency of the adult human heart. Strains specific to the rat heart or that better mimic the developing myocardium would be relevant to examine. For example, cardiomyogenic gene expression in mouse embryonic stem cells was strain dependent [260].

As previously discussed, mechanotransduction is a complicated process. It is bidirectional and integrates many types of signals into an ultimate cell behavior. We evaluate FAK and ERK activation as an assessment of mechanotransduction, but these signaling kinases are involved in multiple downstream transmission pathways. While

FAK activation is generally linked to integrin signaling, ERK activation can occur through integrin and growth factor pathways. To more specifically evaluate mechanotransduction pathways, integrin signaling can be disrupted by knocking down specific alpha subunits with short interfering RNA or activity can be blocked with non-specific echistatin or integrin specific blocking antibodies [261]. Similarly, FAK activation could be blocked with short interfering RNA or expression of the dominant-negative FAK known as FRNK [125]. To evaluate the role of the cytoskeleton in mechanotransduction in CPCs, the cells could be treated with cytochalasin D to prevent actin polymerization or with blebbistatin to inhibit myosin.

In addition to the above limitations, smaller gaps in the experimental methods of Aim 2 remain. While we measure cell spread area, we do not asses the height (or total volume) of the cells. This could potentially play a role in how the cells experience fluid shear stress. We count the number of dividing cells and cells with more than one nucleus based on general immunocytochemistry. To confirm our results and more conclusively show separate cell division and binucleation events a four color stain by immunocytochemistry is necessary: DAPI (total nuclei), Ki67 or aurora b kinase(dividing nuclei), alpha-actinin or tubulin (cytoskeleton/cleavage furrow) and non-muscle myosin II or septin (contractile ring) [168, 262]. A dividing cell would have a dividing nucleus, cleavage furrow and contractile ring. A recently binucleated cell would be positive for a diving nucleus, with a consistent cytoplasm and absence of a contractile ring indicating karyokinesis without cytokinesis. Finally, due to the limitations of our microscope we were unable to evaluate calcium oscillations in strained CPCs. We plan to evaluate calcium handling protein expression in strained CPCs. For calcium oscillation measurements that were taken, we did not distinguish between nuclear and cytoplasmic calcium, nor did we quantify the average amplitude and duration of oscillations.

6.3.3 Future Directions

An innumerable number of culture conditions could be evaluated to asses CPC behavior. Instead of adding to this complexity, it would be more impactful at this juncture to evaluate direct questions regarding mechanotransduction in CPCs. Specific knockdown of integrin subunits or intracellular signaling proteins such as focal adhesion kinase or proteins involved in the linker of nucleoskeleton and cytoskeleton (LINC) complex would elucidate the roles of these pathways. We observed differential activation of focal adhesion kinase and the extracellular signal-regulated kinase, suggesting that they receive input from different upstream signaling events. Overlap between these signaling cascades should be teased apart to determine the influence of different signaling components such as growth factors and extracellular matrix proteins. This may help to identify the common denominator or simplest effective signaling moiety. Such studies may lead to new targets for drug therapy that could potentially be used to activate endogenous progenitor cells.

However, complex microenvironments may be necessary to activate CPCs. Moving forward, in order to more definitively determine the effect of various strains, focus should be placed on a single (or minimal number of) matrix protein(s). To limit the number of matrix conditions, preliminary work on multiple matrices could be performed to screen for a desired outcome (i.e. troponin expression). Then further work evaluating other endpoints could be performed on the matrix that induced the least and greatest troponin expression. This would then allow the investigator to evaluate multiple strain frequencies or multiple strain magnitudes in three-dimensional cultures. Although not considered in this dissertation, electrical stimulation induces stem cell maturation [263]. It may be possible to achieve the same effects by biochemically stimulating calcium signaling in CPCs (i.e. through ATP) or mechanically activating calcium channels in CPCs in three-dimensional cyclic-strain cultures.

Progenitor cell therapy may not prove to be the most effective treatment for MI. In adults, the autologous cell sourcing yields older, less regenerative CPCs and sourcing from younger tissue has its own hurdles in autologous CPC cryopreservation or limitations of allogenic sources. Infusion of stem/progenitor cells may not be necessary for regeneration [34]. Work in our laboratory has shown that the secretome of CPCs may be powerful enough to induce regeneration post-MI [264]. While not fully characterized, it is worth investigating as it may provide an off-the-shelf therapy.

APPENDIX

A.1. Methods and Supplemental Results

A.1.1. Cardiac Progenitor Cell Isolation

CPCs were isolated from adult male Sprague-Dawley rats (about 250g) by removing the heart and homogenizing the tissue, as approved by Emory University's Institute Animal Care and Use Committee. The tissue homogenate was further digested with type-2 collagenase (1 mg/mL in Hank's Balanced Salt Solution (HBSS); Worthington Biochemical) and passed through a 70 μm filter. Cells were then incubated with Dynabeads (Dynal) conjugated to a c-kit antibody (Santa Cruz H-300) prior to magnetic sorting. Sorted cells were plated on a T-75 tissue culture flask and expanded to confluence. Following isolation, CPCs were characterized by flow cytometric analysis of c-kit (Santa Cruz H-300), multi-drug resistance protein (MDR; Santa Cruz H-241), Gata-4 (Santa Cruz H-112) and Nkx2.5 (Santa Cruz H-114). Only clones with >90% c-kit expression were used for subsequent studies. Figure 39 shows representative flow cytometry histograms for c-kit, MDR, Gata-4, and Nxk2.5.

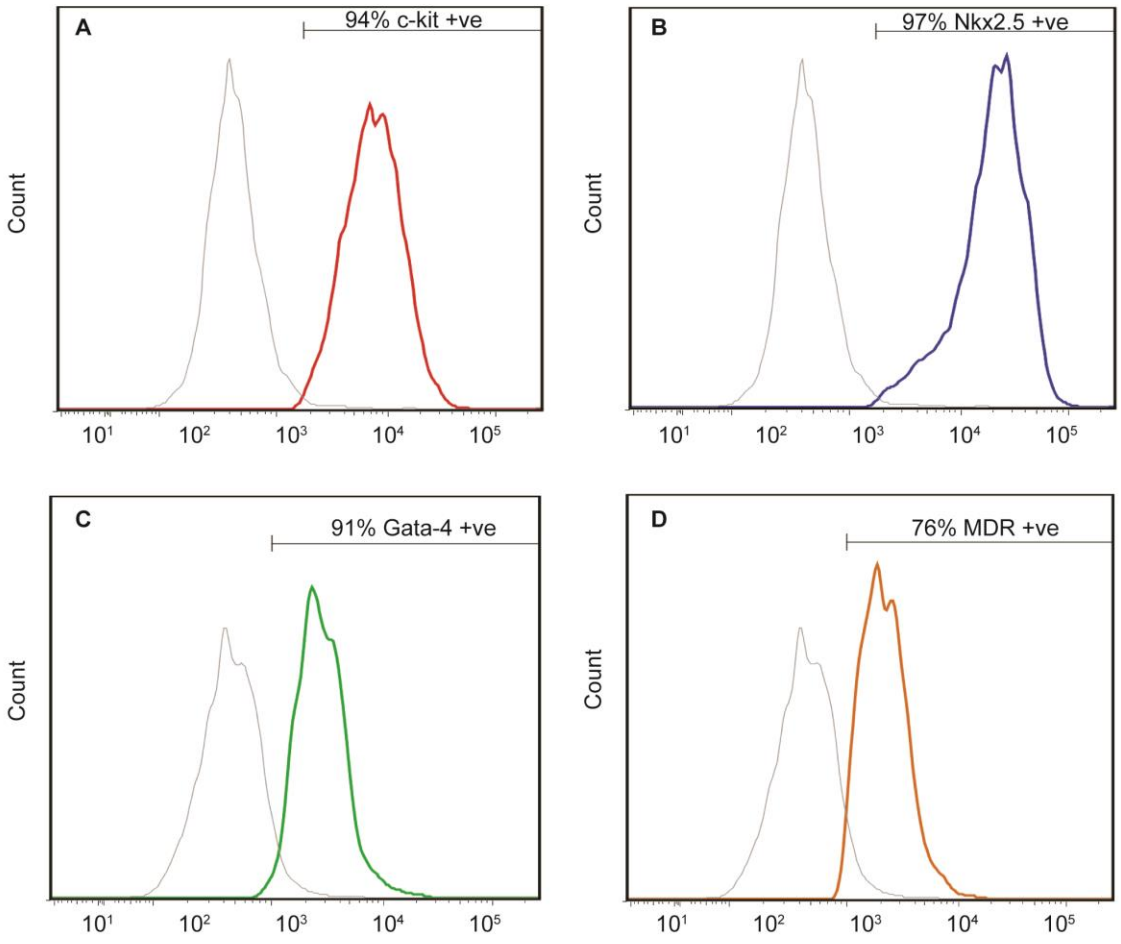

Figure 39. CPC Characterization. CPC clones were assessed by flow cytometry for stem cell markers c-kit (A) and MDR (D) as well as cardiomyogenic markers Nkx2.5 (B) and Gata-4 (C). Lighter histograms represent negative control.

A.1.2. Decellularized cardiac extracellular matrix (cECM) generation

Decellularized porcine ventricular extracellular matrix was obtained and processed into a cell culture coating as previously described [175, 176]. Briefly, porcine ventricular tissue was isolated and cut into small rectangular pieces, rinsed in phosphate buffered saline (PBS, Fisher), and decellularized using 1% sodium dodecyl sulfate (SDS, Fisher) for 4-5 days. The decellularized cECM was then rinsed with Triton X-100 (Integra Chemical Company) for 30 minutes, DI water overnight, frozen at -80°C overnight, lyophilized

(Labconco) overnight, and milled into a fine powder. The powder was digested using pepsin at 1 mg/ml in 0.1M HCl (Fisher) for at least 54 hours prior to use, as modified from a previously published protocol, at a ratio of 10:1 of ECM matrix to pepsin. The material was then raised to a basic pH by adding 1 M NaOH (Fisher), and brought to a salt concentration of 1X PBS through the addition of 10X PBS. Then, the material was brought to physiological pH of 7.4 using HCl and NaOH, and diluted to 6 mg/ml using 1X PBS. The cECM was then frozen at -80°C overnight, lyophilized for 24 hours (Labconco) and stored at -80°C prior to use.

A.1.3. Cell Culture

Matrix solutions were made by reconstituting cECM in sterile water and then diluting to 1 mg/mL in 100 mM acetic acid. Collagen I (COL; rat tail, Invitrogen) was diluted to 1 mg/ml in 100 mM acetic acid. Tissue culture plastic plates were coated with cECM or COL and incubated for 1 hour at 37°C to allow adsorption. Coated plates were then washed twice with 1x PBS to remove acetic acid. CPCs were seeded on top of the coated plates and incubated in the appropriate medium for the desired timepoints (see subsequent methods sections for details specific to each experiment).

A.1.4. RNA and protein isolation

Cell culture was performed as described above in 6-well tissue culture plastic plates coated with 500 µl of the appropriate matrix. Two wells were prepared for each condition with 5 x10^5 cells per well. Cells were cultured in treatment media (Ham's F-12 (Mediatech) + 0.1 µg/mL bFGF (Sigma) + 1x ITS (Cellgro) + 1x Penicillin-Streptomycin-Glutamine (P/S/G, Cellgro)) and media was exchanged every 48 hours. Cells were harvested 2 and 7 days following plating with Trizol (Invitrogen) for isolation of RNA and protein. The Trizol solution was frozen at -80°C until RNA isolation was

performed. RNA and protein extraction were performed according to the manufacturer's protocol. Samples were stored at -20°C.

A.1.5. Reverse transcription and quantitative real-time PCR

RNA quantification and purity was determined by absorbance readings at 260 and 280 nm by a BioTek Synergy2 Spectrophotometer. Reverse transcription was performed with M-MLV (Invitrogen) as follows. Samples were prepared with 2 μg RNA and 0.1 μg hexamers (Thermo Scientific), 0.1 μg oligo dTs (Fermentas), 25 nmol dNTPS (Fermentas) and RNase free water for a final volume of 12 μL. No-template controls were performed by replacing RNA content with RNase free water. Samples were heated at 65°C for 5 minutes to denature the RNA, followed by 25°C for 10 minutes to allow hexamers and oligos to anneal. First strand buffer (1x final concentration, Invitrogen), 0.2 μmol DTT (Invitrogen), 40 units RNaseOUT Inhibitor (Invitrogen) and 200 units M-MLV (Invitrogen) were added to each sample. Samples were heated at 37°C for 60 minutes for reverse transcription, followed by 70°C for 15 minutes to inactivate the enzyme. cDNA products were stored at -20°C.

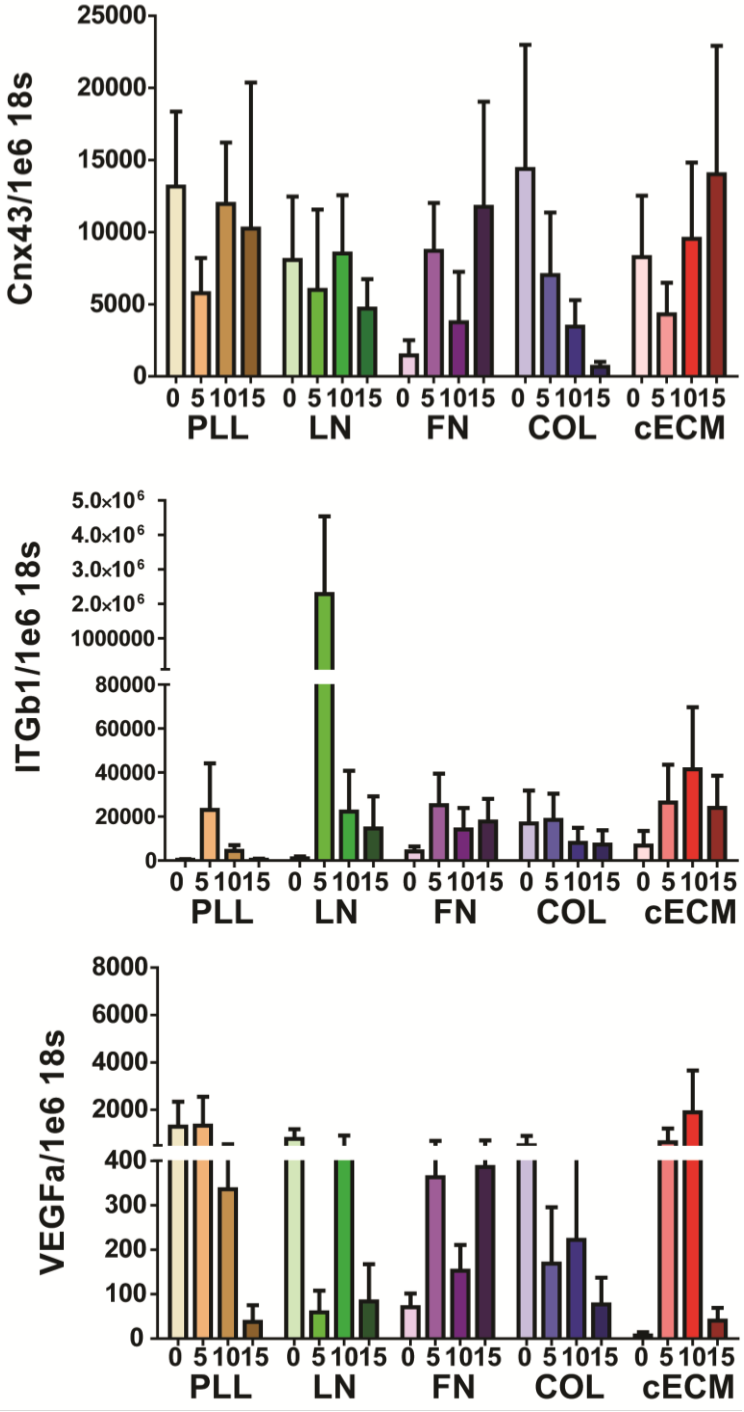

Figure 40. qPCR Results. CPCs were seeded on the appropriate matrix for 6 hours and then cyclic strain was applied for 24 hours. Cells were harvested by trizol and cDNA quantified by qPCR. Cnx43 (top), ITGb1 (middle), VEGFa (bottom); Two-way ANOVA, bars represent mean + SEM; n=2-5; Cnx43 = connexin 43, ITGb1 = integrin beta1,

VEGFa = vascular endothelial growth factor A, PLL = poly-l-lysine, LN = laminin, COL = collagen I, FN = fibronectin, cECM = naturally-derived cardiac extracellular matrix.

Gene expression was measured by quantitative real-time PCR on an Applied Biosystems StepOne Plus Real-Time PCR System. Reaction mixtures contained 7.5 μL Power SYBR Green (Invitrogen), 5.1 μL RNase free water (Hyclone), 1.4 μL of the appropriate primer at 1μM (IDT) and 1 μL 1:5 cDNA (total volume = 15 μL). The running protocol was 95°C for 10 minutes, followed by 40 cycles of 95°C for 15 seconds and 60°C for 60 seconds, for all SYBR Green Primers. A melt-curve was calculated at 2°C intervals with the same cycling conditions. Each sample was run in duplicate. A Taqman gene expression assay was performed to quantify GAPDH expression (Applied Biosystems; 50°C for 2 minutes, 95°C for 10 minutes and then 40 cycles of 95°C for 15 seconds followed by 60°C for 1 minute). Results are normalized to GAPDH and expressed as fold change for cECM relative to COL (ΔΔCt). Primer sequences are listed in Table 1. For array studies, cDNA from 3 separate studies was pooled to a total of 1 μg per plate. Extracellular matrix and adhesion molecule gene array plates were purchased from Qiagen (SABiosciences) and gene levels were normalized to beta-actin housekeeping gene. Data were compared using the logΔΔCt to plot COL vs. cECM and changes ± 2.5-fold were considered significantly up- or downregulated.

Table 1: List of Primers

Name	Forward 5'-3' Reverse 5'-3'	Lineage	Aim of Study
α-Myosin Heavy Chain (α-mhc)	F: AACGCCCAAGCCCACTTGAA R: CATTGGCACGGACTGCGTCA	cardiomyocyte	1
troponinT2 (tropT)	F: AAGGCCAAAGTCACCGGGCG R: TCGGGTGCCTGGCAAGACCT	cardiomyocyte	1
troponinC1 (tropC)	F: GATCTCTTCCGCATGTTTGACA R: TGGCCTGCAGCATCATCTT	cardiomyocyte	1
gata-4	F: ACCTGCTACAGCAGGGTTGGT R: TCTAGCACAACTGCAAGCATGGC	early cardiomyocyte	1
nkx2.5	F: CAAGTGCTCTCCTGCTTTCC R: GGCTTTGTCCAGCTCCACT	early cardiomyocyte	1
smooth muscle (sm) α-actin	F: CCCAGATTCAGGAACAGCAT R: GTTAGCAAGGTCGGATGCTC	smooth muscle	1
smooth muscle (sm) 22α	F: AGCCAGTGAAGGTGCCTGAGAAC R: TGCCCAAAGCCATTAGAGTCCTC	smooth muscle	1
fibroblast specific protein 1 (fsp)	F: GAGGAGGCCCTGGATGTAAT R: CTTCATTGTCCCTGTTGCTG	fibroblast	1
von Willebrand Factor (vwf)	F: CCCACCGGATGGCTAGGTATT R: GAGGCGGATCTGTTTGAGGTT	endothelial	1
tie2	F: TGCCACCATCACTCAATACCA R: AGGCTGGGTTGCTTGATCCT	endothelial	1
*primers were redisgned in Aim 2 to allow for purifacation of standards for standard curves			
troponinC1 (tnnc1)	F: GTAGACGAGGATGGCAGTGG R: ATGCGGAAGAGATCCGACAG	cardiomyocyte	2
troponinT2 (tnnT2)	F: CCAAGGAGCTATGGCAGAGT R: CTTTGGCCTTCCCACGAGTT	cardiomyocyte	2

Table 1 Continued: List of Primers

Name	Forward 5'-3' Reverse 5'-3'	Lineage	Aim of Study
nkx2.5	F: GCACCATGCGGGAAGGCTAT R: GACTGAGAAGGGCGTGTGTG	early cardiomyocyte	2
gata-4	F: ACCTGCTACAGCAGGGTTGGT R: TTCTAGCACAACTGCAAGCATGGC	early cardiomyocyte	2
connexin 43 (Cnx43)	F: TCAGCCTCCAAGGAGTTCCA R: CTAAGCCAAAGACGCAACGC	cardiomyocyte	2
integrin beta1 (ITGb1)	F: TCACCTACTCAGTGAACAGCAA R: ACGCCTGCTACAATTGGGAT		2
vascular endothelial growth factor A (VEGF)	F: GATAGAGTATATCTTCAAGCCG R: CTCATCTCTCCTATGTGCTG	endothelial	2
18s	F: TTCCTTACCTGGTTGATCCTGCCA R: AGCGAGCGACCAAAGGAACCATAA	housekeeping gene	2

A.1.6. Western blot

Protein quantification was performed by microBCA (Thermo Scientific) according to the manufacturer's protocol. Samples were prepared by adding 30 μg protein to appropriate amounts of 5x Laemmli buffer and water to yield a final volume of 25 μL and then boiled for 8 minutes at 95°C. Each sample was then loaded on 12% SDS-PAGE gel. NovexSharp (Invitrogen) protein ladder was loaded at 15 μL. Electrophoresis was performed and gels were transferred to a nitrocellulose membrane. Membranes were immediately blocked with 5% milk in Tris-buffered saline with 1% Tween-20 (TBS-T) overnight at 4°C. Membranes were washed 3 times in 1x TBS-T, then immersed in a 1:1000 primary antibody (Table 2). All antibody solutions, except those from Cell Signaling, were made in 5% milk in 1x TBS-T and incubated with membranes overnight

at 4°C prior to 3 washes with 1x TBS-T. Cell Signaling antibodies were diluted in bovine serum albumin. Membranes were incubated at room temperature for 1 hour in 1:5000 secondary antibody. For all cases, the secondary antibody was HRP-conjugated goat anti-rabbit or goat anti-mouse (Bio-rad). Membranes were exposed on film or Kodak imager and results were quantified with ImageJ and are expressed as fold change for cECM/COL.

Table 2: List of Antibodies and Stains

Antibody	**Supplier**	**Catalog #**	**Host**
c-kit (H-300)	Santa Cruz Biotechnology	sc-5535	Rabbit
Gata-4	Santa Cruz Biotechnology	sc-9053	Rabbit
Nkx2.5	Santa Cruz Biotechnology	sc-14033	Rabbit
HUTS-4 (active integrin beta1)	Millipore	MAB2079Z	Mouse
Integrin beta1	Santa Cruz Biotechnology	sc-8978	Rabbit
pFAK	Cell Signaling	8556P	Rabbit
FAK	Cell Signaling	3285S	Rabbit
pERK	Cell Signaling	9101S	Rabbit
ERK	Cell Signaling	9102S	Rabbit
Connexin 43	Sigma	C8093	Mouse
GAPDH	Santa Cruz Biotechnology	sc-25778	Rabbit
Stain	**Supplier**	**Catalog #**	
DAPI	Invitrogen	D1306	
Rhodamine-Phalloidin	Invitrogen	R415	
Fluorescein 5-maleimide	Sigma	38132	

A.1.7. Determination of proliferation

Cell culture plates were prepared as described above with 125 μL of the appropriate matrix per well of a 24-well plate. CPCs were seeded at a density of 2000 cells per well to allow growth, while removing the possibility of contact inhibition [Hadjipanayi 2009]. The cells were incubated in serum-rich treatment medium (Ham's F-12 (Mediatech) + 10% FBS (Hyclone) + 0.1 μg/mL bFGF (Sigma) + 1x ITS (Cellgro) + 1x P/S/G (Cellgro)). Following 48 hour incubation, the medium was discarded and the cells were lifted from culture plates with TrypLE Express (Invitrogen). The cell solution was diluted 1:100 in Isoton II (Beckman Coulter) and cells were immediately counted in triplicate in a Coulter Counter. Results are expressed as fold change in cell number as final count/initial seed number.

A.1.8. Microfluidic adhesion assay

Individual channels of the microfluidic devices [265] were filled simultaneously with protein solutions of interest, including collagen I (Invitrogen, rat tail), cECM, fibronectin (BD Biosciences, human) and laminin (BD Biosciences, mouse) at 10 μg/mL. Devices were then incubated for 3 hours at 37°C; the channels were rinsed with PBS and blocked with 2% BSA for 0.5 hours at 37°C. CPCs were then seeded at $1x10^6$ cells/mL in growth media (Ham's F-12 (Mediatech) + 0.1 μg/mL bFGF (Sigma) + 10% FBS (Hyclone) + 1x P/S/G (Cellgro) and allowed to adhere for 3 hours at 37°C, and then subjected to step-wise increments of shear stresses from 0 to ~470 dynes/cm^2 for 12 minutes. Results are reported as the fraction of adherent cells over time normalized to starting cell number.

A.1.9. Annexin V staining

Cell culture plates were prepared as described above with 125 μL of the appropriate matrix per well of a 24-well plate. CPCs were seeded at a density of 50,000 cells per

well, in triplicate. Cells were cultured in serum-free media (Ham's F-12 (Mediatech) + 1x P/S/G (Cellgro)). Cells that were not serum-deprived were stained with AnnexinV Alexa Fluor® 647 (Invitrogen) as a negative control. After 12 hour incubation, media from each well was collected and TrypLE Express (Invitrogen) was added to lift the cells from the well. The lifted cells were added to the respective collected media. Cells were centrifuged at >1500 rpm for 5 minutes. The supernatant was removed and the cells were washed with cold 1x PBS. After centrifugation at >1500 rpm for 5 minutes, the supernatant was again removed and the cells were resuspended in 50 μL of Annexin binding buffer. The cell solution was then incubated with 5 μL of AnnexinV Alexa Fluor® 647 (Invitrogen) at room temperature for 15 minutes. After incubation, 400 μL of Annexin binding buffer was added and samples were mixed gently and kept on ice. Cells were analyzed immediately by flow cytometry.

A.1.10. Silanization of Bioflex Plates

Working in a fume hood, 2 mL of 1.0 M NaOH (Sigma) was added to each well of a 6-well Bioflex plate (Flexcell International) and incubated for 1 hour at room temperature. Following incubation, plates were washed in ddH2O for five minutes, three times. With the lids on, each well was treated with 1 mL of 4% (v/v) aminopropyltriethoxysilane (APTES; Sigma) in acetone for 10 minutes at room temperature. Plates were washed three times, treated with 2 mL 0.5% glutaraldehyde (Sigma) in ddH2O at room temperature for 30 minutes and then washed three times again. Matrix proteins were diluted to 100 μg/mL, with 1 mL for each well, as follows: naturally-derived cardiac extracellular matrix (cECM; porcine) in 100 mM acetic acid, collagen I (COL; rat tail, Invitrogen) in 100 mM acetic acid, fibronectin (FN; human, BD Bioscience) in 1X PBS, laminin (LN; mouse, BD Bioscience) in 1X PBS and poly-L-lysine (Sigma) in ddH2O. Matrix proteins were added to the appropriate wells and plates were incubated for 1 hour at 37 °C. Plates were then washed once for 5 minutes in 1X PBS and treated with 1 mL

of 1 M ethanolamine (Sigma) in ddH2O (pH 7.0) for 20 min to quench unreacted gluteraldehyde. Plates were washed three times with 1X PBS and stored dry at 4°C. To sterilize, plates were kept under ultraviolet light for 1 hour prior to use. Functionalization with glutaraldehyde is demonstrated by auto-fluorescence in Figure 41.

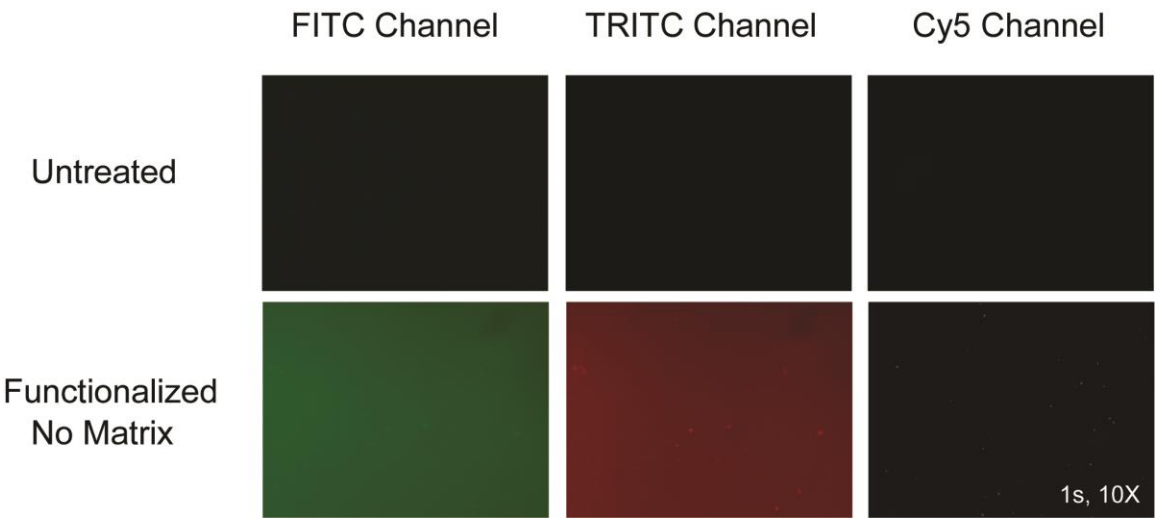

Figure 41. Functionalization of Bioflex plates. Auto-fluorescence in FITC and TRITC channels indicates presence of glutaraldehyde.

A.1.11. Application of Mechanical Tension

CPCs were seeded at a density of $4x10^5$ cells/well on functionalized Bioflex plates and incubated in treatment medium (Ham's F-12 (Mediatech) + 0.1 μg/mL bFGF (Sigma) + 1x insulin transferrin selenium (Cellgro) + 1x penicillin-streptomycin-glutamine (P/S/G, Cellgro)) for 6 hours prior to the application of mechanical tension. Tensile strain was applied through a Flexcell 5000 (Flexcell International). For this, Bioflex plates were loaded onto 25 mm cylindrical loading posts. A cyclic sinusoidal strain regimen of 1 Hz and 0.5 duty cycle, with elongation magnitudes of 5, 10 or 15% was applied to the plates for 24 hours. During this time, cells were maintained in 5% CO2 at 37° C. Approximate stress and strain values achieved in this set-up are presented in Figure 42.

A

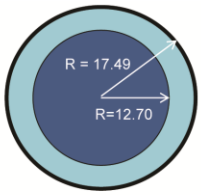

B

Strain (%)	Stress (kPa)
0	0
5	53
10	105
15	158

C

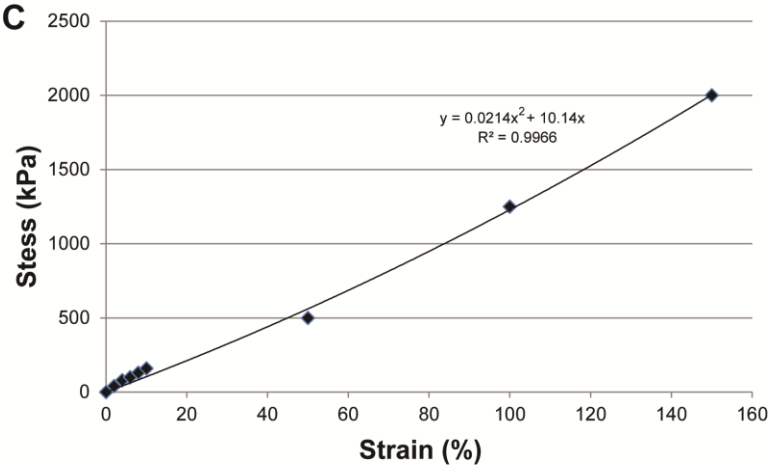

Figure 42. Biaxial strain in Bioflex 6-well plates. (A) Diameter of loading post (dark) and well (light), (B) Relationship of generated strain and estimated stress, (C) Stress and strain relationship of compiled data from: Colombo A (2008) Proc Inst Mech Eng H, 222(8): 1235-45.

To assess activation of focal adhesion kinase and extracellular signal-regulated kinase, CPCs were seeded as described above and allowed to adhere for 20 minutes before lysing with NP-40 lysis buffer. Alternatively, cells were allowed to adhere for the full 6 hours and then strained for either 15 minutes or 24 hours before lysis. Lysates were incubated overnight at 4°C with rocking. Lysates were spun at 10,000 x g for 5 minutes and supernatants used for Western blots.

A.1.12. Strain Transfer Video Microscopy

Untreated StageFlexer membranes (Flexcell International) were functionalized with matrix proteins as described above. For improved visualization CPCs were incubated for 2 hours at 37° C with anti-c-kit antibody conjugated Dynabeads, with rocking. CPCs were seeded at $5x10^5$ cells/membrane and incubated for 6 hours in growth media. Seeded membranes were then placed in a StageFlexer (Flexcell International) attached to the Flexcell 5000. A cyclic sinusoidal strain regimen of 1 Hz and 0.5 duty cycle, with

elongation magnitudes of 5, 10 or 15% was applied and bright field video was captured on an upright microscope (Amscope) with ToupView 3.7 at 20 frames per second. To quantify, a single cell containing two or more beads was identified. The distance between the two beads was traced in FIJI and strain was computed as the difference between the average maximum and minimum distances between the beads over the minimum distance between the beads. This 'measure strain' is compared to the strain reported by the Flexcell 5000.

A.1.13. Immunocytochemistry

After 24 hours of mechanical strain, cells were immediately fixed in 4% paraformaldehyde (Sigma) for 20 minutes at room temperature. Following three washes in 1X PBS, the cells were permeabilized with 0.1% triton in (Sigma) 1X PBS. Cells were again washed and then blocked in 3% bovine serum albumin (Sigma) for 1 hour at room temperature. Cells were then stained with 10 μg/mL fluoresceinyl-maleimide (Sigma) for 1 hour at room temperature in the absence of light, followed by washing and then 1 μg/mL DAPI (company) for 10 minutes. Alternatively, cells were simultaneously stained for 125 μg/mL rhodamine-phalloidin (Invitrogen) and DAPI for 20 minutes at room temperature in the absence of light. Cells were washed prior to imaging. Images were captured on an Olympus IX70 inverted fluorescent microscope.

Cell characteristics were quantified by importing images into CellProfiler 2.1.0. The images were analyzed according to the following pipeline: 1) resized by 0.25, 2) converted to greyscale, 3) nuclei were identified by intensity using a global threshold, automatic smoothing and a threshold correction factor of 1, 4) cells were identified around nuclei by intensity through propagation with per object Otsu thresholding, automatic smoothing and a threshold correction factor of 0.8, 5) cell size, shape and orientation were measured, 6) export to spreadsheet. Exported data was compiled to

calculate cell size, spread area and alignment. This pipeline is summarized in Figure 43. Alignment scores were calculated by measuring the angle between the major axis of each cell and the horizon, taking the standard deviation of all the angles and computing 100* the percent difference of the standard deviation from a Gaussian distribution or: 100*((90/sqrt(3)-Stdev)/(90/sqrt(3)). Circular math was employed to correct for the orientation of cells in orthogonal images.

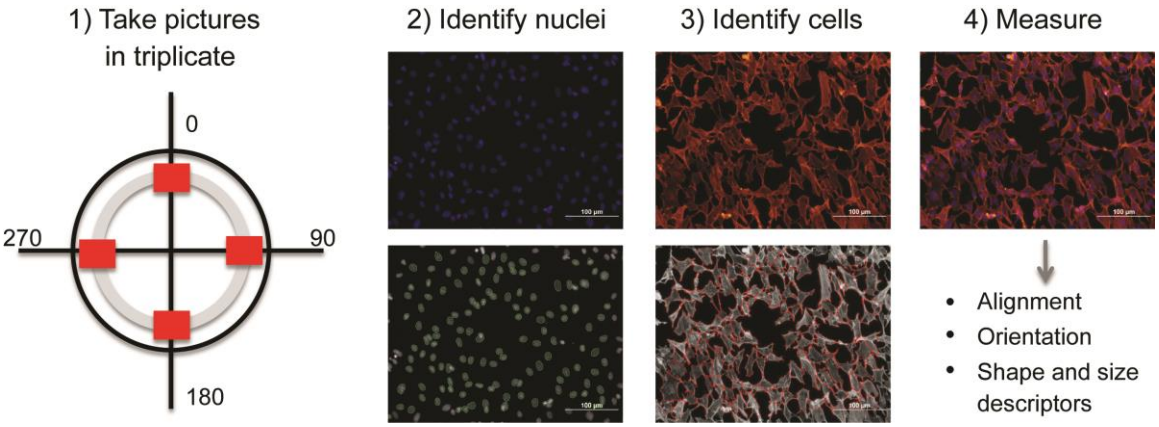

Figure 43. CellProlifer Workflow. Images were acquired at edge of loading post. Nuclei and cells were identified based on intensity. Shape characteristics were measured.

A.1.14. Cytoplasmic Calcium Imaging

Coverslips were coated with 10 ug/cm^2 of the appropriate matrix and allowed to dry. After UV sterilization, 200,000 CPCs were seeded onto each coverslip and cultured for 24 hours. Cells were loaded with 10 μm Fluo-4 (Invitrogen) in 2 mM calcium Tyrode's solution for 20 minutes at room temperature. Cells were washed with 2mM calcium Tyrode's before imaging on an Olympus confocal microscopes under epifluoresence. For each coverslip, a video was acquired at the beginning of a 1 Hz electrical stimulation, showing initial calcium uptake. Two additional videos were acquired with 1 Hz stimulation per coverslip. Videos were quantified by tracing regions of interest around individual cells and evaluating fluorescence over time. The number of active cells with

calcium oscillations and the number of oscillations per active cell in the 90 second period were evaluated.

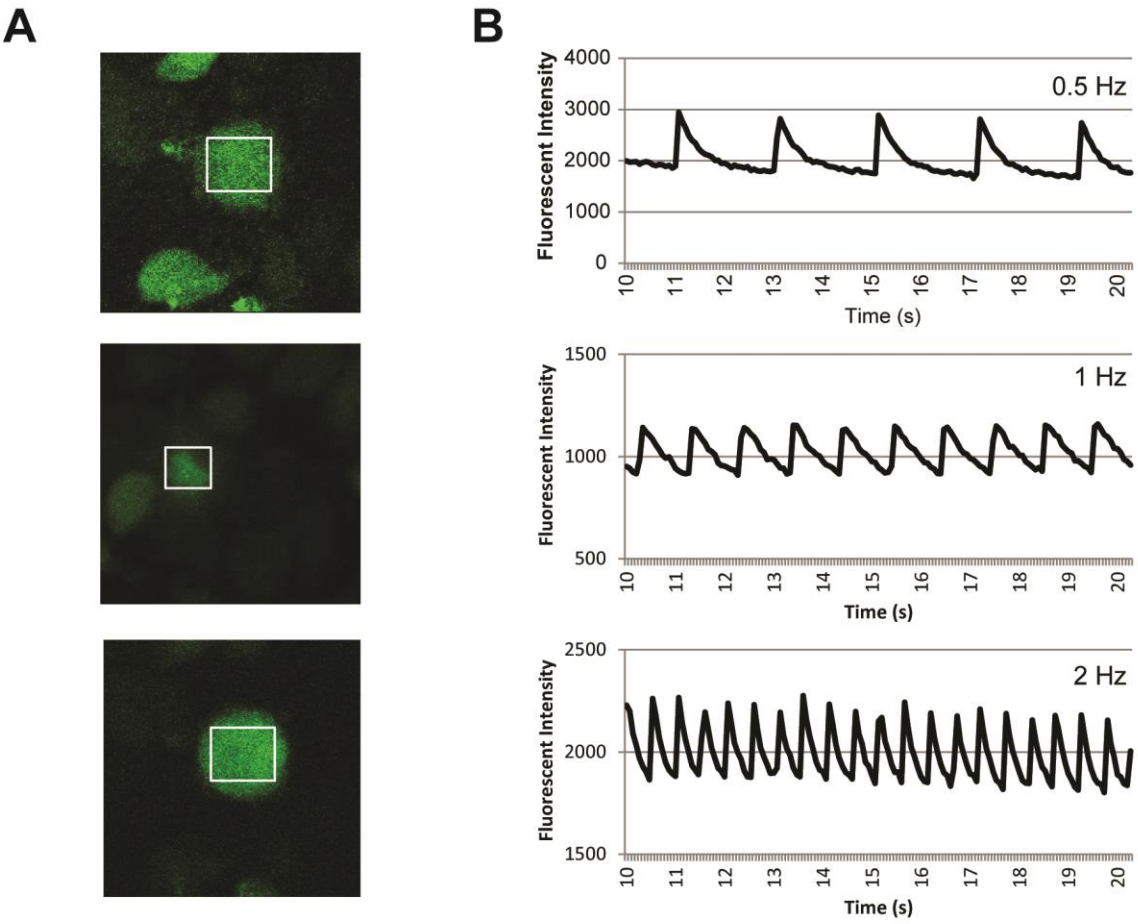

Figure 44. Pacing CPCs. CPCs were seeded on laminin for 3 hours. Cytoplasmic protein was assessed by Fluo-4 during electrical stimulation. Pacing CPCs, though rare, were found for each stimulation frequency. (A) Representative stills, region of interest is enclosed in white box, (B) Intensity traces from matching region of interest in A.

A.1.15. Cytokine ELISAs

After 24 hours of mechanical strain, conditioned media was immediately collected from the wells and stored at -20° C. ELISA kits were purchased from RayBiotech for stem cell factor, hepatocyte growth factor, platelet-derived growth factor and vascular endothelial

growth factor. Experiments were performed according to the manufacturer's protocol. Briefly, diluted conditioned media or standard was added the appropriate well and incubated for 2.5 hours at room temperature. Following washing, the appropriate biotin-conjugated antibody was added to each well and incubated for 1 hour at room temperature. Following washing, a horseradish peroxidase-conjugated streptavidin solution was added to each well and incubated for 45 minutes at room temperature. After additional washing, substrate was added to each well and incubated for 30 minutes at room temperature. Finally, stop solution was added to each well. Plates were read immediately at 450 nm on a BioTek Synergy2 spectrophotometer. Concentrations of each cytokine were calculated based on the standard curve.

A.1.16.Statistical Analysis

Graphpad Prism 3 or 5 software was used for all statistical analysis. In Aim 1, student's t-test with Welch's Correction or paired t-test was performed. P-values of less than 0.05 were considered significant. In Aim 2, two-way ANOVAs were performed for each data set to establish overall effects of matrix and strain on a given endpoint. No post-test results are reported for the two-way ANOVA as we cannot compare between all relevant groups simultaneously. Instead the same data was analyzed by one-way ANOVAs to establish specific effects of matrix or strain, except where noted. All one-way ANOVA post-tests are Tukey's multiple comparison tests allowing for the comparison of all groups to each other. Ultimately, this does not allow for direct comparisons of all culture conditions, but does allow conclusions to be drawn regarding the effect of strain for CPCs cultured on a given matrix and the effect of matrix conditions for a given strain.

REFERENCES

[1] Go AS, Mozaffarian D, Roger VL, Benjamin EJ, Berry JD, Blaha MJ, et al. Heart disease and stroke statistics--2014 update: a report from the American Heart Association. Circulation. 2014;129:e28-e292.

[2] Segers VFM, Lee RT. Stem-cell therapy for cardiac disease. Nature. 2008;451:937-42.

[3] Xie M, Burchfield JS, Hill JA. Pathological ventricular remodeling: therapies: part 2 of 2. Circulation. 2013;128:1021-30.

[4] Matsa E, Sallam K, Wu JC. Cardiac stem cell biology: glimpse of the past, present, and future. Circulation research. 2014;114:21-7.

[5] Burke AP, Virmani R. Pathophysiology of acute myocardial infarction. The Medical clinics of North America. 2007;91:553-72; ix.

[6] Burchfield JS, Xie M, Hill Ja. Pathological ventricular remodeling: mechanisms: part 1 of 2. Circulation. 2013;128:388-400.

[7] Nadal-Ginard B. Myocyte Death, Growth, and Regeneration in Cardiac Hypertrophy and Failure. Circulation Research. 2003;92:139-50.

[8] Swynghedauw B. Molecular mechanisms of myocardial remodeling. Physiological reviews. 1999;79:215-62.

[9] Anversa P, Li P, Zhang X, Olivetti G, Capasso JM. Ischaemic myocardial injury and ventricular remodelling. Cardiovascular research. 1993;27:145-57.

[10] Dobaczewski M, Gonzalez-Quesada C, Frangogiannis NG. The extracellular matrix as a modulator of the inflammatory and reparative response following myocardial infarction. Journal of Molecular and Cellular Cardiology. 2010;48:504-11.

[11] Vannan MA. Ventricular remodelling after myocardial infarction. British heart journal. 1992;68:257-9.

[12] St John Sutton MG, Sharpe N. Left ventricular remodeling after myocardial infarction: pathophysiology and therapy. Circulation. 2000;101:2981-8.

[13] Olivetti G, Capasso JM, Meggs LG, Sonnenblick EH, Anversa P. Cellular basis of chronic ventricular remodeling after myocardial infarction in rats. Circulation research. 1991;68:856-69.

[14] Cheng W, Li B, Kajstura J, Li P, Wolin MS, Sonnenblick EH, et al. Stretch-induced programmed myocyte cell death. The Journal of clinical investigation. 1995;96:2247-59.

[15] Cleutjens JP, Kandala JC, Guarda E, Guntaka RV, Weber KT. Regulation of collagen degradation in the rat myocardium after infarction. Journal of molecular and cellular cardiology. 1995;27:1281-92.

[16] Cleutjens JPM, Creemers EEJM. Integration of concepts: cardiac extracellular matrix remodeling after myocardial infarction. Journal of cardiac failure. 2002;8:S344-8.

[17] Bishop JE, Laurent GJ. Collagen turnover and its regulation in the normal and hypertrophying heart. European heart journal. 1995;16 Suppl C:38-44.

[18] Li YY, McTiernan CF, Feldman aM. Proinflammatory cytokines regulate tissue inhibitors of metalloproteinases and disintegrin metalloproteinase in cardiac cells. Cardiovascular research. 1999;42:162-72.

[19] Jugdutt BI. Ventricular remodeling after infarction and the extracellular collagen matrix: when is enough enough? Circulation. 2003;108:1395-403.

[20] McCain ML, Parker KK. Mechanotransduction: the role of mechanical stress, myocyte shape, and cytoskeletal architecture on cardiac function. Pflügers Archiv : European journal of physiology. 2011;462:89-104.

[21] Barallobre-Barreiro J, Didangelos A, Schoendube Fa, Drozdov I, Yin X, Fernández-Caggiano M, et al. Proteomics Analysis of Cardiac Extracellular Matrix Remodeling in a Porcine Model of Ischemia-Reperfusion Injury. Circulation. 2012;44.

[22] Eghbali M, Weber KT. Collagen and the myocardium: fibrillar structure, biosynthesis and degradation in relation to hypertrophy and its regression. Molecular and cellular biochemistry. 1990;96:1-14.

[23] McCurdy S, Baicu CF, Heymans S, Bradshaw AD. Cardiac extracellular matrix remodeling: fibrillar collagens and Secreted Protein Acidic and Rich in Cysteine (SPARC). Journal of molecular and cellular cardiology. 2010;48:544-9.

[24] Li A-H, Liu PP, Villarreal FJ, Garcia Ra. Dynamic changes in myocardial matrix and relevance to disease: translational perspectives. Circulation research. 2014;114:916-27.

[25] Rienks M, Papageorgiou A-P, Frangogiannis NG, Heymans S. Myocardial extracellular matrix: an ever-changing and diverse entity. Circulation research. 2014;114:872-88.

[26] Berry MF, Engler AJ, Woo YJ, Pirolli TJ, Bish LT, Jayasankar V, et al. Mesenchymal stem cell injection after myocardial infarction improves myocardial compliance. American journal of physiology Heart and circulatory physiology. 2006;290:H2196-203.

[27] Bayomy AF, Bauer M, Qiu Y, Liao R. Regeneration in heart disease-Is ECM the key? Life sciences. 2012;91:823-7.

[28] Bovendeerd PH, Arts T, Huyghe JM, van Campen DH, Reneman RS. Dependence of local left ventricular wall mechanics on myocardial fiber orientation: a model study. Journal of biomechanics. 1992;25:1129-40.

[29] Grossman W, Jones D, McLaurin LP. Wall stress and patterns of hypertrophy in the human left ventricle. The Journal of clinical investigation. 1975;56:56-64.

[30] Andreu I, Luque T, Sancho A, Pelacho B, Iglesias O, Melo E, et al. Heterogeneous micromechanical properties of the extracellular matrix in healthy and infarcted hearts. Acta biomaterialia. 2014.

[31] Leitman M, Lysyansky P, Sidenko S, Shir V, Peleg E, Binenbaum M, et al. Two-dimensional strain-a novel software for real-time quantitative echocardiographic assessment of myocardial function. Journal of the American Society of Echocardiography : official publication of the American Society of Echocardiography. 2004;17:1021-9.

[32] Voigt J-U, Arnold MF, Karlsson M, Hübbert L, Kukulski T, Hatle L, et al. Assessment of Regional Longitudinal Myocardial Strain Rate Derived from Doppler Myocardial Imaging Indexes in Normal and Infarcted Myocardium. Journal of the American Society of Echocardiography. 2000;13:588-98.

[33] Garbern JC, Lee RT. Cardiac stem cell therapy and the promise of heart regeneration. Cell Stem Cell. 2013;12:689-98.

[34] Nadal-Ginard B, Ellison GM, Torella D. The cardiac stem cell compartment is indispensable for myocardial cell homeostasis, repair and regeneration in the adult. Stem cell research. 2014.

[35] Bergmann O, Bhardwaj RD, Bernard S, Zdunek S, Barnabe-Heider F, Walsh S, et al. Evidence for cardiomyocyte renewal in humans. Science. 2009;324:98-102.

[36] Jesty SA, Steffey MA. c-kit+ precursors support postinfarction myogenesis in the neonatal, but not adult, heart. Proceedings of the …. 2012:4-9.

[37] Mohsin S, Siddiqi S, Collins B, Sussman Ma. Empowering adult stem cells for myocardial regeneration. Circulation research. 2011;109:1415-28.

[38] Voog J, Jones DL. Stem cells and the niche: a dynamic duo. Cell Stem Cell. 2010;6:103-15.

[39] Turner NJ, Keane TJ, Badylak SF. Lessons from developmental biology for regenerative medicine. Birth defects research Part C, Embryo today : reviews. 2013;99:149-59.

[40] Williams C, Quinn KP, Georgakoudi I, Black LD. Young developmental age cardiac extracellular matrix promotes the expansion of neonatal cardiomyocytes in vitro. Acta biomaterialia. 2013.

[41] Gershlak JR, Resnikoff JI, Sullivan KE, Williams C, Wang RM, Black LD. Mesenchymal stem cells ability to generate traction stress in response to substrate stiffness is modulated by the changing extracellular matrix composition of the heart during development. Biochemical and biophysical research communications. 2013;439:161-6.

[42] Burgess ML, McCrea JC, Hedrick HL. Age-associated changes in cardiac matrix and integrins. Mechanisms of ageing and development. 2001;122:1739-56.

[43] Barry EL, Mosher DF. Factor XIIIa-mediated cross-linking of fibronectin in fibroblast cell layers. Cross-linking of cellular and plasma fibronectin and of amino-terminal fibronectin fragments. J Biol Chem. 1989;264:4179-85.

[44] Sabri A, Farhadian F, Contard F, Samuel JL, Rappaport L. Fibronectin expression in the cardiovascular system. Herz. 1995;20:118-26.

[45] Yarnitzky T, Volk T. Laminin is required for heart, somatic muscles, and gut development in the Drosophila embryo. Developmental biology. 1995;169:609-18.

[46] Krieg M, Arboleda-Estudillo Y, Puech PH, Käfer J, Graner F, Müller DJ, et al. Tensile forces govern germ-layer organization in zebrafish. Nature cell biology. 2008;10:429-36.

[47] Huang H, Kamm RD, Lee RT. Cell mechanics and mechanotransduction: pathways, probes, and physiology. American journal of physiology Cell physiology. 2004;287:C1-11.

[48] Bhana B, Iyer RK, Chen WLK, Zhao R, Sider KL, Likhitpanichkul M, et al. Influence of substrate stiffness on the phenotype of heart cells. Biotechnology and bioengineering. 2010;105:1148-60.

[49] Barker PCa, Houle H, Li JS, Miller S, Herlong JR, Camitta MGW. Global longitudinal cardiac strain and strain rate for assessment of fetal cardiac function: novel experience with velocity vector imaging. Echocardiography (Mount Kisco, NY). 2009;26:28-36.

[50] Di Salvo G, Russo MG, Paladini D, Pacileo G, Felicetti M, Ricci C, et al. Quantification of regional left and right ventricular longitudinal function in 75 normal fetuses using ultrasound-based strain rate and strain imaging. Ultrasound in medicine & biology. 2005;31:1159-62.

[51] Menasche P, Alfieri O, Janssens S, McKenna W, Reichenspurner H, Trinquart L, et al. The Myoblast Autologous Grafting in Ischemic Cardiomyopathy (MAGIC) trial: first

randomized placebo-controlled study of myoblast transplantation. Circulation. 2008;117:1189-200.

[52] Hare JM, Traverse JH, Henry TD, Dib N, Strumpf RK, Schulman SP, et al. A randomized, double-blind, placebo-controlled, dose-escalation study of intravenous adult human mesenchymal stem cells (prochymal) after acute myocardial infarction. Journal of the American College of Cardiology. 2009;54:2277-86.

[53] Passier R, van Laake LW, Mummery CL. Stem-cell-based therapy and lessons from the heart. Nature. 2008;453:322-9.

[54] Forrester JS, Makkar RR, Marbán E. Long-term outcome of stem cell therapy for acute myocardial infarction: right results, wrong reasons. Journal of the American College of Cardiology. 2009;53:2270-2.

[55] Breitbach M, Bostani T, Roell W, Xia Y, Dewald O, Nygren JM, et al. Potential risks of bone marrow cell transplantation into infarcted hearts. 2015;110:1362-70.

[56] Asano S, Hoshikawa Y, Yamane Y, Ikeda M, Wakasa H. An intrapulmonary teratoma associated with bronchiectasia containing various kinds of primordium: a case report and review of the literature. Virchows Archiv : an international journal of pathology. 2000;436:384-8.

[57] Cooke MJ, Stojkovic M, Przyborski Sa. Growth of teratomas derived from human pluripotent stem cells is influenced by the graft site. Stem cells and development. 2006;15:254-9.

[58] Torella D, Ellison GM, Nadal-Ginard B, Indolfi C. Cardiac stem and progenitor cell biology for regenerative medicine. Trends in cardiovascular medicine. 2005;15:229-36.

[59] Zaruba M-M, Soonpaa M, Reuter S, Field LJ. Cardiomyogenic potential of C-kit(+)-expressing cells derived from neonatal and adult mouse hearts. Circulation. 2010;121:1992-2000.

[60] Beltrami AP, Barlucchi L, Torella D, Baker M, Limana F, Chimenti S, et al. Adult cardiac stem cells are multipotent and support myocardial regeneration. Cell. 2003;114:763-76.

[61] Linke A, Müller P, Nurzynska D, Casarsa C, Torella D, Nascimbene A, et al. Stem cells in the dog heart are self-renewing, clonogenic, and multipotent and regenerate infarcted myocardium, improving cardiac function. Proceedings of the National Academy of Sciences of the United States of America. 2005;102:8966-71.

[62] Urbanek K, Torella D, Sheikh F, De Angelis A, Nurzynska D, Silvestri F, et al. Myocardial regeneration by activation of multipotent cardiac stem cells in ischemic heart failure. Proceedings of the National Academy of Sciences of the United States of America. 2005;102:8692-7.

[63] Urbanek K, Cesselli D, Rota M, Nascimbene A, De Angelis A, Hosoda T, et al. Stem cell niches in the adult mouse heart. Proceedings of the National Academy of Sciences of the United States of America. 2006;103:9226-31.

[64] Leri A, Kajstura J, Anversa P. Cardiac stem cells and mechanisms of myocardial regeneration. Physiological reviews. 2005;85:1373-416.

[65] Messina E, De Angelis L, Frati G, Morrone S, Chimenti S, Fiordaliso F, et al. Isolation and expansion of adult cardiac stem cells from human and murine heart. Circulation research. 2004;95:911-21.

[66] Marbán E, Cingolani E. Heart to heart: cardiospheres for myocardial regeneration. Heart rhythm : the official journal of the Heart Rhythm Society. 2012;9:1727-31.

[67] Makkar RR, Smith RR, Ke C, Malliaras K, Thomson LEJ, Berman DLSCCMDaLMPaAMMSbPVJMDcSD. Intracoronary cardiosphere-derived cells for heart regeneration after myocardial infarction (CADUCEUS): a prospective, randomised phase 1 trial. The Lancet. 2012;379:895-094.

[68] Bolli R, Chugh AR, D'Amario D, Loughran JH, Stoddard MF, Ikram S, et al. Cardiac stem cells in patients with ischaemic cardiomyopathy (SCIPIO): initial results of a randomised phase 1 trial. The Lancet. 2011;378:1847-57.

[69] Fuchs E, Tumbar T, Guasch G. Socializing with the neighbors: stem cells and their niche. Cell. 2004;116:769-78.

[70] Mearns BM. Intramyocardial injections are safe. Nature Reviews Cardiology. 2009;6:441-.

[71] Christman KL, Lee RJ. Biomaterials for the treatment of myocardial infarction. Journal of the American College of Cardiology. 2006;48:907-13.

[72] Davis ME, Motion JPM, Narmoneva Da, Takahashi T, Hakuno D, Kamm RD, et al. Injectable self-assembling peptide nanofibers create intramyocardial microenvironments for endothelial cells. Circulation. 2005;111:442-50.

[73] Kofidis T, de Bruin JL, Hoyt G, Lebl DR, Tanaka M, Yamane T, et al. Injectable bioartificial myocardial tissue for large-scale intramural cell transfer and functional recovery of injured heart muscle. The Journal of thoracic and cardiovascular surgery. 2004;128:571-8.

[74] Kofidis T, Lebl DR, Martinez EC, Hoyt G, Tanaka M, Robbins RC. Novel injectable bioartificial tissue facilitates targeted, less invasive, large-scale tissue restoration on the beating heart after myocardial injury. Circulation. 2005;112:I173-7.

[75] Kutschka I, Chen IY, Kofidis T, Arai T, von Degenfeld G, Sheikh AY, et al. Collagen matrices enhance survival of transplanted cardiomyoblasts and contribute to functional improvement of ischemic rat hearts. Circulation. 2006;114:I167-73.

[76] Thompson Ca, Nasseri Ba, Makower J, Houser S, McGarry M, Lamson T, et al. Percutaneous transvenous cellular cardiomyoplasty. Journal of the American College of Cardiology. 2003;41:1964-71.

[77] Zhang P, Zhang H, Wang H, Wei Y, Hu S. Artificial matrix helps neonatal cardiomyocytes restore injured myocardium in rats. Artificial organs. 2006;30:86-93.

[78] Kichula ET, Wang H, Dorsey SM, Szczesny SE, Elliott DM, Burdick JA, et al. Experimental and computational investigation of altered mechanical properties in myocardium after hydrogel injection. Ann Biomed Eng. 2014;42:1546-56.

[79] Burdick Ja, Vunjak-Novakovic G. Engineered microenvironments for controlled stem cell differentiation. Tissue engineering Part A. 2009;15:205-19.

[80] Borg TK, Rubin K, Lundgren E, Borg K, Obrink B. Recognition of extracellular matrix components by neonatal and adult cardiac myocytes. Developmental biology. 1984;104:86-96.

[81] Lundgren E, Terracio L, Mårdh S, Borg TK. Extracellular matrix components influence the survival of adult cardiac myocytes in vitro. Experimental cell research. 1985;158:371-81.

[82] Votteler M, Kluger PJ, Walles H, Schenke-Layland K. Stem cell microenvironments--unveiling the secret of how stem cell fate is defined. Macromolecular bioscience. 2010;10:1302-15.

[83] Hilenski LL, Terracio L, Borg TK. Myofibrillar and cytoskeletal assembly in neonatal rat cardiac myocytes cultured on laminin and collagen. Cell and tissue research. 1991;264:577-87.

[84] Shanker AJ, Yamada K, Green KG, Yamada Ka, Saffitz JE. Matrix-protein-specific regulation of Cx43 expression in cardiac myocytes subjected to mechanical load. Circulation research. 2005;96:558-66.

[85] Philp D, Chen SS, Fitzgerald W, Orenstein J, Margolis L, Kleinman HK. Complex extracellular matrices promote tissue-specific stem cell differentiation. Stem cells (Dayton, Ohio). 2005;23:288-96.

[86] Schenke-layland K, Nsair A, Handel BV, Angelis E, Gluck JM, Votteler M, et al. Biomaterials Recapitulation of the embryonic cardiovascular progenitor cell niche. Biomaterials. 2011;32:2748-56.

[87] Battista S, Guarnieri D, Borselli C, Zeppetelli S, Borzacchiello A, Mayol L, et al. The effect of matrix composition of 3D constructs on embryonic stem cell differentiation. Biomaterials. 2005;26:6194-207.

[88] Bornstein P, Sage EH. Matricellular proteins: extracellular modulators of cell function. Current opinion in cell biology. 2002;14:608-16.

[89] Murphy WL, McDevitt TC, Engler AJ. Materials as stem cell regulators. Nature Materials. 2014;13:547-57.

[90] Hynes RO. The extracellular matrix: not just pretty fibrils. Science (New York, NY). 2009;326:1216-9.

[91] Wijelath ES, Rahman S, Namekata M, Murray J, Nishimura T, Mostafavi-Pour Z, et al. Heparin-II domain of fibronectin is a vascular endothelial growth factor-binding domain: enhancement of VEGF biological activity by a singular growth factor/matrix protein synergism. Circ Res. 2006;99:853-60.

[92] Sun Z, Martinez-Lemus La, Trache A, Trzeciakowski JP, Davis GE, Pohl U, et al. Mechanical properties of the interaction between fibronectin and alpha5beta1-integrin on vascular smooth muscle cells studied using atomic force microscopy. American journal of physiology Heart and circulatory physiology. 2005;289:H2526-35.

[93] Maruthamuthu V. Cell-ECM traction force modulates endogenous tension at cell–cell contacts. Proceedings of the …. 2011.

[94] Yin S, Zhang X, Zhan C, Wu J, Xu J, Cheung J. Measuring single cardiac myocyte contractile force via moving a magnetic bead. Biophysical journal. 2005;88:1489-95.

[95] Zimmermann W-H, Eschenhagen T. Cardiac tissue engineering for replacement therapy. Heart failure reviews. 2003;8:259-69.

[96] Mayer SE, de Cotten MV, Moran NC. Dissociation of the augmentation of cardiac contractile force from the activation of myocardial phosphorylase by catecholamines. The Journal of pharmacology and experimental therapeutics. 1963;139:275-82.

[97] Engler A, Bacakova L, Newman C, Hategan A, Griffin M, Discher D. Substrate compliance versus ligand density in cell on gel responses. Biophysical journal. 2004;86:617-28.

[98] Jacot JG, McCulloch AD, Omens JH. Substrate stiffness affects the functional maturation of neonatal rat ventricular myocytes. Biophysical journal. 2008;95:3479-87.

[99] Jacot JG. Cardiac Myocyte Force Development during Differentiation and Maturation. 2010;1188:121-7.

[100] Engler AJ, Carag-Krieger C, Johnson CP, Raab M, Tang H-Y, Speicher DW, et al. Embryonic cardiomyocytes beat best on a matrix with heart-like elasticity: scar-like rigidity inhibits beating. Journal of cell science. 2008;121:3794-802.

[101] Trappmann B, Gautrot JE, Connelly JT, Strange DGT, Li Y, Oyen ML, et al. Extracellular-matrix tethering regulates stem-cell fate. Nature materials. 2012;11:642-9.

[102] Engler AJ, Sen S, Sweeney HL, Discher DE. Matrix elasticity directs stem cell lineage specification. Cell. 2006;126:677-89.

[103] Evans ND, Minelli C, Gentleman E, LaPointe V, Patankar SN, Kallivretaki M, et al. Substrate stiffness affects early differentiation events in embryonic stem cells. European cells & materials. 2009;18:1-13; discussion -4.

[104] Arshi A, Nakashima Y, Nakano H, Eaimkhong S, Evseenko D, Reed J, et al. Rigid microenvironments promote cardiac differentiation of mouse and human embryonic stem cells. Science and Technology of Advanced Materials. 2013;14:025003-.

[105] Yang C, Tibbitt MW, Basta L, Anseth KS. Mechanical memory and dosing influence stem cell fate. 2014;13:645-52.

[106] McBeath R, Pirone DM, Nelson CM, Bhadriraju K, Chen CS. Cell shape, cytoskeletal tension, and RhoA regulate stem cell lineage commitment. Developmental cell. 2004;6:483-95.

[107] Choi YS, Vincent LG, Lee AR, Kretchmer KC, Chirasatitsin S, Dobke MK, et al. The alignment and fusion assembly of adipose-derived stem cells on mechanically patterned matrices. Biomaterials. 2012;33:6943-51.

[108] Tay CY, Yu H, Pal M, Leong WS, Tan NS, Ng KW, et al. Micropatterned matrix directs differentiation of human mesenchymal stem cells towards myocardial lineage. Experimental cell research. 2010;316:1159-68.

[109] Pijnappels Da, Schalij MJ, Ramkisoensing Aa, van Tuyn J, de Vries AaF, van der Laarse A, et al. Forced alignment of mesenchymal stem cells undergoing cardiomyogenic differentiation affects functional integration with cardiomyocyte cultures. Circulation research. 2008;103:167-76.

[110] McDevitt TC, Angello JC, Whitney ML, Reinecke H, Hauschka SD, Murry CE, et al. In vitro generation of differentiated cardiac myofibers on micropatterned laminin surfaces. 2001.

[111] Walsh KB, Parks GE. Changes in cardiac myocyte morphology alter the properties of voltage-gated ion channels. Cardiovascular research. 2002;55:64-75.

[112] Terracio L, Miller B, Borg TK. Effects of cyclic mechanical stimulation of the cellular components of the heart: in vitro. In vitro cellular & developmental biology. 1988;24.

[113] Guilak F, Cohen DM, Estes BT, Gimble JM. Control of stem cell fate by physical interactions with the extracellular matrix. Cell Stem Cell. 2009;5:17-26.

[114] Gavara N, Roca-Cusachs P, Sunyer R, Farré R, Navajas D. Mapping cell-matrix stresses during stretch reveals inelastic reorganization of the cytoskeleton. Biophysical journal. 2008;95:464-71.

[115] Wang N, Ingber DE. Control of cytoskeletal mechanics by extracellular matrix, cell shape, and mechanical tension. Biophysical journal. 1994;66:2181-9.

[116] Smith PG, Deng L, Fredberg JJ, Maksym GN. Mechanical strain increases cell stiffness through cytoskeletal filament reorganization. American journal of physiology Lung cellular and molecular physiology. 2003;285:L456-63.

[117] Miller CE, Donlon KJ, Toia L, Wing CL, Chess PR. Cyclic strain induces proliferation of cultured embryonic heart cells. In Vitro Cellular & Developmental Biology. 2000;36.

[118] Clause KC, Tinney JP, Liu LJ. Engineered early embryonic cardiac tissue increases cardiomyocyte proliferation by cyclic mechanical stretch via p38-MAP kinase phosphorylation. Tissue Engineering. 2009;15.

[119] Jang J-Y, Lee SW, Park SH, Shin JW, Mun C, Kim S-H, et al. Combined effects of surface morphology and mechanical straining magnitudes on the differentiation of mesenchymal stem cells without using biochemical reagents. Journal of biomedicine & biotechnology. 2011;2011:860652-.

[120] Waldman LK, Fung YC, Covell JW. Transmural Myocardial Deformation in the Canine Left Ventricle Normal in Vivo Three-Dimensional Finite Strains. 1984.

[121] Costa KD, May-newman K, Farr D, Dell WGO, Culloch ADMC, Omens JH, et al. Three-dimensional residual strain in midanterior canine left ventricle. 1997:1968-76.

[122] Gopalan SM, Flaim C, Bhatia SN, Hoshijima M, Knoell R, Chien KR, et al. Anisotropic stretch-induced hypertrophy in neonatal ventricular myocytes micropatterned on deformable elastomers. Biotechnology and bioengineering. 2003;81:578-87.

[123] Sadoshima J, Jahn L, Takahashi T, Kulik T, Izumo S. Molecular Characterization of the Stretch-induced Adaptation of Cultured Cardiac Cells. Journal of Biological Chemistry. 1992;267:10551-60.

[124] Lammerding JAN. Mechanotransduction in cardiac myocytes. Annals of the New York …. 2004;1015:53-70.

[125] Yamada K, Green KG, Samarel AM, Saffitz JE. Distinct pathways regulate expression of cardiac electrical and mechanical junction proteins in response to stretch. Circulation research. 2005;97:346-53.

[126] Schmelter M, Ateghang B, Helmig S, Wartenberg M, Sauer H. Embryonic stem cells utilize reactive oxygen species as transducers of mechanical strain-induced cardiovascular differentiation. FASEB journal : official publication of the Federation of American Societies for Experimental Biology. 2006;20:1182-4.

[127] Kurazumi H, Kubo M, Ohshima M, Yamamoto Y, Takemoto Y, Suzuki R, et al. The effects of mechanical stress on the growth, differentiation, and paracrine factor production of cardiac stem cells. PloS one. 2011;6:e28890-e.

[128] Guo B, Li Y, Han R, Zhou H, Wang M. Angiotensin II upregulation of cardiomyocyte adiponectin production is nitric oxide/cyclic GMP dependent. The American journal of the medical sciences. 2011;341:350-5.

[129] Sadoshima J, Izumo S. The cellular and molecular response of cardiac myocytes to mechanical stress. Annual review of physiology. 1997;59:551-71.

[130] Akhyari P, Fedak PWM, Weisel RD, Lee TYJ, Verma S, Mickle DAG, et al. Mechanical stretch regimen enhances the formation of bioengineered autologous cardiac muscle grafts. Circulation. 2002;106:I-137.

[131] Mihic A, Li J, Miyagi Y, Gagliardi M, Li S-H, Zu J, et al. The effect of cyclic stretch on maturation and 3D tissue formation of human embryonic stem cell-derived cardiomyocytes. Biomaterials. 2014;35:2798-808.

[132] Kurazumi H, Li T-S, Takemoto Y, Suzuki R, Mikamo A, Guo C-Y, et al. Haemodynamic unloading increases the survival and affects the differentiation of cardiac stem cells after implantation into an infarcted heart. European journal of cardio-thoracic surgery : official journal of the European Association for Cardio-thoracic Surgery. 2014:1-7.

[133] Rowlands AS, George PA, Cooper-white JJ. Directing osteogenic and myogenic differentiation of MSCs : interplay of stiffness and adhesive ligand presentation. American journal of physiology Cell physiology. 2008;295:1037-44.

[134] Lee J, Abdeen Aa, Zhang D, Kilian Ka. Directing stem cell fate on hydrogel substrates by controlling cell geometry, matrix mechanics and adhesion ligand composition. Biomaterials. 2013;34:8140-8.

[135] De Lisio M, Jensen T, Sukiennik Ra, Huntsman HD, Boppart MD. Substrate and strain alter the muscle-derived mesenchymal stem cell secretome to promote myogenesis. Stem cell research & therapy. 2014;5:74-.

[136] Mackenna DA, Dolfi F, Vuori K, Ruoslahti E. Extracellular Signal – regulated Kinase and c-Jun NH 2 -terminal Kinase Activation by Mechanical Stretch Is Integrin-dependent and Matrix-specific in Rat Cardiac Fibroblasts. 1998.

[137] Subramony SD, Dargis BR, Castillo M, Azeloglu EU, Tracey MS, Su A, et al. The guidance of stem cell differentiation by substrate alignment and mechanical stimulation. Biomaterials. 2013;34:1942-53.

[138] Kasten A, Müller P, Bulnheim U, Groll J, Bruellhoff K, Beck U, et al. Mechanical integrin stress and magnetic forces induce biological responses in mesenchymal stem cells which depend on environmental factors. Journal of cellular biochemistry. 2010;111:1586-97.

[139] Gong Z, Niklason LE. Small-diameter human vessel wall engineered from bone marrow-derived mesenchymal stem cells (hMSCs). FASEB journal : official publication of the Federation of American Societies for Experimental Biology. 2008;22:1635-48.

[140] Wang N, Butler JP, Ingber DE. Mechanotransduction across the cell surface and through the cytoskeleton. Science. 1993;260:1124-7.

[141] Hoffman BD, Grashoff C, Schwartz Ma. Dynamic molecular processes mediate cellular mechanotransduction. Nature. 2011;475:316-23.

[142] Hynes RO. Integrins: bidirectional, allosteric signaling machines. Cell. 2002;110:673-87.

[143] Buxboim A, Ivanovska IL, Discher DE. Matrix elasticity, cytoskeletal forces and physics of the nucleus: how deeply do cells 'feel' outside and in? Journal of cell science. 2010;123:297-308.

[144] Discher DE, Janmey P, Wang Y-l. Tissue Cells Feel and Respond to the Stiffness of Their Substrate. Science. 2005;310:1139-43.

[145] Dalby MJ, Gadegaard N, Oreffo ROC. Harnessing nanotopography and integrin–matrix interactions to influence stem cell fate. Nature Materials. 2014;13:558-69.

[146] Trappmann B, Chen CS. How cells sense extracellular matrix stiffness : a material's perspective. Current Opinion in Biotechnology. 2013.

[147] Lund AW, Yener B, Stegemann JP, Plopper GE. The natural and engineered 3D microenvironment as a regulatory cue during stem cell fate determination. Tissue engineering Part B, Reviews. 2009;15:371-80.

[148] Vogel V, Sheetz M. Local force and geometry sensing regulate cell functions. Nature reviews Molecular cell biology. 2006;7:265-75.

[149] Elosegui-Artola A, Bazellières E, Allen MD. Rigidity sensing and adaptation through regulation of integrin types. Nature materials. 2014;13.

[150] Schwartz MA, Simone DW. Cell Adhesion Receptors in Mechanotransduction. Current opinion in cell biology. 2008;20:551-6.

[151] Ross RS, Borg TK. Integrins and the Myocardium. Circulation Research. 2001;88:1112-9.

[152] Lal H, Verma SK, Foster DM, Golden HB, Reneau JC, Watson LE, et al. Integrins and proximal signaling mechanisms in cardiovascular disease. Fronteirs in Bioscience. 2009;14:2307-34.

[153] Galbraith CG, Yamada KM, Galbraith Ja. Polymerizing actin fibers position integrins primed to probe for adhesion sites. Science (New York, NY). 2007;315:992-5.

[154] Maitra N, Flink IL, Bahl JJ, Morkin E. Expression of a and b integrins during terminal differentiation of cardiomyocytes. 2000;47:715-25.

[155] Hornberger LK, Singhroy S, Cavalle-garrido T, Tsang W, Keeley F, Rabinovitch M. Synthesis of Extracellular Matrix and Adhesion Through B1 Myocyte Proliferation. Circulation research. 2000;87:508-15.

[156] Ross RS, Pham C, Shai S-y, Goldhaber JI, Fenczik C, Glembotski CC, et al. 1 Integrins Participate in the Hypertrophic Response of Rat Ventricular Myocytes. 1998:1160-72.

[157] Li R, Wu Y, Manso AM, Gu Y, Liao P, Israeli S, et al. B1 Integrin Gene Excision in the Adult Murine Cardiac Myocyte Causes Defective Mechanical and Signaling Responses. The American journal of pathology. 2012;180:952-62.

[158] Fässler R, Rohwedel J, Maltsev V, Bloch W, Lentini S, Guan K, et al. Differentiation and integrity of cardiac muscle cells are impaired in the absence of beta 1 integrin. Journal of cell science. 1996;109 (Pt 1:2989-99.

[159] Hubbi ME, Ahn EH, Downey J, Afzal J, Kim DH, Rey S, et al. Matrix Rigidity Controls Endothelial Differentiation and Morphogenesis of Cardiac Precursors. Science Signaling. 2012;5:ra41-ra.

[160] Riveline D, Zamir E, Balaban NQ, Schwarz US, Ishizaki T, Narumiya S, et al. Focal Contacts as Mechanosensors : Externally Applied Local Mechanical Force Induces Growth of Focal Contacts by an mDia1-dependent and. 2001;153:1175-85.

[161] Katsumi A, Orr aW, Tzima E, Schwartz MA. Integrins in mechanotransduction. The Journal of biological chemistry. 2004;279:12001-4.

[162] Guan J-L. Role of focal adhesion kinase in integrin signaling. The International Journal of Biochemistry & Cell Biology. 1997;29:1085-96.

[163] H Lal SKVMSRSGGLDMF, Dostal DE. Stretch-Induced MAP kinase Activation in Cardiac Myocytes: Differential Regulation through B1-Integrin and Focal Adhesion Kinase. J Molecular Cell Cardiol. 2007;43:137-47.

[164] Torsoni AS, Marin TM, Velloso La, Franchini KG. RhoA/ROCK signaling is critical to FAK activation by cyclic stretch in cardiac myocytes. American journal of physiology Heart and circulatory physiology. 2005;289:H1488-96.

[165] Weinbaum JS, Schmidt JB, Tranquillo RT. Combating Adaptation to Cyclic Stretching by Prolonging Activation of Extracellular Signal-Regulated Kinase. Cellular and Molecular Bioengineering. 2013;6:279-86.

[166] Sordella R, Jiang W, Chen G-C, Curto M, Settleman J. Modulation of Rho GTPase signaling regulates a switch between adipogenesis and myogenesis. Cell. 2003;113:147-58.

[167] French KM, Boopathy AV, DeQuach JA, Chingozha L, Lu H, Christman KL, et al. A naturally derived cardiac extracellular matrix enhances cardiac progenitor cell behavior in vitro. Acta Biomater. 2012;8:4357-64.

[168] Li M, Naqvi N, Yahiro E, Liu K, Powell PC, Bradley WE, et al. C-Kit Is Required for Cardiomyocyte Terminal Differentiation. Circulation research. 2008;102:677-85.

[169] van Berlo JH, Kanisicak O, Maillet M, Vagnozzi RJ, Karch J, Lin S-CJ, et al. C-Kit+ Cells Minimally Contribute Cardiomyocytes To the Heart. Nature. 2014;509:337-41.

[170] Miyamoto S, Kawaguchi N, Ellison GM, Matsuoka R, Shin'oka T, Kurosawa H. Characterization of long-term cultured c-kit+ cardiac stem cells derived from adult rat hearts. Stem cells and development. 2010;19:105-16.

[171] Leri A, Kajstura J, Anversa P. Role of cardiac stem cells in cardiac pathophysiology: a paradigm shift in human myocardial biology. Circulation research. 2011;109:941-61.

[172] Urbanek K, Rota M, Cascapera S, Bearzi C, Nascimbene A, De Angelis A, et al. Cardiac stem cells possess growth factor-receptor systems that after activation regenerate the infarcted myocardium, improving ventricular function and long-term survival2005.

[173] Cesselli D, Beltrami AP, D'Aurizio F, Marcon P, Bergamin N, Toffoletto B, et al. Effects of age and heart failure on human cardiac stem cell function. The American journal of pathology. 2011;179:349-66.

[174] Itzhaki-Alfia A, Leor J, Raanani E, Sternik L, Spiegelstein D, Netser S, et al. Patient characteristics and cell source determine the number of isolated human cardiac progenitor cells. Circulation. 2009;120:2559-66.

[175] Singelyn JM, DeQuach Ja, Seif-Naraghi SB, Littlefield RB, Schup-Magoffin PJ, Christman KL. Naturally derived myocardial matrix as an injectable scaffold for cardiac tissue engineering. Biomaterials. 2009;30:5409-16.

[176] DeQuach Ja, Mezzano V, Miglani A, Lange S, Keller GM, Sheikh F, et al. Simple and high yielding method for preparing tissue specific extracellular matrix coatings for cell culture. PloS one. 2010;5:e13039-e.

[177] Johnson TD, DeQuach Ja, Gaetani R, Ungerleider J, Elhag D, Nigam V, et al. Human versus porcine tissue sourcing for an injectable myocardial matrix hydrogel. Biomaterials Science. 2014:13-7.

[178] Singelyn JM, Sundaramurthy P. Catheter-Deliverable Hydrogel Derived From Decellularized Ventricular Extracellular Matrix Increases Endogenous Cardiomyocytes and Preserves Cardiac Function. Journal of the American College of Cardiology. 2012;59.

[179] Singelyn JM, Christman KL. Injectable materials for the treatment of myocardial infarction and heart failure: the promise of decellularized matrices. Journal of cardiovascular translational research. 2010;3:478-86.

[180] Seif-Naraghi SB, Salvatore Ma, Schup-Magoffin PJ, Hu DP, Christman KL. Design and characterization of an injectable pericardial matrix gel: a potentially autologous scaffold for cardiac tissue engineering. Tissue engineering Part A. 2010;16:2017-27.

[181] Singelyn JM, Christman KL. Modulation of material properties of a decellularized myocardial matrix scaffold. Macromolecular bioscience. 2011;11:731-8.

[182] Badylak SF. Decellularized allogeneic and xenogeneic tissue as a bioscaffold for regenerative medicine: factors that influence the host response. Annals of biomedical engineering. 2014;42:1517-27.

[183] Grover GN, Rao N, Christman KL. Myocardial matrix-polyethylene glycol hybrid hydrogels for tissue engineering. Nanotechnology. 2014;25:014011-.

[184] Seif-Naraghi SB, Singelyn JM, Salvatore Ma, Osborn KG, Wang JJ, Sampat U, et al. Safety and efficacy of an injectable extracellular matrix hydrogel for treating myocardial infarction. Science translational medicine. 2013;5:173ra25-ra25.

[185] Müller-Ehmsen J, Whittaker P, Kloner Ra, Dow JS, Sakoda T, Long TI, et al. Survival and development of neonatal rat cardiomyocytes transplanted into adult myocardium. Journal of molecular and cellular cardiology. 2002;34:107-16.

[186] Rota M, Padin-Iruegas ME, Misao Y, De Angelis A, Maestroni S, Ferreira-Martins J, et al. Local activation or implantation of cardiac progenitor cells rescues scarred infarcted myocardium improving cardiac function. Circulation research. 2008;103:107-16.

[187] Terrovitis JV, Smith RR, Marbán E. Assessment and optimization of cell engraftment after transplantation into the heart. Circulation research. 2010;106:479-94.

[188] Hadjipanayi E, Mudera V, Brown RA. Close dependence of fibroblast proliferation on collagen scaffold matrix stiffness. Journal of tissue engineering and regenerative medicine. 2009;3:77-84.

[189] Wang HB, Dembo M, Wang Y-L. Substrate flexibility regulates growth and apoptosis of normal but not transformed cells. Journal of Physiology-Cell. 2000;279:C1345-C50.

[190] Miskon A, Mahara A, Uyama H, Yamaoka T. A suspension induction for myocardial differentiation of rat mesenchymal stem cells on various extracellular matrix proteins. Tissue engineering Part C, Methods. 2010;16:979-87.

[191] Bratt-Leal AM, Carpenedo RL, McDevitt TC. Engineering the Embryoid Body Microenvironment to Direct Stem Cell Differentiation. Biotechnology Progress. 2009;25:43-51.

[192] Young DA, Ibrahim DO, Hu D, Christman KL. Injectable hydrogel scaffold from decellularized human lipoaspirate. Acta biomaterialia. 2011;7:1040-9.

[193] Lien CL, Wu C, Mercer B, Webb R, Richardson Ja, Olson EN. Control of early cardiac-specific transcription of Nkx2-5 by a GATA-dependent enhancer. Development (Cambridge, England). 1999;126:75-84.

[194] Hsieh PCH, Segers VFM, Davis ME, MacGillivray C, Gannon J, Molkentin JD, et al. Evidence from a genetic fate-mapping study that stem cells refresh adult mammalian cardiomyocytes after injury. Nature medicine. 2007;13:970-4.

[195] Oh H, Bradfute SB, Gallardo TD, Nakamura T, Gaussin V, Mishina Y, et al. Cardiac progenitor cells from adult myocardium: homing, differentiation, and fusion after infarction. Proceedings of the National Academy of Sciences of the United States of America. 2003;100:12313-8.

[196] Phelps Ea, Landázuri N, Thulé PM, Taylor WR, García AJ. Bioartificial matrices for therapeutic vascularization. Proceedings of the National Academy of Sciences of the United States of America. 2010;107:3323-8.

[197] Nussbaum J, Minami E, Laflamme Ma, Virag JaI, Ware CB, Masino A, et al. Transplantation of undifferentiated murine embryonic stem cells in the heart: teratoma formation and immune response. FASEB journal : official publication of the Federation of American Societies for Experimental Biology. 2007;21:1345-57.

[198] Shai S-Y, Harpf AE, Babbitt CJ, Jordan MC, Fishbein MC, Chen J, et al. Cardiac Myocyte-Specific Excision of the beta1 Integrin Gene Results in Myocardial Fibrosis and Cardiac Failure. Circulation Research. 2002;90:458-64.

[199] Popov C, Radic T, Haasters F, Prall WC, Aszodi a, Gullberg D, et al. Integrins α2β1 and α11β1 regulate the survival of mesenchymal stem cells on collagen I. Cell death & disease. 2011;2:e186-e.

[200] Salasznyk RM, Williams Wa, Boskey A, Batorsky A, Plopper GE. Adhesion to Vitronectin and Collagen I Promotes Osteogenic Differentiation of Human Mesenchymal Stem Cells. Journal of biomedicine & biotechnology. 2004;2004:24-34.

[201] Rutschow S, Li J, Schultheiss H-P, Pauschinger M. Myocardial proteases and matrix remodeling in inflammatory heart disease. Cardiovascular research. 2006;69:646-56.

[202] Seiffert M, Beck SC, Schermutzki F, Muller CA, Erickson HP, Klein G. Mitogenic and adhesive effects of tenascin-C on human hematopoietic cells are mediated by various

functional domains. Matrix biology : journal of the International Society for Matrix Biology. 1998;17:47-63.

[203] Badylak SF. The extracellular matrix as a biologic scaffold material. Biomaterials. 2007;28:3587-93.

[204] Singelyn JM, Dequach JA, Christman KL. Engineering anatomically shaped human bone grafts with human mesenchymal stem cells (hMSCs). Science-Business eXchange. 2009;2:2406-8.

[205] Badylak S, Obermiller J, Geddes L, Matheny R. Extracellular matrix for myocardial repair. The heart surgery forum. 2003;6:E20-6.

[206] Rane Aa, Christman KL. Biomaterials for the treatment of myocardial infarction a 5-year update. Journal of the American College of Cardiology. 2011;58:2615-29.

[207] Spradling A, Drummond-Barbosa D, Kai T, others. Stem cells find their niche. NATURE-LONDON-. 2001;414:98-104.

[208] Pankov R. Fibronectin at a glance. Journal of Cell Science. 2002;115:3861-3.

[209] Konstandin MH, Toko H, Gastelum GM, Quijada PJ, De La Torre a, Quintana M, et al. Fibronectin is Essential for Reparative Cardiac Progenitor Cell Response Following Myocardial Infarction. Circulation Research. 2013.

[210] Xu Y, Gurusiddappa S, Rich RL, Owens RT, Keene DR, Mayne R, et al. Multiple Binding Sites in Collagen Type I for the Integrins 1 1 and 2 1. Journal of Biological Chemistry. 2000;275:38981-9.

[211] Jokinen J, Dadu E, Nykvist P, Kapyla J, White DJ, Ivaska J, et al. Integrin-mediated Cell Adhesion to Type I Collagen Fibrils. Journal of Biological Chemistry. 2004;279:31956-63.

[212] Alcaraz J, Xu R, Mori H, Nelson CM, Mroue R, Spencer Va, et al. Laminin and biomimetic extracellular elasticity enhance functional differentiation in mammary epithelia. The EMBO journal. 2008;27:2829-38.

[213] Ponce ML, Nomizu M, Delgado MC, Kuratomi Y, Hoffman MP, Powell S, et al. Identification of Endothelial Cell Binding Sites on the Laminin 1 Chain. 1999:688-94.

[214] Tashiro K-i, Monji A, Yoshida I, Hayashi Y, Matsuda K, Tashiro N, et al. An IKLLI-containing peptide derived from the laminin α1 chain mediating heparin-binding, cell adhesion, neurite outgrowth and proliferation, represents a binding site for integrin α3β1 and heparan sulphate proteoglycan. Biochem. 1999;126:119-26.

[215] Mazia D. Adhesion of cells to surfaces coated with poly-lysine. Application to Electron Microscopy. 1975;66:198-200.

[216] Chiquet M. Regulation of extracellular matrix gene expression by mechanical stress. Matrix biology. 1999;18:417-26.

[217] Pimentel RC. Autocrine Regulation of Myocyte Cx43 Expression by VEGF. Circulation Research. 2002;90:671-7.

[218] Guo D, Kassiri Z, Oudit GY. Role of Signaling Pathways in the Myocardial Response to Biomechanical Stress and in Mechanotransduction in the Heart. 2011:141-66.

[219] Gwak S-J, Bhang SH, Kim I-K, Kim S-S, Cho S-W, Jeon O, et al. The effect of cyclic strain on embryonic stem cell-derived cardiomyocytes. Biomaterials. 2008;29:844-56.

[220] Guo X-M, Zhao Y-S, Chang H-X, Wang C-Y, E L-L, Zhang X-A, et al. Creation of engineered cardiac tissue in vitro from mouse embryonic stem cells. Circulation. 2006;113:2229-37.

[221] Watt FM, Hogan BL. Out of Eden: stem cells and their niches. Science (New York, NY). 2000;287:1427-30.

[222] Kornbergs L, Earpo HS, Parsonsn JT, Schallerv M. Clustering Increases Phosphorylation of a Focal. 1992:23439-42.

[223] Boutahar N, Guignandon A, Vico L, Lafage-Proust M-H. Mechanical strain on osteoblasts activates autophosphorylation of focal adhesion kinase and proline-rich tyrosine kinase 2 tyrosine sites involved in ERK activation. The Journal of biological chemistry. 2004;279:30588-99.

[224] Chaturvedi LS, Marsh HM, Basson MD. Src and focal adhesion kinase mediate mechanical strain-induced proliferation and ERK1/2 phosphorylation in human H441 pulmonary epithelial cells. American journal of physiology Cell physiology. 2007;292:C1701-13.

[225] Kumar A, Murphy R, Robinson P, Wei L, Boriek AM. Cyclic mechanical strain inhibits skeletal myogenesis through activation of focal adhesion kinase, Rac-1 GTPase, and NF-kappaB transcription factor. FASEB journal : official publication of the Federation of American Societies for Experimental Biology. 2004;18:1524-35.

[226] Wang JG, Miyazu M, Matsushita E, Sokabe M, Naruse K. Uniaxial cyclic stretch induces focal adhesion kinase (FAK) tyrosine phosphorylation followed by mitogen-activated protein kinase (MAPK) activation. Biochemical and biophysical research communications. 2001;288:356-61.

[227] Huang X, Yang N, Fiore VF, Barker TH, Sun Y, Morris SW, et al. Matrix stiffness-induced myofibroblast differentiation is mediated by intrinsic mechanotransduction. American journal of respiratory cell and molecular biology. 2012;47:340-8.

[228] Wei X, Li T, Hagen B, Zhang P, Sanchez PG, Williams K, et al. Short-term mechanical unloading with left ventricular assist devices after acute myocardial infarction conserves calcium cycling and improves heart function. JACC Cardiovascular interventions. 2013;6:406-15.

[229] Lyford GL, Strege PR, Shepard A, Ou Y, Ermilov L, Miller SM, et al. alpha(1C) (Ca(V)1.2) L-type calcium channel mediates mechanosensitive calcium regulation. American journal of physiology Cell physiology. 2002;283:C1001-8.

[230] Ruwhof C, van Wamel JET, Noordzij LaW, Aydin S, Harper JCR, van der Laarse a. Mechanical stress stimulates phospholipase C activity and intracellular calcium ion levels in neonatal rat cardiomyocytes. Cell Calcium. 2001;29:73-83.

[231] Kondratev D, Gallitelli MF. Increments in the concentrations of sodium and calcium in cell compartments of stretched mouse ventricular myocytes. Cell Calcium. 2003;34:193-203.

[232] Kuo P-L, Lee H, Bray M-A, Geisse Na, Huang Y-T, Adams WJ, et al. Myocyte shape regulates lateral registry of sarcomeres and contractility. The American journal of pathology. 2012;181:2030-7.

[233] Ren J, Avery J, Zhao H, Schneider JG, Ross FP, Muslin AJ. Beta3 integrin deficiency promotes cardiac hypertrophy and inflammation. Journal of molecular and cellular cardiology. 2007;42:367-77.

[234] Woitasky N, Maxeiner H, Krehbiehl N, Mu A, Weigand MA, Abdallah Y, et al. New insights into paracrine mechanisms of human cardiac progenitor cells. European Journal of Heart Failure. 2010.

[235] Ferreira-Martins J, Rondon-Clavo C, Tugal D, Korn Ja, Rizzi R, Padin-Iruegas ME, et al. Spontaneous Calcium Oscillations Regulate Human Cardiac Progenitor Cell Growth. Circulation Research. 2009;105:764-74.

[236] Ferreira-Martins J, Ogorek B, Cappetta D, Matsuda a, Signore S, D'Amario D, et al. Cardiomyogenesis in the Developing Heart Is Regulated by C-Kit-Positive Cardiac Stem Cells. Circulation Research. 2012;110:701-15.

[237] Tufan H, Zhang XH. Cardiac progenitor cells engineered with Pim-1 (CPCeP) develop cardiac phenotypic electrophysiological properties as they are co-cultured with neonatal myocytes. … and cellular cardiology. 2012;53:695-706.

[238] Ishikawa S, Kuno A, Tanno M, Miki T, Kouzu H, Itoh T, et al. Role of connexin-43 in protective PI3K-Akt-GSK-3 signaling in cardiomyocytes. 2012;1:2536-44.

[239] Song D, Liu X, Liu R, Yang L, Zuo J, Liu W. Connexin 43 hemichannel regulates H9c2 cell proliferation by modulating. 2010:472-82.

[240] Wu X, Huang W, Luo G, Alain LA. Hypoxia induces connexin 43 dysregulation by modulating matrix metalloproteinases via MAPK signaling. 2013:155-62.

[241] Lee C-y, Lou J, Wen K-k, McKane M, Eskin SG, Ono S. Actin depolymerization under force is governed by lysine 113 : glutamic acid 195-mediated. 2013:1-6.

[242] Gerdes aM, Capasso JM. Structural remodeling and mechanical dysfunction of cardiac myocytes in heart failure. Journal of molecular and cellular cardiology. 1995;27:849-56.

[243] McSpadden LC, Kirkton RD, Bursac N. Electrotonic loading of anisotropic cardiac monolayers by unexcitable cells depends on connexin type and expression level. American journal of physiology Cell physiology. 2009;297:C339-51.

[244] Ahuja P, Perriard E, Pedrazzini T, Satoh S, Perriard J-C, Ehler E. Re-expression of proteins involved in cytokinesis during cardiac hypertrophy. Experimental cell research. 2007;313:1270-83.

[245] Kuang D, Zhao X, Xiao G, Ni J, Feng Y, Wu R, et al. Stem cell factor/c-kit signaling mediated cardiac stem cell migration via activation of p38 MAPK. Basic research in cardiology. 2008;103:265-73.

[246] Ding L, Saunders TL, Enikolopov G, Morrison SJ. Endothelial and perivascular cells maintain haematopoietic stem cells. Nature. 2012;481:457-62.

[247] Broudy VC. Stem cell factor and hematopoiesis. Blood. 1997;90:1345-64.

[248] Hoch RV, Soriano P. Roles of PDGF in animal development. Development. 2003;130:4769-84.

[249] Battegay EJ, Rupp J, Iruela-Arispe L, Sage EH, Pech M. PDGF-BB modulates endothelial proliferation and angiogenesis in vitro via PDGF beta-receptors. J Cell Biol. 1994;125:917-28.

[250] Boopathy AV, Lin P, Somasuntharam I, Fiore VF, Cabigas EB, Ban K, et al. The modulation of cardiac progenitor cell function by hydrogel-dependent Notch1 activation. Biomaterials. 2014;35.

[251] Nakamura T, Mizuno S. The discovery of hepatocyte growth factor (HGF) and its significance for cell biology, life sciences and clinical medicine. Proceedings of the Japan Academy Series B, Physical and biological sciences. 2010;86:588-610.

[252] Morimoto H, Takahashi M, Izawa A, Ise H, Hongo M, Kolattukudy PE, et al. Cardiac overexpression of monocyte chemoattractant protein-1 in transgenic mice prevents cardiac dysfunction and remodeling after myocardial infarction. Circ Res. 2006;99:891-9.

[253] Narasimhan P, Liu J, Song YS, Massengale JL, Chan PH. VEGF Stimulates the ERK 1/2 signaling pathway and apoptosis in cerebral endothelial cells after ischemic conditions. Stroke; a journal of cerebral circulation. 2009;40:1467-73.

[254] Chang HJ, Park JS, Kim MH, Hong MH, Kim KM, Kim SM, et al. Extracellular signal-regulated kinases and AP-1 mediate the up-regulation of vascular endothelial growth factor by PDGF in human vascular smooth muscle cells. International journal of oncology. 2006;28:135-41.

[255] Jung YD, Nakano K, Liu W, Gallick GE, Ellis LM. Extracellular signal-regulated kinase activation is required for up-regulation of vascular endothelial growth factor by serum starvation in human colon carcinoma cells. Cancer research. 1999;59:4804-7.

[256] Roger VL, Go AS, Lloyd-Jones DM, Adams RJ, Berry JD, Brown TM, et al. Heart disease and stroke statistics--2011 update: a report from the American Heart Association. Circulation. 2011;123:e18-e209.

[257] Wang QD, Pernow J, Sjoquist PO, Ryden L. Pharmacological possibilities for protection against myocardial reperfusion injury. Cardiovascular research. 2002;55:25-37.

[258] Kakkar R, Lee RT. Intramyocardial fibroblast myocyte communication. Circulation research. 2010;106:47-57.

[259] Chaudhuri O, Mooney DJ. Stem-cell differentiation: Anchoring cell-fate cues. Nature materials. 2012;11:568-9.

[260] Shimko VF, Claycomb WCC. Effect of Mechanical Loading on Three-dimensional cultures of ESC-derived CMs. 2008;14:49-58.

[261] Cho H, Balaji S, Sheikh AQ, Hurley JR, Tian YF, Collier JH, et al. Regulation of endothelial cell activation and angiogenesis by injectable peptide nanofibers. Acta biomaterialia. 2011;8:154-64.

[262] Liu Z, Yue S, Chen X, Kubin T, Braun T. Regulation of cardiomyocyte polyploidy and multinucleation by CyclinG1. Circulation research. 2010;106:1498-506.

[263] Radisic M, Park H, Shing H, Consi T, Schoen FJ, Langer R, et al. Functional assembly of engineered myocardium by electrical stimulation of cardiac myocytes cultured on scaffolds. Proceedings of the National Academy of Sciences of the United States of America. 2004;101:18129-34.

[264] Gray WD, French KM, Ghosh-Choudhary SK, Maxwell JT, Brown ME, Platt MO, et al. Identification of Therapeutic Covariant microRNA Clusters in Hypoxia Treated Cardiac Progenitor Cell Exosomes using Systems Biology. Circulation research. 2014:1-10.

[265] Lu H, Koo LY, Wang WM, Lauffenburger Da, Griffith LG, Jensen KF. Microfluidic shear devices for quantitative analysis of cell adhesion. Analytical chemistry. 2004;76:5257-64.